Order Number 9236593

Investigations of the water oxidation complex in PS II

Shim, Hyunsuk, Ph.D.

University of Illinois at Urbana-Champaign, 1992

U·M·I
300 N. Zeeb Rd.
Ann Arbor, MI 48106

INVESTIGATIONS OF THE WATER OXIDATION COMPLEX IN PS II

BY

HYUNSUK SHIM

B.S., Yonsei University, 1984

THESIS

Submitted in partial fulfillment of the requirements
for the degree of Doctor of Philosophy in Biophysics
in the Graduate College of the
University of Illinois at Urbana-Champaign, 1992

Urbana, Illinois

UNIVERSITY OF ILLINOIS AT URBANA-CHAMPAIGN

THE GRADUATE COLLEGE

DECEMBER 1991

WE HEREBY RECOMMEND THAT THE THESIS BY

HYUNSUK SHIM

ENTITLED INVESTIGATIONS OF THE WATER OXIDATION COMPLEX IN PS II

BE ACCEPTED IN PARTIAL FULFILLMENT OF THE REQUIREMENTS FOR

THE DEGREE OF DOCTOR OF PHILOSOPHY

Peter G Debrunner

Director of Thesis Research

Dennis E. Buetow

Head of Department

Committee on Final Examination†

Peter G Debrunner

Chairperson

Dennis E Buetow

† Required for doctor's degree but not for master's.

O-517

ABSTRACT

In this thesis an attempt was made to take the water oxidizing complex apart in a controlled way and to reconstitute it to its functional form.

The mechanism of photosynthetic water oxidation has been probed by the use of the substrate analogue NH_2OH in 1 M NaCl treated PSII membranes lacking the 17 and 23 kD extrinsic proteins. A plot of the Mn released versus [NH_2OH] shows a sigmoidal shape. The results were interpreted in terms of a cooperativity model. The plot of Mn release versus oxygen evolving activity shows that all 4 Mn in the reaction center are essential for active oxygen evolution.

1 M $CaCl_2$ treated PSII membranes, which lack all 3 extrinsic polypeptides (17, 23, and 33 kD) have low oxygen evolving activity in spite of the full complement of 4 Mn per reaction center. If the light intensity is sufficiently low, 1 M $CaCl_2$ treated PSII evolve the same number of oxygen molecules per photon as 1 M NaCl treated PSII. Therefore, removal of the 33 kD polypeptide did not inactivate the Mn center and all Mn centers are intact. When the light intensity is high, there is possible alternative electron donors to P_{680}^+ in 1 M $CaCl_2$ treated PSII (e.g., Chl). As a result, the fluorescence and the oxygen evolving activity are low. I analyzed the fluorescence data of the S_1 -> S_2 transition in DCMU-treated samples. The transition time of $CaCl_2$ PSII is 1.4 times longer than that of NaCl PSII. This slow-down of the S_1 -> S_2

transition rate is not the main reason for slow donor side and there are other reports that indicate the slow-down of the S_3 -> S_0 transition rate. It is likely that other S state transitions, including the dark reaction, are slowed down as well.

I reconstituted 37 % of the oxygen evolving activity with 40 % Mn concentration in the reconstituted sample. Therefore, about 40 % of the centers have all 4 Mn while the other 60 % of the centers have no Mn. It is very plausible that Mn rebinding also involves cooperativity. Other divalent transition metals like Fe^{2+} and Co^{2+} apparently compete for the Mn binding sites and may form mixed metal clusters.

This thesis is dedicated to

my parents,

and my husband

ACKNOWLEDGEMENTS

I would like to express my gratitude to Professor Peter G. Debrunner for his encouragement and enthusiasm during my graduate studies. I also thank Professor Govindjee for his ideas and support. This project could not have been possible without his knowledge and insights.

I thank Dr. William Coleman for his help during the early stage of this project. Also, I acknowledge everyone in Debrunner's and Govindjee's laboratories for their intellectual and social interactions: Phil Nyman, Mike Hendrich, Yaomin Xia, Jorge Rodriguez, Peeter Pirn, Chunhe Xu, and Jiancheng Cao. They have all been helpful in ways which are too numerous to mention. I would like to thank Loretta Skowron and David Kramer for their help in Mn and fluorescence measurements.

Finally, I would like to express my gratitude to my parents and family for their support and generosity, and Chang-Hyon Yun, for being a wonderful husband and a friend.

TABLE OF CONTENTS

ABBREVIATIONS

BSA	bovine serum albumin
Chl	chlorophyll
Cyt	cytochrome
DCIP	2,6-Dichloroindophenol
DCMU	(diuron) 3-(3,4-dichlorophenyl)-1,1-dimethylurea
EDTA	ethylenediamine tetraacetic acid
EPR	electron paramagnetic resonance
ESEEM	electron spin echo envelope modulation
EXAFS	extended x-ray absorption fine structure
Hepes	N-2-hydroxyethylpiperazine-N'-2-ethanesulfonic acid
HQ	hydroquinone
ICP	inductively coupled plasma
MES	2-[N-Morpholino]ethanesulfonic acid
OEC	oxygen evolving complex
Pheo	pheophytin
PPBQ	phenyl-p-benzoquinone
PQ	plastoquinone
PQH_2	plastoquinol
PSII	photosystem II
RC	reaction center
SDS-PAGE	sodium dodecyl sulfate polyacrylamide gel electrophoresis
WOC	water oxidizing complex

Chapter I: GENERAL INTRODUCTION

I-1. Introduction

Photosynthesis not only provides the food and energy for all higher forms of life, but also produces the oxygen that allowed aerobic life to evolve. Photosynthesis occurs in subcellular organelles called chloroplasts (Rawn, 1989). The chloroplast is enclosed by a double membrane. The aqueous region enclosed by the inner membrane is called the stroma. Suspended within the stroma is a continuous membrane called the thylakoid membrane, which encloses an internal space known as the lumen. The light reactions of photosynthesis occur within this membrane.

The reaction begins when an antenna pigment absorbs photons and transfers the excitation energy over the array of pigments. The excitation energy is trapped at a reaction center where a primary charge separation takes place. This light-driven oxidation-reduction occurs in two distinguishable reaction centers, PSI and PSII, that are connected by a series of electron carriers as illustrated in the so-called Z-scheme in figure 1 (Andréasson and Vänngård, 1988; Govindjee and Coleman, 1991). PSII includes the WOC which is the topic of this thesis. PSI provides the charge separation to reduce $NADP^+$. PSI is removed from the thylakoids to study the mechanism of water oxidation.

The function of PSII is to act as a water-plastoquinone oxido-reductase. Water is oxidized to oxygen and plastoquinone (PQ) is

Figure 1. The Z-scheme of photosynthetic electron transport in plants and cyanobacteria. The vertical position of each electron carrier corresponds to its reduction potential at pH 7.

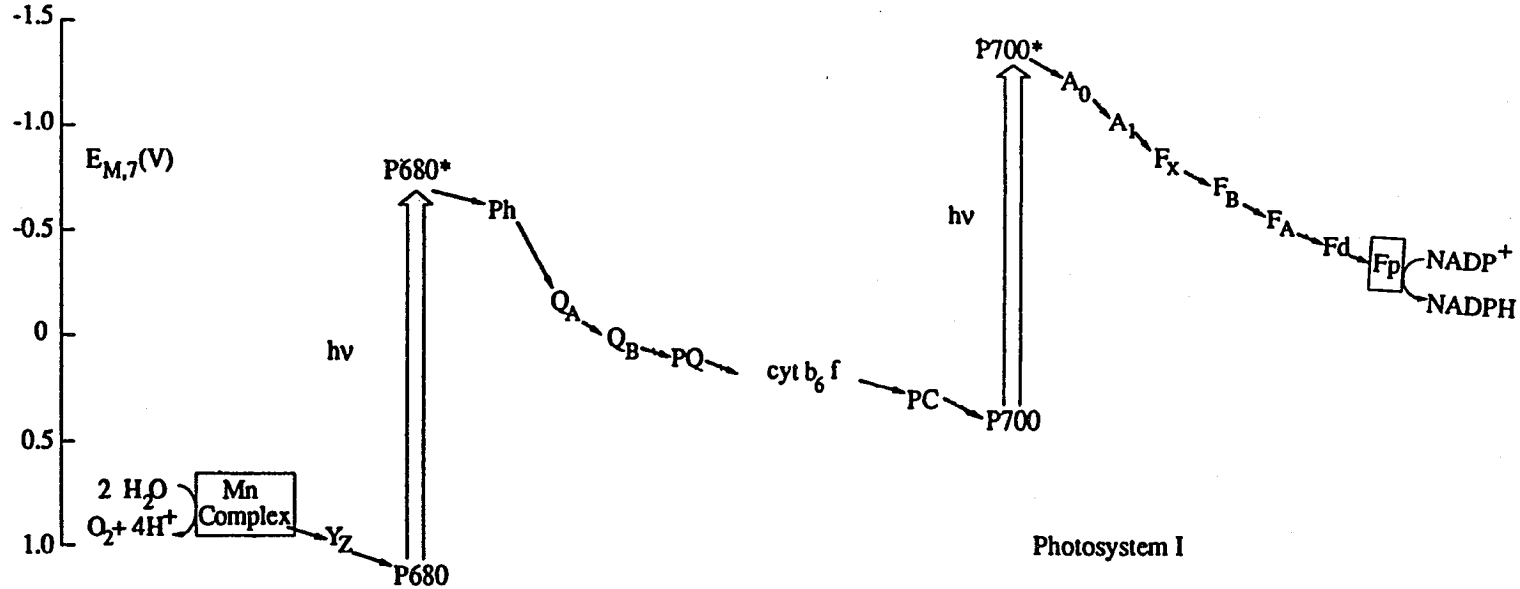

reduced to plastoquinol (PQH_2): $2H_2O + 2PQ + 4\ hv \rightarrow O_2 + 2\ PQH_2$ (Govindjee and Wasielewski, 1989). Oxygen is evolved and 4 protons are released in the lumen, while 4 protons are picked up from the stroma for the production of PQH_2. To accomplish the four-electron oxidation of water with one-electron photochemistry, PSII is thought to cycle through five successive intermediate states (S_0, S_1, S_2, S_3, and S_4), the S_4 state spontaneously decaying to produce S_0 and O_2 as described by the Kok cycle (Kok et al., 1970) shown in figure 2.

The catalytic site of photosynthetic water oxidation is known to involve a manganese cluster. An absolute manganese requirement for the functioning of the water oxidation is well documented (reviewed by Pecoraro, 1988). Quantitation of manganese in PSII has indicated a stoichiometry of four tightly bound manganese ions per center (Cheniae and Martin, 1970, 1971; Radmer and Cheniae, 1977; Yocum et al., 1981). Although extensive studies over the past few decades have shown that Mn are involved in the water oxidation, the mechanism of the reaction and the structure of the manganese-containing oxygen evolving complex are poorly understood (Govindjee et al., 1985; Renger and Wydrzynski, 1990). In this thesis, I studied the mechanism of water oxidation by the Mn complex in the PSII by deleting and reconstituting Mn.

Figure 3 shows a possible model for the organization of PSII in higher plants and green algae (excluding the light harvesting Chl a/Chl b complex). There are at least 8 polypeptides: (I) 47 kD (CP-47), an internal Chl a-protein antenna complex which fluoresces

Figure 2. The Mn complex is believed to cycle through five oxidation states in the course of accumulating oxidizing equivalents from P680 and then applying them to two water molecules and releasing molecular oxygen. The five S states of the Kok cycle (Kok et al., 1970).

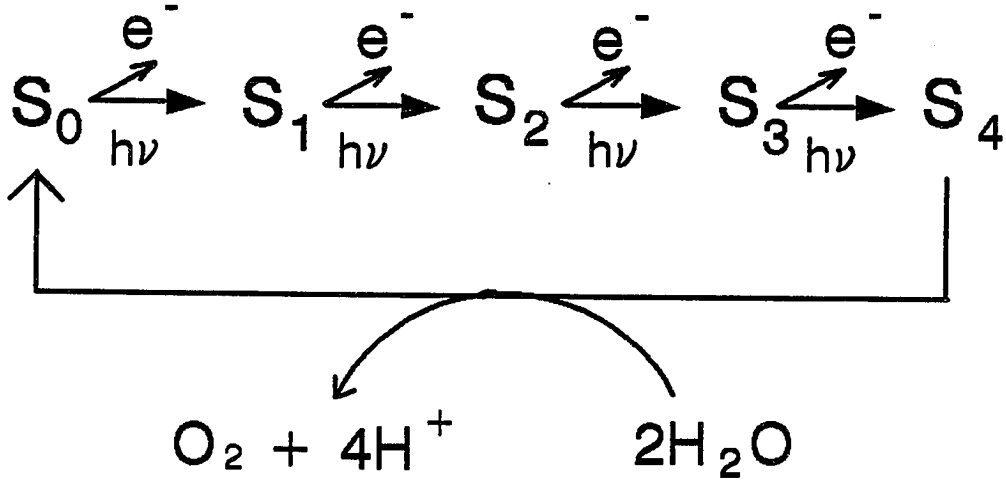

Figure 3. A possible model for the organization of proteins and Mn within the water oxidizing complex of PSII. There are at least 8 polypeptides: 47 kD, 43 kD, D-1 (34 kD), D-2 (32 kD), cyt $\underline{b}_{559}$ (4 and 9 kD), and three extrinsic polypeptides (33, 23, and 17 kD).

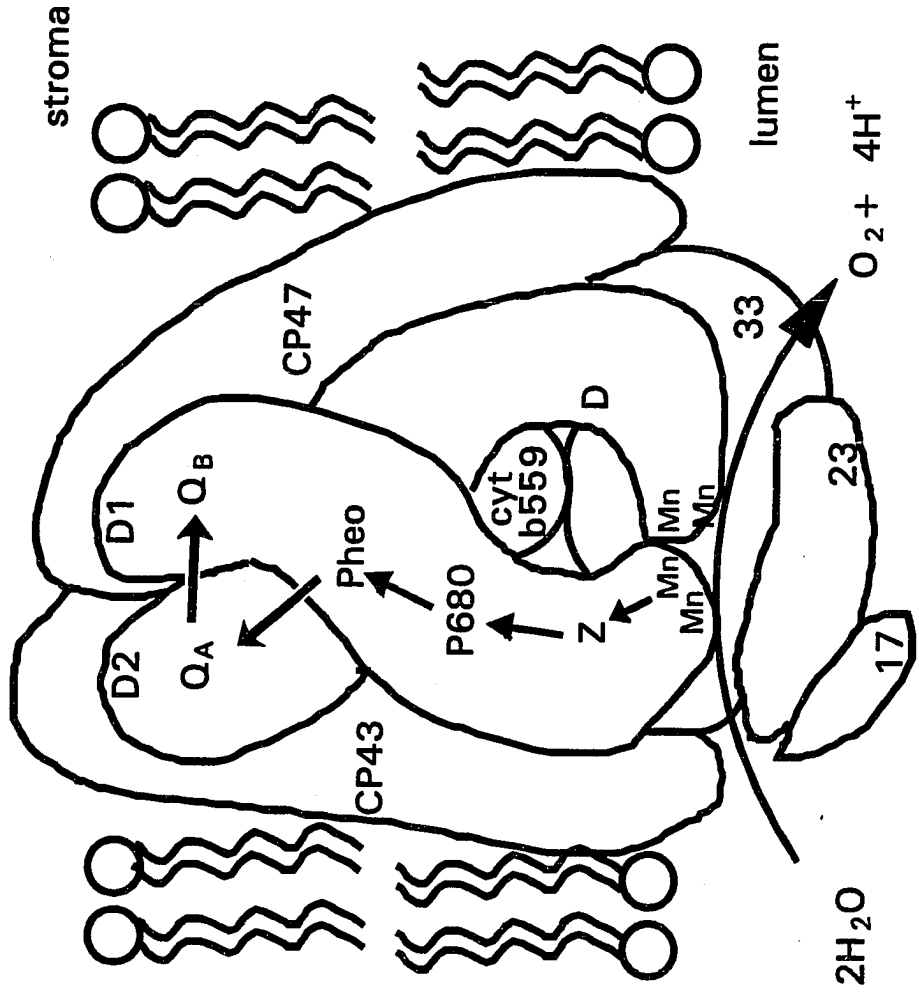

at 696 nm at 77 K; (II) 43 kD (CP-43), a distal Chl a-protein antenna complex which fluoresces at 685 nm at 77 K; (III) D-1, a 32 kD Q_B-binding protein to which herbicides can also bind; (IV) D-2, a 34 kD Q_A-binding protein; (V) cytochrome b-559 having two polypeptides of 4 and 9 kD; (VI) Y-33, a 33 kD extrinsic polypeptide that is involved in oxygen evolution; (VII) Y-23, a 23 kD extrinsic polypeptide that stimulates oxygen evolution and is required for Ca^{2+} and Cl^- binding to the membrane; (VIII) Y-17, a 17 kD extrinsic polypeptide whose function is less clearly defined. An additional low molecular weight (5 kD) polypeptide is also known to exist in PSII (see e.g., a review on PSII by Ikeuchi, 1991).

The following chapter I-2 will discuss the present knowledge of PSII to the extent needed in this thesis.

I-2. Current model of the WOC

The catalytic site of photosynthetic water oxidation is known to involve a manganese cluster which is driven by the photochemistry of PSII through a sequence of five states of the water oxidation complex.

PSII is a large membrane protein complex and since no crystal structure is available, other biochemical and biophysical techniques were applied to investigate the water oxidation mechanism.

Much information about the structure has come from x-ray absorption spectroscopy. The shape and position of the X-ray

absorption edge are sensitive to the oxidation state, types of ligands, and site symmetry in a coordination complex (Srivastava and Nigam, 1972). The EXAFS data indicate that there are at least 2 Mn atoms which are separated by 2.7 Å. The best fit to the data also suggests that there is a short Mn-(C or N or O) distance of 1.78 Å. These are typical of μ-oxo-bridged Mn. A long Mn-Mn separation of 3.3 Å has also been observed. Comparisons with model compounds suggest that the cluster contains bridging oxide or hydroxide ligands connecting the Mn atoms, perhaps with carboxylate bridges connecting the 3.3 Å Mn pair (see figure 4) (George et al., 1989; Sauer et al., 1991).

I-2-1 S_1 state

For PSII in the dark-adapted S_1 state the edge inflection energy occurs at about 6551.3 eV, which is in the range observed for Mn^{3+} complexes (Cole et al., 1987).

The S_1 state EPR signal appears as a broad, low field feature (g = 5) at X-band in parallel field, while no signal is observable in the standard perpendicular field mode. The g-value and lineshape of the S_1 state EPR signal are consistent with a transition of an S = 1 spin state (Dexheimer et al., 1990). Since S = 2 for one Mn^{3+}, the effective spin of 1 must be the result of couplings of at least two Mn.

Figure 4. A possible model for the Mn complex in the WOC based on EXAFS data. The EXAFS data indicate that there are at least 2 Mn atoms which are separated by 2.7 Å, and there is a short Mn-(C or N or O) bond of 1.78 Å (μ-oxo-bridged Mn). A long Mn-Mn separation of 3.3 Å has been also observed. Comparisons with model compounds suggest that the cluster contains bridging oxide or hydroxide and carboxylates connecting the 3.3 Å Mn pair (George et al., 1989).

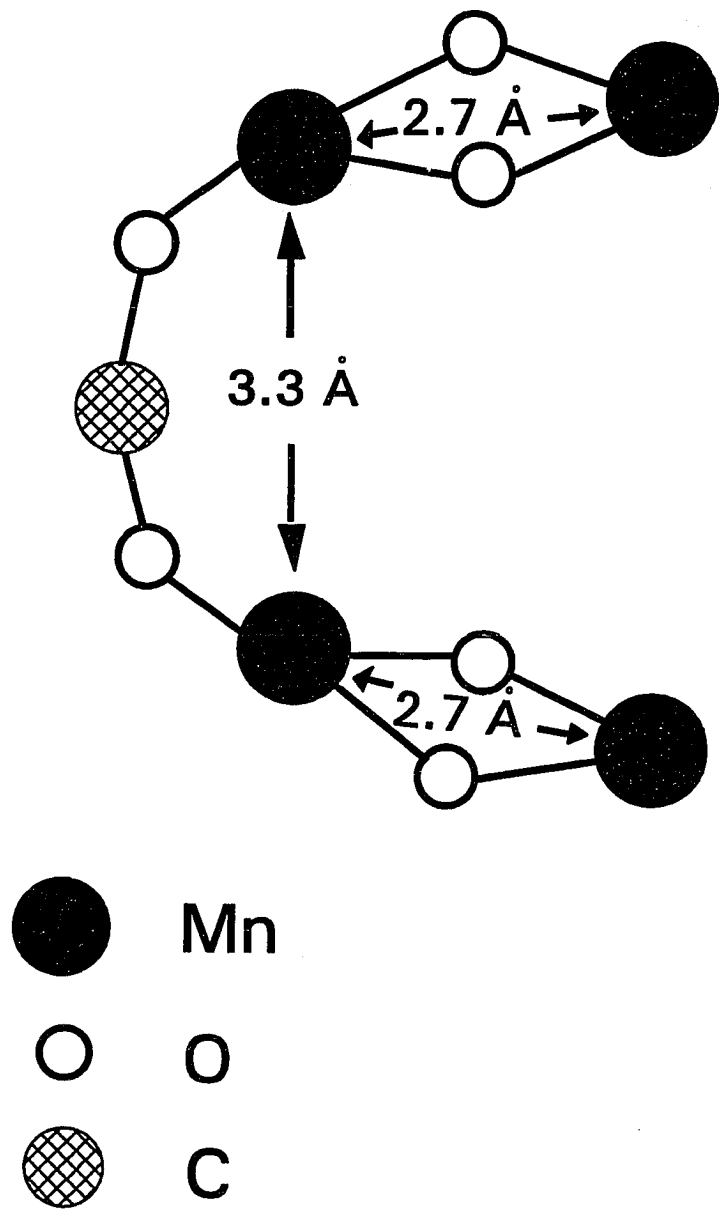

I-2-2 S_2 state

The first information on the redox state of the functional Mn became available with the discovery of a low-temperature g = 2 multiline EPR signal (Dismukes and Siderer, 1981), which characterizes S_2 (Brudvig et al., 1983). EPR expects signals from half-integer spins, and at least 2 out of the 5 states are expected to have EPR signals. The fact that the S_2 state of the Mn complex displays S = 1/2 type EPR signals suggests that the S_0 state and S_4 states, which differ from S_2 by two electrons, might do so too. Unfortunately, no signals from either of these states have been observed yet.

Two types of the S_2 state EPR signals at g = 1.98 and g = 4.1 have been observed (figure 5). The amplitude of both signals was shown to oscillate with the number of illuminating flashes with a period of 4 (Zimmermann and Rutherford, 1986). The S_2 state multiline signal can be captured by cooling a sample of PSII membranes to 77 K after illumination in the presence of DCMU at 273 K or by illumination at 200 K. DCMU blocks electron flow beyond Q_A and thus allows only one turnover of PSII. The multiline signal covers a span of 150 mT and consists of 16-20 lines that are approximately evenly spaced and have numerous small peaks and shoulders (a = 75 - 90 G) (Hansson et al., 1986). Illumination between 120 K and 160 K results in decreasing yields of the S_2 state multiline signal with decreasing illumination temperature, and compensating increases in production of the S_2 state g = 4.1 signal (about 1000 G, featureless), the other signal of the S_2

Figure 5. S_2 state EPR signal of PSII. The spectrum obtained as described in II-9, shows both the multiline signal at g = 1.98 and the (unresolved) g = 4.1 signal. Instrumental conditions: microwave frequency = 9.46 GHz, microwave power = 0.80 mW, modulation frequency = 100 kHz, modulation amplitude = 20 G, and temperature = 6.5 K.

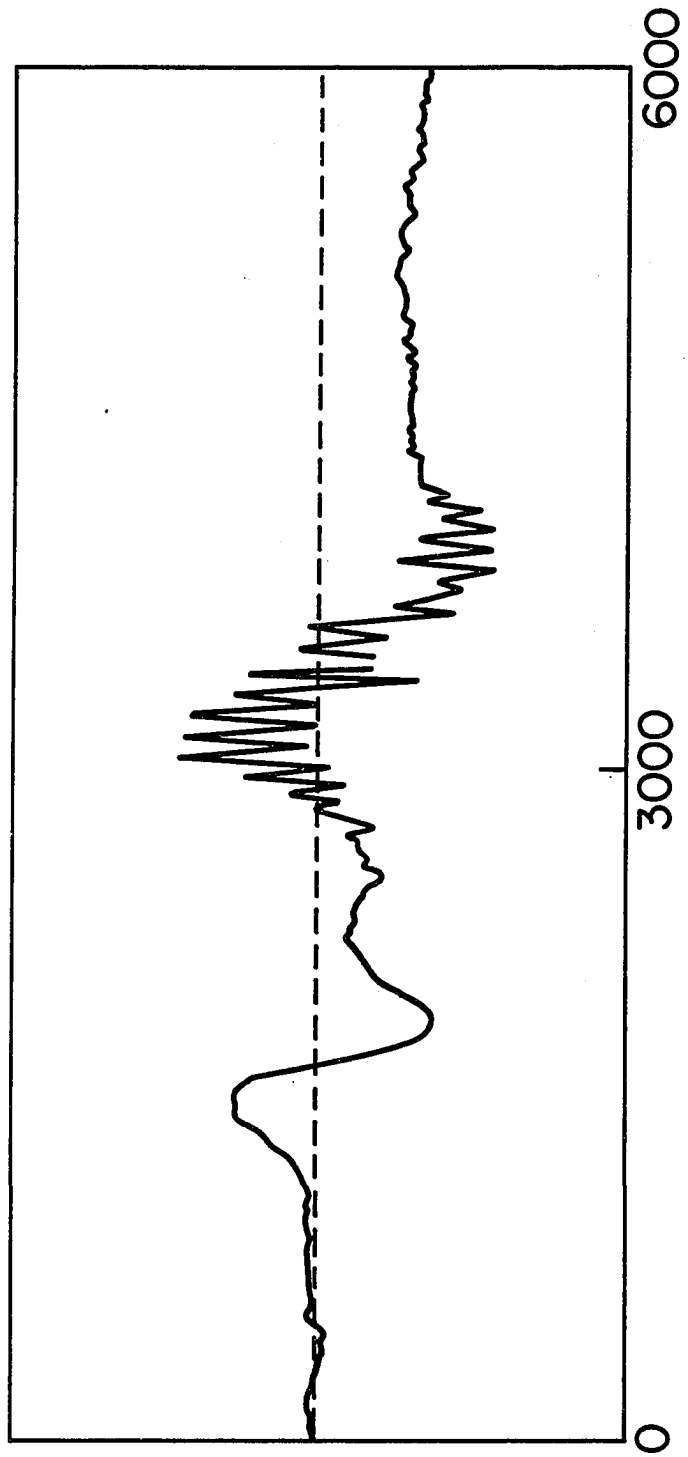

state. Kim et al. (1990) showed evidence of a multinuclear Mn origin for the S_2 g = 4.1 signal. The g = 4.1 EPR signal obtained from oriented PSII membranes under conditions of ammonia inhibition of oxygen evolution shows at least 16 Mn hyperfine lines with a regular spacing of approximately 36 G.

EPR studies of the temperature dependence of power saturation suggest that the multiline center is an antiferromagnetically coupled Mn dimer (Mn^{3+} (S = 2)-Mn^{4+} (S = 3/2) of maximum spin = 7/2). The spin coupling problem of the Mn tetramer can be simplified by assuming that two out of four Mn are in the same oxidation state (either (+3, +3) or (+4, +4)) and couple to a net spins of zero. The remaining two Mn with spins S = 2 and S = 3/2 then couple to net spins of 1/2, 3/2, 5/2, 7/2. One possibility is to assign the multiline and 4.1 signals to the ground (S = 1/2) and first excited (S = 3/2) states of S = 7/2 multiplet (Pace et al., 1991).

Goodin et al. (1984) showed a shift to higher energy (1.2 eV) in the X-ray absorption K-ed8ge energy of Mn upon advancement from the S_1 state to the S_2 state. This shift suggests a metal centered oxidation from Mn^{3+} - Mn^{3+} -> Mn^{3+} - Mn^{4+}.

ESEEM experiments were performed on the S_2 multiline EPR signal. The Fourier transform of the light-minus-dark time domain ESEEM data shows a peak at 5.8 MHz in ^{14}N samples which is absent upon substitution with ^{15}N. The ESEEM due to ^{14}N may be from an amino acid ligand, such as a histidine. The first suggestion of a histidine-Mn cluster as a model for the oxygen evolving complex was made by Padhye et al. (1986).

I-2-3 S_3 state

Conversion of S_2 to the S_3 state does not change the EXAFS, suggesting no change in the redox state of Mn during this photoinduced transition (Guiles et al., 1990). Thus, the possibility that the positive charge is located on an intermediate other than Mn. The idea that a redox active ligand, other than Mn, may function in the oxygen evolution complex was first suggested by Kambara and Govindjee (1985).

A modified multiline EPR signal was obtained upon calcium depletion of PSII membranes in the dark. Illumination of Ca depleted PSII at 0°C generates a new intermediate in the water oxidizing reaction from a site which is conformationally coupled to the Mn cluster (Boussac et al., 1989, 1990; Sivaraja et al., 1989). It gives rise to an EPR spectrum identified as modified S_3 state signal (symmetric lineshpe with width 165 G, g = 2.0; figure 6). Boussac et al. (1989) observed the modified S_3 EPR signal in Ca-depleted PSII membranes, and a similar intermediate was observed if $2Cl^-$ was replaced by F^- (Baumgarten et al., 1990). This signal has been attributed to a free radical (possibly an oxidized histidine in magnetic contact with the Mn) based on its g-value ≈2 in combination with its extremely large linewidth at the low temperature or high microwave powers required to saturate it (Boussac et al., 1990). However, it remains to be proven whether S_3 in normal PSII has anything to do with histidine.

Figure 6. EPR signal of calcium depleted PSII membranes in the modified S_3 state. The calcium depleted PSII membranes were prepared by removing calcium along with the 17 and 23 kD extrinsic proteins from the PSII membranes and reconstituting the 17 and 23 kD proteins. The calcium depleted PSII membranes were illuminated at 0°C. Instrumental conditions are as figure 5.

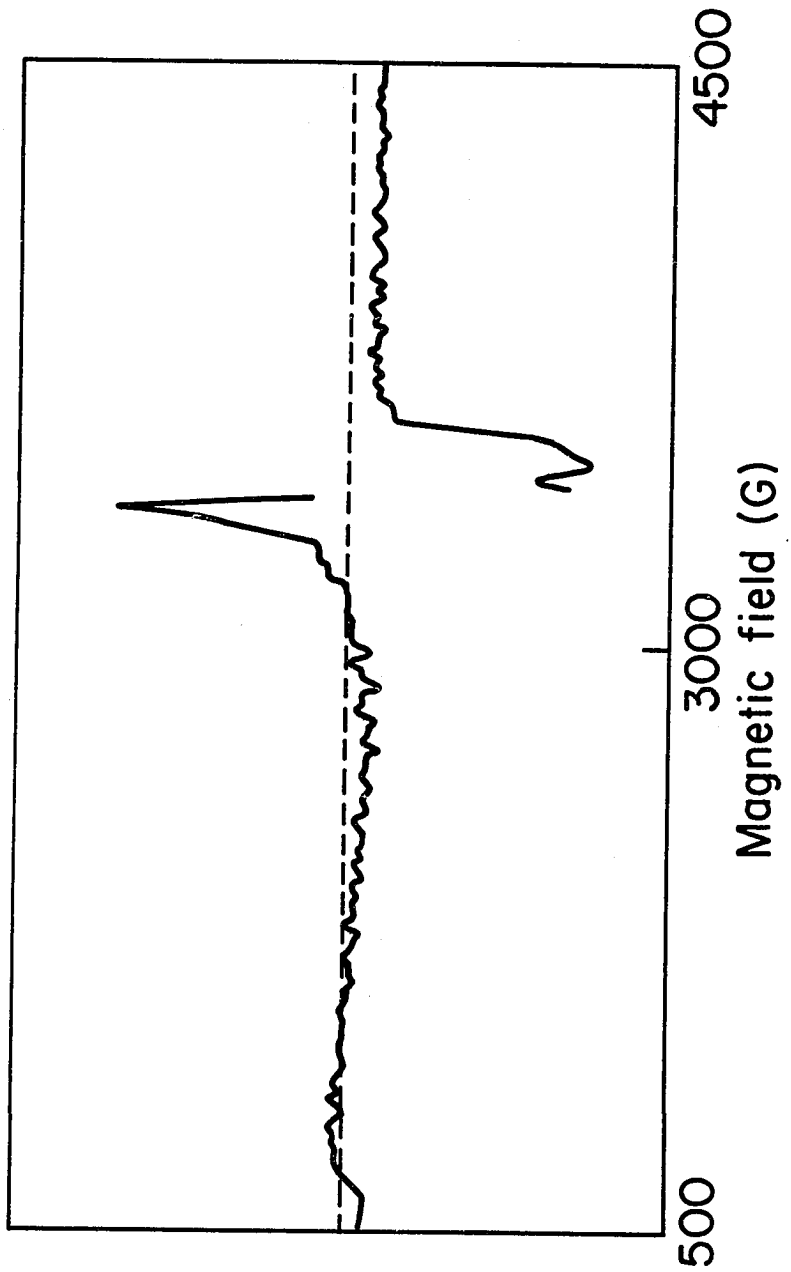

I-2-4 Extrinsic polypeptides

The oxygen evolution by PSII of plants involves a cluster of 4 Mn atoms linked to the reaction center complex and three extrinsic polypeptides with molecular masses of 17, 23, and 33 kD as shown in figure 3. Some of the functions of the extrinsic polypeptides have been determined by studying the effects of their selective removal and rebinding in purified PSII.

The 17 and 23 kD proteins can be released in the PSII membranes with 1.0 M NaCl (Miyao and Murata, 1983), and the 33 kD protein with 1.0 M $CaCl_2$ (Ono and Inoue, 1983a, b) or 2.6 M urea (Miyao and Murata, 1984). The reconstitution with the extrinsic proteins is sequential; the rebinding occurs in the order of 33 kD, then 23 kD and finally the 17 kD protein (Miyao and Murata, 1987).

The functions of these proteins, which have so far been elucidated, are as follows: The 33 kD protein (i) stabilizes the Mn cluster (Miyao and Murata, 1984; Kuwabara et al., 1985), (ii) accelerates the S state transition from S_3 to S_0 (Miyao et al., 1987a, b), (iii) reduces the chloride requirement from 200 mM to 30 mM (Miyao and Murata, 1985) and (iv) provides a binding site for the 23 kD protein (Murata et al., 1983). The 23 kD protein (i) stabilizes the calcium site (Murata and Miyao, 1985; Kuwabara et al., 1985; Murata et al., 1983), (ii) reduces the chloride requirement from 30 mM to 10 mM (Miyao and Murata, 1985), and (iii) provides the binding site for the 17 kD protein (Miyao and Murata, 1983). The 17 kD protein sustains oxygen-evolution activity at chloride concentrations below 10 mM (Akabori et al., 1984; Miyao

and Murata, 1985). The cyanobacteria, which have an oxygen evolving PSII, are devoid of the 17 and 23 kD extrinsic proteins (Stewart et al., 1985; Vermaas et al., 1988). Apparently, the smaller extrinsic proteins are not required for oxygen evolution and rather provide structural and/or regulatory benefits for higher plants. Furthermore, recent studies on a genetically engineered Synechocystis sp. PCC 6803 mutant lacking the 33 kD polypeptide suggest that in cyanobacteria even this protein may not be required for oxygen evolution (Burnap and Sherman, 1990).

I-2-5 Calcium

The modified multiline EPR signal obtained upon calcium depletion of PSII membranes (dark adapted) is shown in figure 7. The increased number of hyperfine lines and narrower Mn hyperfine splittings compared to the normal S_2 state multiline signal indicate a redistribution of spin density within the Mn cluster. The same type of modified multiline signal can be obtained by Sr^{2+} replacement of Ca^{2+}. Calcium depletion facilitates access of NH_2OH to the OEC and of diphenylcarbazide to Z^+. Diphenylcarbazide is an efficient electron donor to Z^+ in PSII membranes in which Mn is removed or dislocated. These observations suggest a possible "gatekeeper" role for calcium in limiting access of substrate water to the Mn cluster (Tso et al., 1991). For a review on the role of calcium in the oxygen evolving complex, see Ghanotakis and Yocum (1990).

Figure 7. Modified S_2 state multiline EPR signal from PSII membranes that are depleted of calcium (see legend of figure 6) without illumination. The increased number of hyperfine lines and narrower Mn hyperfine splittings compared to the normal S_2 state multiline signal indicate a redistribution of spin density within the Mn cluster. Instrumental conditions are same as figure 5.

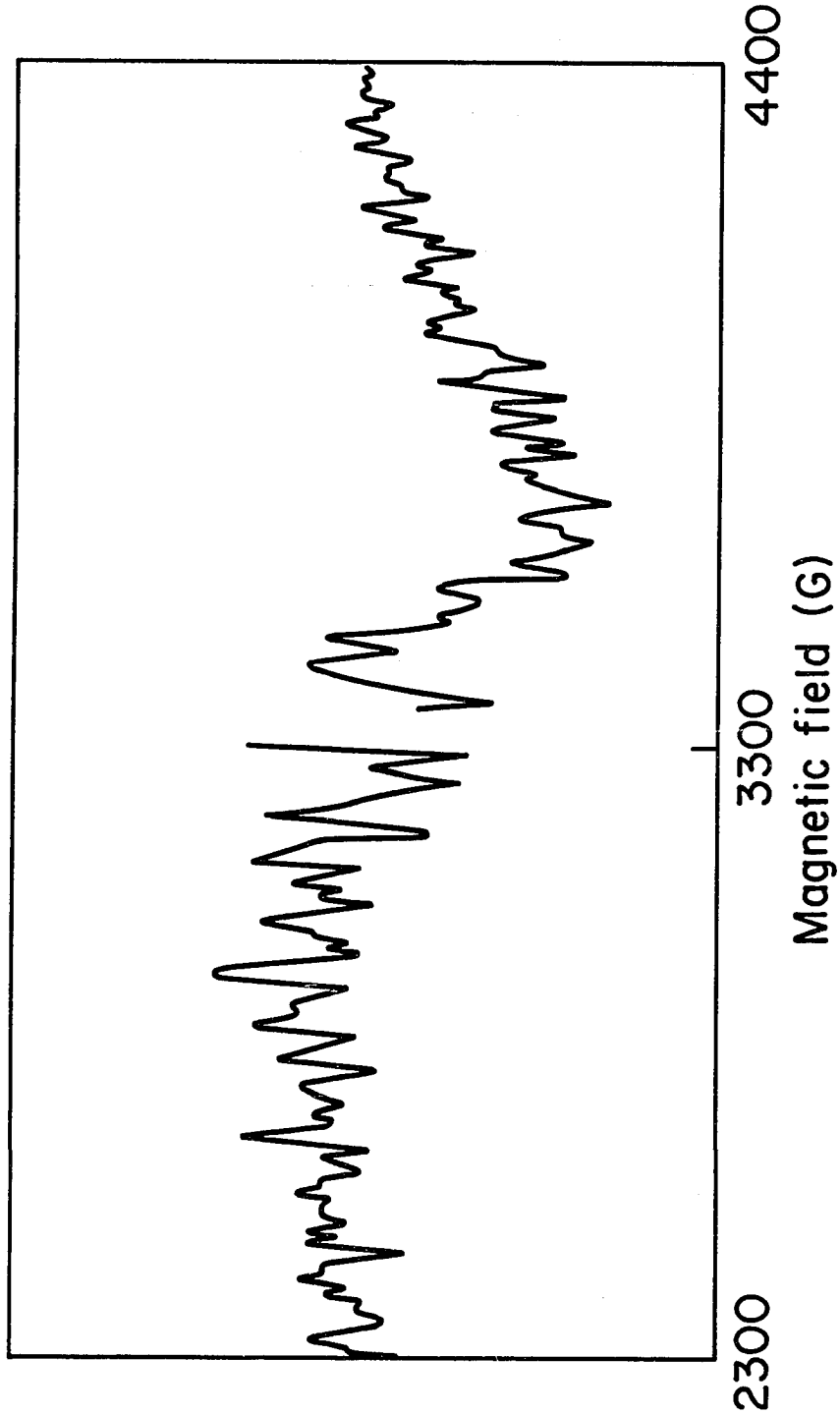

I-2-6 Chloride

The function of Cl^- in the process of photosynthetic water oxidation is still poorly understood. Cl is a well-established cofactor of oxygen evolution. Significantly higher Cl concentrations are required for maximal activity in PSII depleted of the extrinsic polypeptides.

The two possible roles of Cl^- in the WOC are as follows;

(1) Cl^- activates O_2 evolving activity by acting as charge-neutralizing counterions in the environment of the active site of the oxygen evolving reaction (Coleman and Govindjee, 1987; Homann, 1988).

(2) Cl^- possibly binds to Mn, acting to facilitate electron transfer among the Mn atoms (Sandusky and Yocum, 1984), or the anion, occupies a site close to, but not on Mn (Brudvig et al., 1989).

The possibility of a direct binding of Cl^- to the Mn complexes has been investigated by EXAFS and EPR. Yachandra et al. (1986) failed to observe evidence of Cl^- in the first coordination sphere of the Mn complex with EXAFS. Haddy et al. (1989) reported that Br^- substitution for Cl^- did not change the superhyperfine structure of the multiline EPR signal.

I-2-7 Z and D

Debus et al. (1988a) and Vermaas et al. (1988) showed that the slow electron donor, D, is Tyr-160 in the protein D-2, and Debus et al. (1988b) and Metz et al. (1989) showed the fast electron donor,

Z, is Tyr 161 in the protein D-1 in the cyanobacterium *Synechocystis sp.* PCC 6803.

Hoganson and Babcock (1989) estimated the center-to center distance between $P680^+$ and Z^+ as 10-15 Å by the line broadening of the P_{680}^+ EPR spectrum in the presence of Z^+.

From measurements of the EPR signal of D^+ Styring and Rutherford (1987) showed that, after three flashes, D^+ decays slowly in the dark at room temperature in the fraction of centers that were in the S_0 state ($t_{½}$ of 50 min in PSII membranes). This reaction, which is the only known function of D, is accompanied by 2a conversion of S_0 to S_1. The concentration of S_1 was estimated from the amplitude of the S_2 state multiline EPR signal that could be generated by illumination at 200 K (Styring and Rutherford, 1988). These observations indicate that D^+ accepts an electron from S_0 in a dark reaction in which D and S_1 are formed.

I-2-8 Cytochrome b-559

Although the role of Cyt b-559 in the OEC is not known, its EPR signal is an important indicator of whether the electron transfer pathway is intact or not. Cyt b-559 has two different forms characterized by reduction midpoint potential, low-, and high-potential Cyt b-559. Low-potential Cyt b-559 is normally oxidized (reduction potential of ≈ 0 mV) and depletion of the 17 and 23 kD extrinsic polypeptides results in loss of high-potential Cyt b-559 (g_z = 3.1, g_y = 2.2, g_x = 1.5) and appearance of low potential Cyt b-559 (g_z = 2.9, g_y = 2.1, g_x = 1.5) (Miller and Brudvig, 1991).

Cyt b-559 is an alternative electron donor to P680 when PSII is illuminated at 77 K, a temperature that is too low for S state transitions. Thompson and Brudvig (1988) investigated the pathway of oxidation of Cyt b-559 in PSII by EPR and showed that it proceeds via oxidation of a Chl molecule. They proposed that this photooxidation of chlorophyll is the first step in photoinhibition of PSII. The unique susceptibility of PSII to photoinhibition is probably due to the very high redox potential of P680. Therefore, it was proposed that the function of Cyt b-559 is to reduce photooxidized chlorophyll and protect PSII from photoinhibition.

I-2-9 NH_2OH effect

The analysis of the mechanism of water oxidation has been approached by the use of substrate analogues such as NH_2OH, N_2H_2 and H_2O_2, which act as redox-active inhibitors of water oxidation (Bennoun and Joliot, 1969; Cheniae and Martin, 1971; Velthuys and Kok, 1978). Radmer and Cheniae (1977) reported that NH_2OH binds to manganese within the active site of the complex. NH_2OH releases between two and four Mn(II) ions per PSII (Cheniae and Martin, 21971; Yocum et al., 1981) and, at comparable concentrations, extrinsic proteins (Tamura and Cheniae, 1985). NH_2OH is at least partially consumed to form N_2 in the light (Radmer, 1983).

Preincubation with low (micromolar) concentrations of NH_2OH in the S_1 state results in the retardation of the flash-induced yield of O_2 by two steps (Bouges, 1971; Velthuys and Kok, 1978). In

addition to its reaction with the OEC, NH_2OH at millimolar concentrations also interrupts electron transfer to the reaction center between Z and P_{680} (Den Haan et al., 1976). The reactivity of spinach thylakoid membranes with NH_2OH in the dark and in the light has been reported to differ (Guiles et al., 1986; Andreasson et al., 1986; Sivaraja and Dismukes, 1988). Conflicting results claiming a faster release of Mn and a larger yield under illumination (Cheniae and Martin, 1971; Horton and Croze, 1977) or in the dark (Sharp and Yocum, 1981) have appeared.

In addition to its well-known binding on the donor side of PSII, hydroxylamine binds in the dark to a second high affinity site (K_D < 10 μM; < 7 NH_2OH/ PSII) that structurally interacts with the primary electron acceptor FeQ_A^- (the first high affinity site is the Mn site which results in two-electron reduction) (Sivaraja and Dismukes, 1988). Binding in the dark to this acceptor site causes conversion of the normal g = 1.9 EPR signal for FeQ_A^- to g = 2.1 on the first turnover.

There is no evidence yet reported for the release of protons or N_2 in the dark reaction of PSII with NH_2OH, while a single flash generates both protons (Forster and Junge, 1986a; Forster and Junge, 1986b) and N_2 (Radmer, 1983; Radmer and Ollinger, 1983) in NH_2OH treated samples. Also, evidence favoring S_2 as the target for the two electron reduction instead of S_1 has come from Mn x-ray absorption edge experiments. These studies show that binding of NH_2OH causes no change in the edge energy when binding occurs in the dark S_1 state, while a decrease by 1.2 - 1.3 eV occurs only

after illumination to form what would normally be the S_2 sate. By contrast, the S_2 state in untreated PSII samples exhibits an increase in edge energy by 1.1 - 1.2 eV. This decrease by 2.4 eV in the S_2 state edge energy in the presence of NH_2OH was attributed to the reduction of the Mn cluster by 2 equivalents (Guiles et al., 1986). Inhibition at this site is reversed by illumination, which consumes the NH_2OH. Therefore the cumulative evidence favors the following reaction (Sivaraja and Dismukes, 1988).

$$(S_2)WOC \cdot Mn_2^{III,IV} + 2NH_2OH \rightarrow (S_0)WOC \cdot Mn_2^{II,III} + N_2 + 2H_2O + 2H^+$$

Since NH_2OH is capable of further reduction of S_0, the reaction may continue as follows;

$$S_0 + xNH_2OH \rightarrow 3Mn^{2+} \text{ (free)} + Mn \text{ (bound)}.$$

I-3. Purpose and scope of the present thesis

The requirement for 4 Mn/PSII for optimal activity does not necessarily imply that all four are directly involved in water oxidation. There have been a lot of reports claiming that not all of the Mn are essential for active oxygen evolution (see reviews by Dismukes (1986) and Sauer et al. (1991)). The mechanism of photosynthetic water oxidation and, particularly, the role of Mn in it, has been probed in this thesis by the use of the substrate analogue NH_2OH, which acts as redox-active inhibitor of water

oxidation. NH_2OH at a concentration of 10 - 500 μM is known to cause irreversible inhibition in the dark due to the release of Mn and proteins from the PSII membranes.

Chapter III deals with the effect of NH_2OH effect on PSII in terms of Mn release and oxygen evolution. Earlier studies of this effect did not take account of the simultaneous release of extrinsic polypeptides, although the latter are known to affect the Cl^- and Ca^{2+} requirements for optimum activity of the PSII. To simplify the interpretation of the results I chose to work on PSII that are already devoid of the 17 and 23 kD extrinsic proteins. Preliminary studies had shown that treatment of PSII membranes with 81 M NaCl released the two smaller extrinsic polypeptides but left the oxygen evolution intact. This simpler system was therefore chosen to investigate the effect of NH_2OH on Mn release and oxygen evolution. The results turned out to be interpretable in terms of a cooperativity model.

During the process of selecting the simplest fully functional system for investigating the effect of NH_2OH, it was observed that 1 M $CaCl_2$ treated PSII membranes, which lack all 3 extrinsic polypeptides, behave quite differently from NaCl treated samples, which still have the 33 kD polypeptides. In chapter IV, I have studied these differences using NH_2OH treatment, varying light intensity, Chl a fluorescence, and EPR spectroscopy.

Finally in chapter V, I have reexamined in more detail the conditions for photoactivation of the oxygen evolving system of the Mn-depleted system by Mn readdition. Furthermore, I have studied

whether any other metal ions will replace Mn in the Mn binding sites and thus inhibit oxygen evolution. In view of the well-known damaging effect of strong light, it was inevitable to study the effect of photoinhibition to understand the limit of photoactivation.

The major conclusions obtained in this thesis are: (1) 3 (or possibly 4) NH_2OH molecules interact cooperatively with the WOC; (2) PSII samples lacking all 3 extrinsic polypeptides not only have the full complement of four Mn per RC but also evolve the same number of O_2 molecules per photon as PSII samples lacking the 17 8and 23 kD proteins only if the light intensity and therefore the electron transfer rates are sufficiently low; (3) Co^{2+} and Fe^{2+} can not reconstitute the oxygen evolving activity in Mn depleted PSII, but they compete for the Mn binding sites and interfere with Mn reconstitution.

Chaper II: MATERIALS AND METHODS

II-1. Isolation of PSII membranes from spinach

PSII membranes from spinach chloroplasts were prepared according to the method of Berthold et al. (1981) with slight modifications.

Fresh spinach was bought from market and kept in the dark coldroom (4°C) before use. Medium size spinach leaves were washed and deveined. 600 g spinach leaves were ground in 3 l of 0.35 M sucrose, 20 mM Hepes (pH 7.5), 2 mM EDTA, 2 mM $MgCl_2$, and 1 g/l BSA and ground in a conventional grinder for 20-30 s at full speed. After grinding, the homogenate was filtered and squeezed through 4 layers of cheesecloth and then centrifuged for 5 min at 3000 x g. The resulting pellet was resuspended in the same buffer (1.5 l, i.e., half volume) and homogenized twice with a tissue grinder and then centrifuged for 20 s at 1200 x g; the supernatant was centrifuged for 5 min at 4000 x g. The resulting pellet was resuspended in 1.5 l of buffer which contained 20 mM MES (pH 6.5), 5 mM $MgCl_2$, 2 mM EDTA, 1 g/l BSA and centrifuged for 7 min at 4900 x g. The pellet was resuspended in the same buffer at a chlorophyll concentration of 2.67 mg Chl/ml, and 20 % Triton buffer (20 % w/v Triton X-100 in buffer A) was added dropwise (final concentration of Triton X-100 was 25 mg/mg Chl at a Chl concentration of 2 mg Chl/ml) while the suspension was placed on ice in the coldroom (4°C), stirring at low speed. After the suspension had been stirred

for 30 min from the beginning of Triton buffer addition, it was centrifuged for 20 min at 40,000 x g and then washed twice with 2 mM EDTA in buffer A by centrifugation for 20 min at 40,000 x g. The resulting pellet was washed once with buffer B and resuspended in the same buffer. The final samples were frozen quickly and stored in a -80 °C freezer.

List of buffers

Buffer A: 15 mM NaCl, 5 mM $MgCl_2$, and 20 mM MES (pH 6.5)

Buffer B: 0.4 M sucrose, 15 mM NaCl, 5 mM $MgCl_2$, and 20 mM MES (pH 6.5)

Buffer C: 0.4 M sucrose, 15 mM NaCl, 15 mM $CaCl_2$, and 20 mM MES (pH 6.5)

Buffer D: 0.4 M sucrose, 200 mM NaCl, 15 mM $CaCl_2$, and 20 mM MES (pH 6.5)

Buffer E: 0.8 M sucrose, 110 mM NaCl, 15 mM $CaCl_2$, and 20 mM MES (pH 6.5)

Buffer F: 0.4 M sucrose, 15 mM NaCl, and 20 mM MES (pH 6.5)

II-2. Removal of two extrinsic polypeptides.

The two extrinsic polypeptides of 17 and 23 kD can be removed 2by 1 M NaCl wash (Åkerlund et al., 1982; Miyao and Murata, 1983; Ghanotakis et al., 1984). PSII membranes were thawed and resuspended in buffer B at 1.5 mg Chl/ml and mixed with 1/3 volume of medium containing 4 M NaCl in buffer B, to a final concentration of 1 M NaCl at 1 mg Chl/ml. After treatment for 1 hour in the coldroom (4°C) with stirring at low speed, the samples were

centrifuged for 20 min at 40,000 x g. The resulting pellet was washed twice with buffer C (buffer C contains 15 mM $CaCl_2$) and resuspended in the same medium.

II-3. Removal of three extrinsic polypeptides

The three extrinsic polypeptides of 17, 23, and 33 kD can be removed by 1 M $CaCl_2$ wash (Ono and Inoue, 1983a). PSII membranes were thawed and resuspended in buffer B at 3 mg Chl/ml and mixed with the same volume of a medium containing 2 M $CaCl_2$ in buffer B to a final concentration of 1 M $CaCl_2$ at 1.5 mg Chl/ml. After treatment for 1 hour in the coldroom (4°C), stirring at low speed, the samples were centrifuged for 20 min at 40,000 x g. The resulting pellet was washed twice with buffer D (buffer D contains 200 mM NaCl and 15 mM $CaCl_2$) and resuspended in the same buffer.

II-4. NH_2OH treatment

For treatment with NH_2OH, the 1 M NaCl treated PSII membranes (from II-2) were resuspended to a chlorophyll concentration of 1.6 - 2 mg Chl/ml (pH 6.5). The membranes were dark-adapted prior to incubation with NH_2OH in order to favor a higher population of the S_1 state. NH_2OH was then added in the dark to the desired concentration, the suspension was agitated by a Vortex shaker, and kept inside the centrifuge for 30 min at 4°C. The supernatant was analyzed for Mn as described in section II-8 and the pellet was

washed with NH_2OH free-medium (buffer C) before resuspending in the same buffer.

II-5. Photoactivation

Prior to photoactivation, Mn was extracted by NH_2OH treatment. NH_2OH treatment of PSII membranes for photoactivation was done as described in section II-4, with the following additions: (1) four repetitive washings were done to ensure removal of NH_2OH; and (2) the extracted/ washed membranes (≥ 2mg Chl/ml) were resuspended in buffer E before use or storage at -80°C (Blubaugh and Cheniae, 1990). 0.8 M sucrose in buffer E helps to achieve better photoactivation than 0.4 M sucrose. NH_2OH treated membranes were centrifuged and the pellet was resuspended in 0.8 M sucrose, 110 mM NaCl, 1 mM $MnCl_2$, 20 mM MES (pH 6.5), and 20 mM $CaCl_2$ to 250 μg Chl/ml. The sample was transferred to a transparent beaker (sample thickness 2 mm, 2.5 ml volume in 100 ml beaker at a time) and was allowed to equilibrate at room temperature in the dark for 5 min. DCIP was added in the desired concentration, the sample was covered with clear plastic wrap, shaken gently for 5 more minutes and then illuminated from the top for a given time under fluorescent white light of adjustable brightness for various durations. Samples were kept completely dark all the time except for the illumination.

II-6. Chl a fluorescence

All samples for Chl a fluorescence were diluted to 10 μg Chl/ml. The 77 K fluorescence spectra and fluorescence transient measurements were made using a laboratory-built spectrofluorometer (Blubaugh, 1987). The exciting light was provided by a Kodak 4200 projector with two Corning blue glass filters (CS4-76 and CS5-57). Fluorescence emission was detected by a S-20 EMI9558B photomultiplier through a Bausch and Lomb monochromator with 1 mm slit widths (bandpass: 3.3 nm). The photomultiplier was protected from the exciting light by a red Corning filter (CS2-61). Signals were stored and analyzed by a Biomation 805 waveform recorder and a LSI-11 computer.

Chl a fluorescence decay kinetics after single flashes of light were measured on an instrument described by Robinson et al. (1983) and Eaton-Rye (1987). The samples were diluted to 5 μg Chl/ml and transferred to a dark reaction vessel (100 ml) and dark-adapted at room temperature for 10 minutes. A flow cuvette was filled from the vessel by using optimized gas pressure. The illumination volume of the sample was 0.6 ml. At the end of each measurement, the sample in the cuvette was exchanged with that in the vessel by the pressure. Using a weak measuring flash, the level of Chl a fluorescence yield of the sample was measured at 685 nm (10 nm bandwidth) by a EMI 9558A photomultiplier tube. The measuring light was fired at variable times after each actinic flash. The actinic (FX-124, EG&G) and the measuring flashes

(Stroboslave 1539A, General Radio) were filtered with Corning CS4-96 filters; both had a 2.5 μs duration at half-maximal peak (Eaton-Rye and Govindjee, 1988).

Q_A^- concentration was calculated from the variable Chl a fluorescence according to Joliot and Joliot (1964) using the formula given in Mathis and Paillotin (1981); there is a hyperbolic relationship between the fluorescence yield F(t) and the fraction q(t) of closed reaction centers (i.e., q = 1 when $[Q_A^-]$ is maximum) at time t:

$$\frac{F(t) - F_o}{F_{max} - F_o} = \frac{(1 - p)q(t)}{1 - pq(t)}$$

where F_{max} is the maximum fluorescence yield when all Q_A is in the reduced state, F_o is the minimum fluorescence yield when all Q_A is in the oxidized state, and p is the connection parameter which reflects the probability of intersystem energy transfer from a closed unit to any other unit in the system. In this work, p is assumed to be 0.5, as measured earlier for chloroplasts (Forbush and Kok, 1968). Thus, q(t) can be represented by the following formula:

$$q(t) = \frac{2F_v(t)}{F_v^{max} + F_v(t)}$$

where $F_v(t) = F(t) - F_o$ and $F_v^{max} = F_{max} - F_o$.

II-7. Gel electrophoresis

SDS-polyacrylamide gel electrophoresis was performed according to the method of Laemmli (1970). Better results were obtained with a slightly modified procedure. Mostly, 13.5 % SDS-PAGE with 4 M urea was run at a constant voltage of 120 V with 25 μl samples (0.75 mg Chl/ml). The relative amounts of polypeptides were determined from the peak heights in the densitogram given by a densitometer.

II-8. EPR measurement

Low temperature EPR spectroscopy of the S_2 state was carried out on a Bruker ER-200D X-band EPR spectrometer equipped with an Oxford helium flow cryostat.

EPR samples were prepared as follows. The PSII membranes were resuspended in buffer B to 6-8 mg Chl/ml concentration and kept at 0 °C in the dark for 1 hour. The "light" samples were illuminated inside the EPR cavity for temperatures up to 200 K; higher temperature illumination was done in a CO_2-ethanol bath (temperature was measured with a copper-constantan thermocouple). The light source was a 1000 W projector using a water filter and Corning red filter, CS 2-73.

Room temperature EPR spectra for the quantification of Mn^{2+} were taken with 0.3 ml Wilmad Suprasil flat cells in a TM110 cavity. Small aliquots of samples (390 μl at 2 mg Chl/ml) were

mixed well with 10 μl of 10 N HCl (0.25 M) and heated to 70°C for 1 min. After cooling back to room temperature, they were transferred into the flat cells. EPR measurements were carried out with a Bruker ER200D X-band EPR spectrometer. Spectra were taken at 9.70 GHz with 20 mW power and 100 kHz field modulation of 16 G amplitude. The peak-to-peak amplitude of all six Mn hyperfine lines was measured and compared with the amplitude of a standard Mn^{2+} solution. According to Yocum et al. (1981), this method allows a quantitative determination of all Mn in a sample.

II-9. Determination of Chl concentration

15 μl of sample was mixed with 5 ml of 80 % (v/v) aceton and the absorbance was measured at 646.6 nm and 663.6 nm. The Chl concentration was determined according to the following (Porra et al., 1989):

$$[\text{Chl}]\ (\mu\text{g Chl/ml}) = (17.76\ A_{646.6} + 7.34\ A_{663.6}) \times \text{diluting factor}\ (5015/15)$$

The concentration of reaction center can be calculated from [Chl] as follows:

$$[\text{Reaction Center}]\ (\text{M}) = \frac{[\text{Chl}]\ (\text{g/l})}{900 \times 250}$$

where the molecular weight of Chl is 900 and one reaction center contains 250 Chl (Miller and Brudvig, 1991).

II-10. Oxygen evolving activity

The oxygen evolution activity was assayed on a Yellow Spring Model 53 monitor equipped with a Teflon-membrane covered Clark-type oxygen electrode in the presence of 200 μM PPBQ as electron acceptor at 10 μg Chl/ml. The exciting light of intensity 1200 $\mu E \cdot m^{-2} \cdot s^{-1}$ was provided by a Kodak 4200 projector lamp filtered through 1 inch of 5 % $CuSO_4$ solution and a Corning yellow glass, CS2-71.

II-11. DCIP reduction

The assay medium for DCIP photoreduction contained 50 μM DCIP and 10 μg Chl/ml sample in the final resuspending medium of each preparation. The exciting light (1200 $\mu E \cdot m^{-2} \cdot s^{-1}$) was provided by a Kodak 4200 projector lamp filtered through 1 inch of 5 % $CuSO_4$ solution and a Corning yellow glass, CS2-71. The rates were determined by following the disappearance of absorbance at 600 nm, essentially as described (Tamura and Cheniae, 1985).

II-12. Plasma emission

The metal concentrations of the samples were measured using inductively coupled argon plasma spectrometry (ICP). This is an atomic emission technique. The liquid sample is peristaltically pumped through a fixed cross-flow nebulizer. The sample enters a

quartz torch where it is delivered through the middle of an argon plasma, about 8000 °C. The intense heat of the plasma provides the energy for the sample atoms to emit light at their characteristic wavelengths. There is a separate slit and detector for each element so that there is simultaneous detection of emission intensities of the measured elements for each sample.

The emission intensities are proportional to the elemental concentrations. Known standards are measured to provide standard curves that are used to calculate individual unknown concentrations. The instrument in use at the Illinois State Water Survey is a Thermo Jarrell-Ash MARK III Model 1100 vacuum direct reader.

Chapter III: NH_2OH EFFECT

Much insight into the mechanism of O_2 evolution from the water oxidation complex (WOC) of photosynthetic membranes has come from studies of inhibitors which are substrate analogues such as NH_2OH (see section I-2-9). Messinger et al. (1991) reported that in dark-adapted samples with a highly populated S_1 state, NH_2OH leads via a two step sequence of one-electron reductions to the formal redox state S_{-1}. The oscillation patterns of oxygen yield of NH_2OH treated PSII are almost independent of $[S_0]/[S_1]$ of the initial S-states before addition of NH_2OH while those of NH_2NH_2 treated PSII are markedly different.

$$S_1 \xrightarrow{+NH_2OH} S_0 \xrightarrow{+NH_2OH} S_{-1}$$

$$S_1 \xrightarrow{+NH_2NH_2} S_{-1} \quad \text{and} \quad S_0 \xrightarrow{+NH_2NH_2} S_{-2}$$

NH_2OH at concentrations of 0.01 - 0.5 mM releases Mn (Cheniae and Martin, 1971; Sivaraja and Dismukes, 1988). In this chapter, the mechanism of NH_2OH inhibition of the WOC in the dark was investigated by comparing the steady-state O_2 rate and Mn release by NH_2OH from carefully selected preparations in which interference from polypeptide release was avoided.

III-1. Determination of standard preparation

III-1-1 Rationale

The mechanism of photosynthetic water oxidation has been studied by the use of NH_2OH, a substrate analogues which acts as redox-active inhibitor of water oxidation (see e.g., Bennoun and Joliot, 1969; Cheniae and Martin, 1971; Velthuys and Kok, 1978). There is much indirect evidence suggesting that NH_2OH binds to Mn within the WOC (Radmer and Cheniae, 1977; Babcock, 1987). Binding to a lower affinity site occurs in the presence of an excess of NH_2OH, causing irreversible inhibition in the dark due to the release of Mn (Cheniae and Martin, 1971; Yocum et al., 1981) and proteins from the WOC (Tamura and Cheniae, 1985). Since NH_2OH releases not only Mn from the oxygen evolving complex but also some of the extrinsic polypeptides, which influence, at the very least, the conditions for optimum activity, the question arises if the interaction of NH_2OH with the WOC can be studied in a simpler system that still shows normal oxygen evolution activity but avoids interference with the dissociation of extrinsic polypeptides. One obvious choice is to work with PSII devoid of some extrinsic polypeptides. The preliminary experiments discussed below show that PSII treated with 1 M NaCl to remove the 17 kD and 23 kD polypeptides is a suitable system which shows full activity in an appropriate buffer. This preparation, referred to as "NaCl PSII" was therefore adopted for all subsequent measurements of Mn release and oxygen evolution after treatment with NH_2OH. PSII treated with

1 M $CaCl_2$ to remove all extrinsic polypeptides, however, shows diminished oxygen evolution under standard assay conditions; this preparation was therefore rejected for the present study but will be discussed further in chapter IV.

III-1-2 Results

In order to monitor the presence or the absence of various extrinsic polypeptides, SDS-PAGE was run as described in section II-7 on PSII samples. Since the usual NH_2OH treatment is done with 0 to 0.5 mM concentration, we chose 0.3 mM to monitor its effect on the polypeptide release. Figure 8 shows a 13 % gel run with 4 M Urea. Lane 1 has the molecular weight standards, lane 2 is for control PSII membranes, lane 3 is for 0.3 mM NH_2OH treated PSII membranes, lane 4 is for 2 M NaCl treated PSII membranes, lane 5 is for the supernatant of the NH_2OH treated PSII membranes, and lane 6 is for the supernatant of the 2 M NaCl treated PSII membranes. It is obvious from figure 8 that 0.3 mM NH_2OH releases the 17 and 23 kD polypeptides, but not the 33 kD polypeptide. Therefore, to study the NH_2OH effect and to exclude the effect of partial depletion of 2extrinsic polypeptides, it is appropriate to use NaCl treated PSII membranes which are already depleted of the 17 and 23 kD polypeptides.

Figure 9 shows the polypeptide composition of PSII membranes treated with different concentrations of NaCl. Lane 1 and 2 are from pellets obtained after treatment with 1 M and 0.5 M NaCl, while lanes 3 and 4 are from the corresponding supernatants. While

Figure 8. SDS-PAGE patterns of spinach PSII samples. The 13 % gel was prepared according to II-7. Lanes: (1) molecular weight standards (66, 45, 29, and 14 kD); (2) control PSII membranes; (3) 0.3 mM NH_2OH treated PSII membranes; (4) 2 M NaCl treated PSII membranes; (5) supernatant of 0.3 mM NH_2OH treated PSII membranes; and (6) supernatant of 2 M NaCl treated PSII membranes. Sample volume, 25 μl. [Chl], 0.75 mg Chl/ml. Locations of 17 and 23 kD polypeptides are marked.

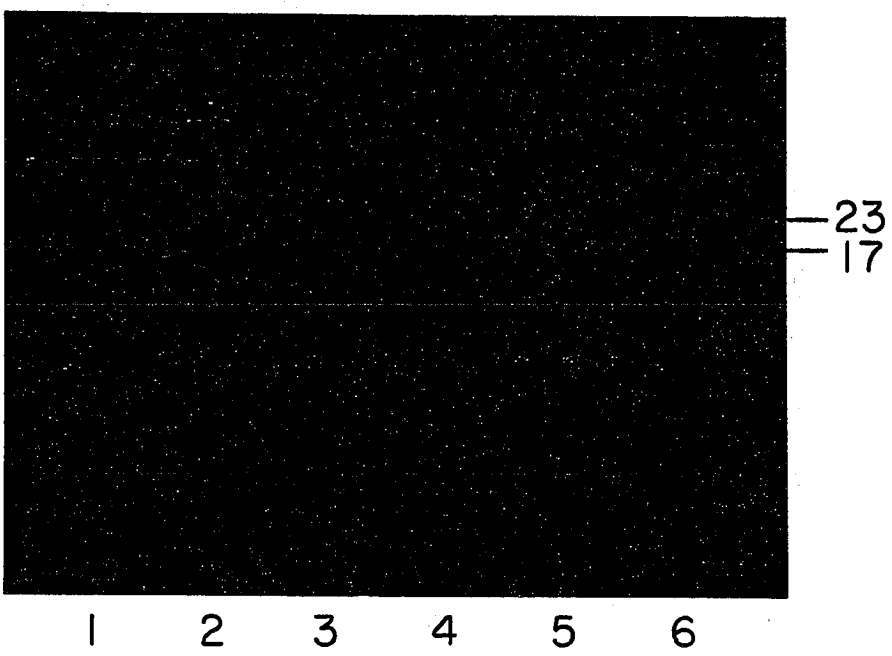

Figure 9. SDS-PAGE patterns of spinach PSII samples. The 13 % gel was prepared according to II-7. Lanes: (1) 1 M NaCl treated PSII membranes; (2) 0.5 M NaCl treated PSII membranes; (3) supernatant of 1 M NaCl treated PSII membranes; and (4) supernatant of 0.5 M NaCl treated PSII membranes. Sample volume, 25 μl. [Chl], 0.75 mg Chl/ml. Locations of 17 and 23 kD polypeptides are marked.

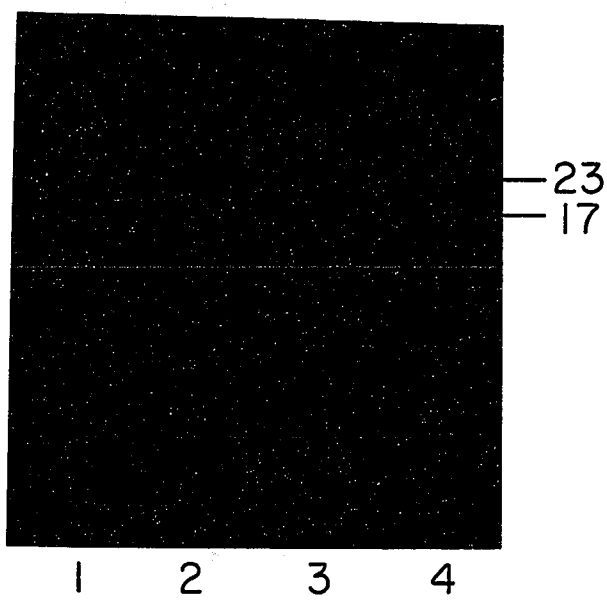

Table 1.

Mn content of spinach PSII membranes after NaCl treatments

	Without 15 mM $CaCl_2$ in the washing and resuspending medium	With 15 mM $CaCl_2$ in the washing and resuspending medium
PSII membranes	100 %*	100 %*
0.5 M NaCl treated PSII	88 %	100 %
1 M NaCl treated PSII	69 %	100 %
2 M NaCl treated PSII	68 %	100 %

* 100 % corresponds to 4.2 Mn/RC. Mn was measured by room temperature EPR spectra. The sample contains 0.25 M HCl and heat-treated (70°C) for 1 minute. The resuspending medium contains 0.4 M sucrose, 15 mM NaCl, and 20 mM MES (pH 6.5).

NaCl treatment was done at 1 mg Chl/ml for 1 hr at 4°C in the dark.

Table 2.

Mn content of spinach PSII membranes after NaCl and NH_2OH treatments

	Without 15 mM $CaCl_2$ in the washing and resuspending medium	With 15 mM $CaCl_2$ in the washing and resuspending medium
PSII membranes	100 %*	100 %*
0.5 M NaCl treated + 0.5 mM NH_2OH treated PSII	30 %	34 %
1 M NaCl treated + 0.5 mM NH_2OH treated PSII	8 %	11 %
2 M NaCl treated + 0.5 mM NH_2OH treated PSII	7 %	10 %

* 100 % corresponds to 4.2 Mn/RC. NH_2OH treatment was done at a Chl concentraiton of 1.6 - 2 mg Chl/ml (pH 6.5). NaCl treated PSII membranes were dark-adapted prior to the incubation with NH_2OH and were treated with NH_2OH for 30 minutes at 4°C in the dark.

See legend of Table 1 for other detail of NaCl treatment.

0.5 M NaCl treatment did not remove all of the 17 and 23 kD polypeptides, 1 M NaCl treatment removed them completely. Thus, the PSII membranes treated with 1 M NaCl were adopted as the standard preparation in the subsequent study. It remains to be shown that a suitable buffer can be found for this preparation.

The Mn content of PSII treated with different concentrations of NaCl with and without 15 mM $CaCl_2$ (buffer B and buffer C, see p. 32) in the washing and resuspending medium was determined by room temperature EPR according to II-8. The results are listed in Table 1 relative to untreated PSII membranes which contain 4.2 ± 0.1 Mn per reaction center (RC) of PSII. NaCl treatment did not affect the oxygen evolving activity of PSII membranes as long as 15 mM $CaCl_2$ was added to the resuspending buffer (0.4 M sucrose, 15 mM NaCl, and 20 mM MES (pH 6.5)). It is clear from Table 1 that PSII membranes that lack the 17 and 23 kD polypeptides lose no Mn as long as 15 mM $CaCl_2$ is present. In the absence of $CaCl_2$, however, the loss of Mn is noticeable at 1 - 2 M NaCl. Moreover, 30 mM NaCl had the same effect as 15 mM $CaCl_2$ in the washing and resuspending medium (100 % oxygen evolving activity and 100 % Mn content). Therefore, the factor which keeps the WOC intact is the ionic strength rather than a specific ion (Ca^{2+}).

Table 2 shows the Mn content in NaCl treated PSII membranes with and without 15 mM $CaCl_2$ in the washing and resuspending medium (0.4 M sucrose, 15 mM NaCl, and 20 mM MES (pH 6.5)) followed by 0.5 mM NH_2OH treatment. Here again 1 M NaCl gave identical results to that of 2 M NaCl treatment. Thus, 1 M NaCl treated PSII is an appropriate sample to study the NH_2OH effect.

Table 3 shows the effect of salts on oxygen evolving activity and Mn content of PSII membranes lacking 3 extrinsic polypeptides (17, 23, and 33 kD). When 200 mM NaCl and 15 mM $CaCl_2$ were included in the resuspension medium (buffer D, see p. 32), PSII membranes did not lose any Mn upon treatment with 1 M $CaCl_2$. However, the oxygen evolution activity measured at 1200 $\mu E \cdot m^{-2} \cdot s^{-1}$ decreased to 40 % of the original value. Further results on 1 M $CaCl_2$ treated PSII will be given in chapter IV.

III-1-3 Discussion

The results given above demonstrate that PSII treated with 1 M NaCl and subsequently suspended in buffer C lacks the 17 and 23 kD polypeptides and still has full O_2 evolving activity. This preparation satisfies the criteria stated at the beginning of this section and was therefore selected as the standard for the following work.

The results of this section confirmed earlier work (Miyao and Murata, 1983, 1985; Ono and Inoue, 1983a, b). Many authors use 2 M NaCl treatment to delete the 2 extrinsic polypeptides rather than 1 M NaCl (e.g., Dekker et al., 1984; De Paula et al., 1986) while the results in this section show that 1 M NaCl treatment is sufficient for this purpose.

1 M $CaCl_2$ treated spinach PSII membranes were considered inappropriate because they had only 40 % of the oxygen evolving activity found in the original PSII membranes at 1200 $\mu E \cdot m^{-2} \cdot s^{-1}$.

Table 3.

Effect of salts on Mn content and rate of oxygen evolution in 1 M $CaCl_2$ treated PSII membranes that lack the 17, 23, and 33 kD polypeptides.

Salt concentration in the resuspending medium[a]	Mn content	oxygen evolution
200 mM NaCl + 15 mM $CaCl_2$	100 %	40 %
200 mM NaCl	-	15 %
15 mM $CaCl_2$	-	15 %
10 mM NaCl	50 %*	5 %

[a] The resuspension medium contained 0.4 M sucrose, 20 mM MES (pH 6.5) and the salts as noted in this column.

100 % corresponds to 4.2 Mn/RC. PSII membranes without 1 M $CaCl_2$ treatment also had 4 Mn/RC; 100% corresponds to the oxygen evolving activity of the PSII membranes without 1 M $CaCl_2$ treatment; it was 600 μM O_2/mg Chl/ml; The oxygen evolving assay was done in the presence of 200 μM PPBQ as electron acceptor at 10 μg Chl/ml. The exciting light had an intensity of 1200 $\mu E \cdot m^{-2} \cdot s^{-1}$.

III-2. NH_2OH effect versus time

III-2-1 Rationale

Since the effect of NH_2OH is dependent both upon concentration (Sivaraja and Dismukes, 1988) and on the duration of the treatment (Cheniae and Martin, 1971), it is desirable to determine both these dependencies. In this section we measured the Mn released from NaCl treated PSII in the presence of 80 - 250 μM NH_2OH at 4°C in the dark as a function of time.

III-2-2 Results

Figure 10 shows the time dependence of the effect of 125 μM NH_2OH (A) and 250 μM NH_2OH (B) treatment on the Mn release in NaCl PSII. NH_2OH was added to the NaCl PSII, the sample was transferred to the EPR cell, and the released Mn was measured by the 6-line EPR spectrum taken at room temperature every 3 minutes.

Figure 11 shows the Mn release at three other concentrations of NH_2OH (80, 130, and 180 μM) as a function of time. In this experiment, a different protocol was followed. The NaCl PSII was treated with NH_2OH and centrifuged to collect the supernatant to measure the Mn released.

I also tried the same experiment at room temperatures but abandoned this approach when I found that NH_2OH released the 33 kD polypeptides even at 130 μM concentration while 0.5 mM NH_2OH did not release the 33 kD protein significantly at 4°C.

Figure 10. Time dependence of Mn release by 125 μM NH_2OH (A) and 250 μM NH_2OH (B) treatment of 1 M NaCl treated PSII membranes lacking the 17 and 23 kD polypeptides. After NH_2OH addition to the NaCl PSII, the sample was transferred to the EPR cell, an EPR spectrum was taken every 3 minutes and analyzed for Mn^{2+} as described in II-8. NH_2OH treatment was done at a Chl concentration of 1.6-2 mg/ml (pH 6.5) in the dark.

A

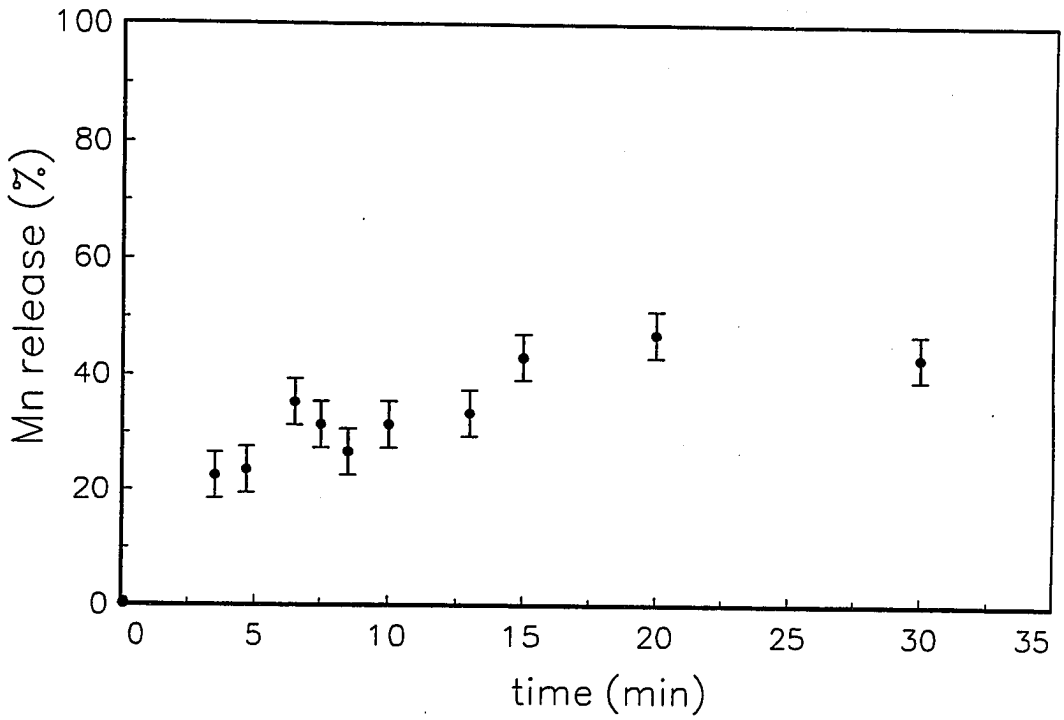

B

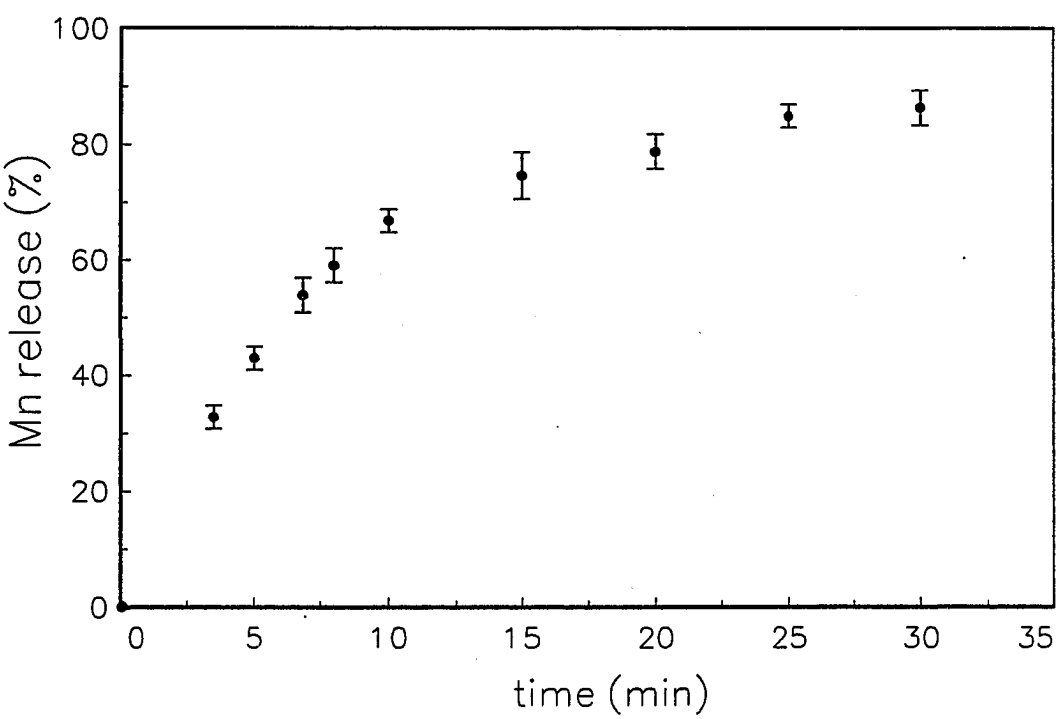

Figure 11. Time dependence of Mn release by 80 μM (a), 130 μM (b), and 180 μM (c) NH_2OH from 1 M NaCl treated PSII membranes lacking the 17 and 23 kD polypeptides. The NaCl PSII was treated with NH_2OH and centrifuged to collect the supernatant. The Mn^{2+} in the supernatant was determined from the 6-line EPR signal at room temperature as described in II-8. NH_2OH treatment was done at a Chl concentration of 1.6-2 mg Chl/ml (pH 6.5). NaCl PSII was dark-adapted prior to the incubation with NH_2OH and was treated with NH_2OH for 30 minutes at 4°C in the dark.

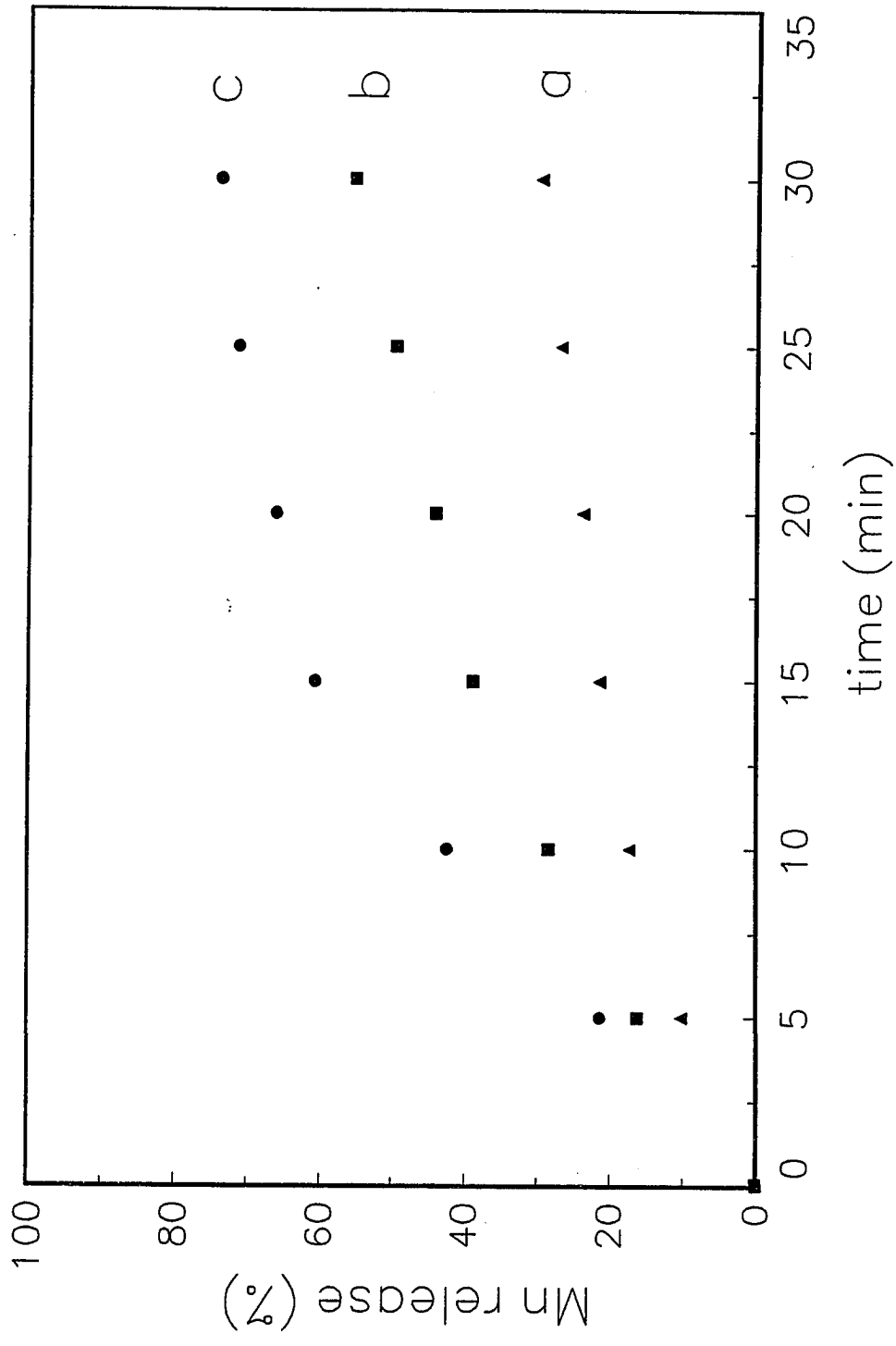

III-2-3 Discussion

Figure 12 shows the combined results of figures 10 and 11 in terms of Mn released per NH_2OH. Obviously, the Mn release was proportional to the NH_2OH concentration within the rather large experimental uncertainty. The more accurate data of the next 2section will show deviations from proportionality.

III-3. Effect of different concentrations of NH_2OH

III-3-1 Rationale

Sivaraja and Dismukes (1988) reported Mn release from PSII membranes by different concentrations of NH_2OH. Their results are complicated, however, by the release of two extrinsic polypeptides at concentration of less than 300 μM NH_2OH. By using the NaCl PSII, it was possible to study the NH_2OH effect with no interference from the extrinsic polypeptides and to analyze the data in terms of a cooperativity model.

III-3-2 Results

NaCl PSII lacking the 17 and 23 kD proteins was treated by NH_2OH at 4°C in the dark for 30 minutes. The samples were then centrifuged, and the Mn^{2+} released into the supernatant was determined by room temperature EPR. The pellet was washed three times and resuspended for the determination of the oxygen evolving activity. Table 4 shows 3 sets of data of Mn released by various concentrations of NH_2OH. Table 5 shows corresponding sets of data of changes in oxygen evolving activity at 1200 $\mu E \cdot m^{-2} \cdot s^{-1}$.

Figure 12. Time dependence of Mn release from figure 10 and figure 11 divided by NH_2OH concentrations. (a) 80 μM NH_2OH; (b) 125 μM NH_2OH; (c) 130 μM NH_2OH; (d) 180 μM NH_2OH; (e) 250 μM NH_2OH.

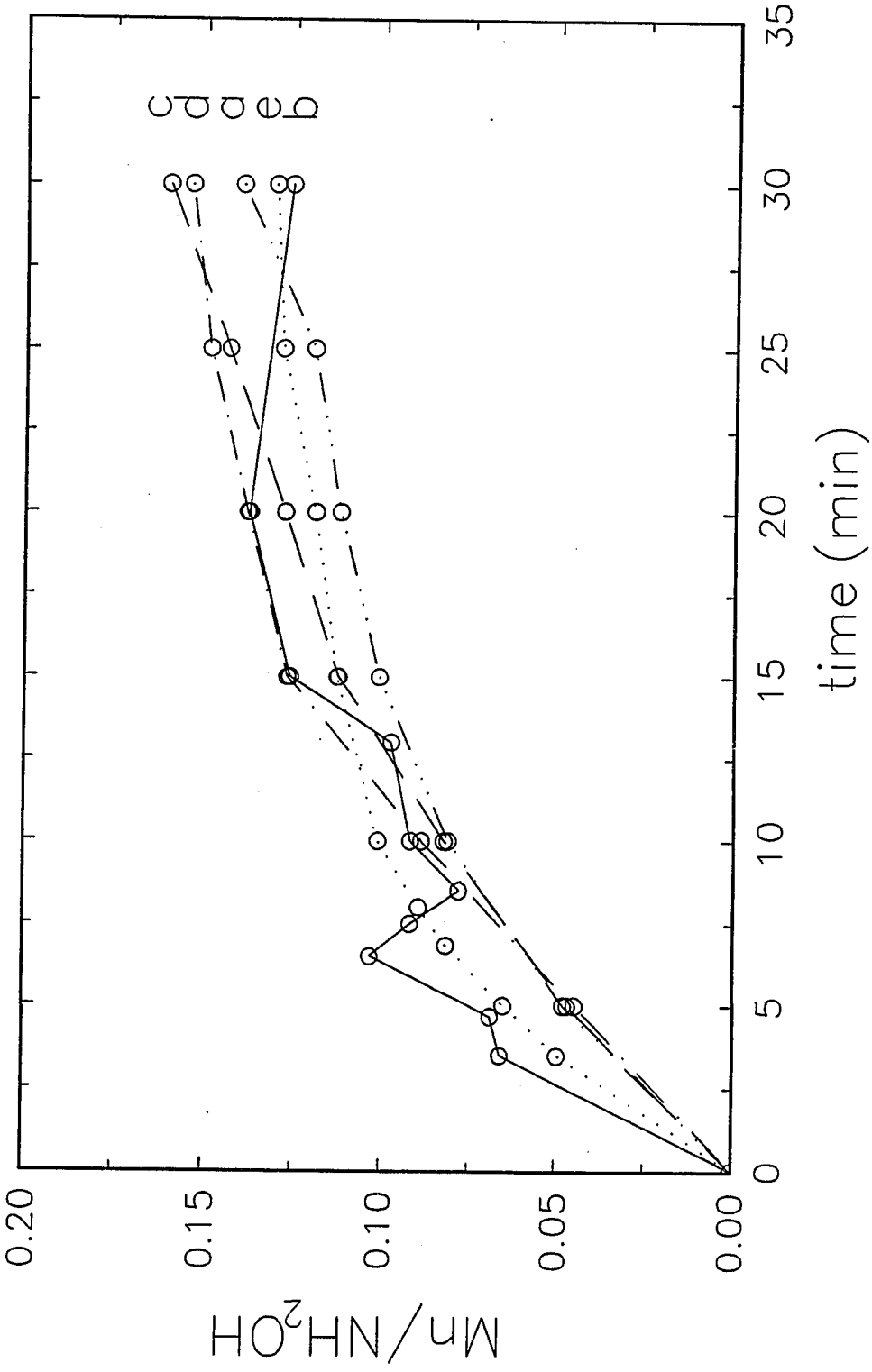

60

Figures 13 and 14 are plots of the data in Tables 4 and 5. Figure 15 is derived from figures 13 and 14 and shows the oxygen evolving activity versus Mn release from the reaction center.

III-3-3 Discussion

The plot of Mn^{2+} released from NaCl PSII as a function of NH_2OH concentration in figure 13 has a sigmoidal shape. As will be discussed shortly, the sigmoidal shape of the curve as opposed to a hyperbolic shape means the Mn release by NH_2OH is cooperative, that is, more than one molecule of NH_2OH reacts with the WOC, and the reactions of these molecules are not independent of each other. The discussion below follows that of Forster and Junge (1985), who studied flash induced proton release as a function of NH_2OH concentration.

A simple example of cooperativity would arise in the reversible binding of n hydroxylamines, H, to one metal center, M, according to the reaction (Stryer, 1981):

$$M + nH \leftrightarrow MH_n$$

with dissociation constant K',

$$K' = \frac{[M][H]^n}{[MH_n]}$$

Defineing y as the fraction of metal complexed,

$$y \quad \frac{[MH_n]}{[M] + [MH_n]} = \frac{[H]^n}{K' + [H]^n}$$

$$[H]^n (1 - y) = y K'$$

$$n \log [H] = \text{const} + \log \frac{y}{1-y}$$

Table 4

Mn release from NaCl PSII by various concentrations of NH_2OH

[NH_2OH] μM	Mn release Exp. 1	Mn release Exp. 2	Mn release Exp. 3	Mean value	Standard deviation
10	4 %	5 %	5 %	4.7	0.6
20	7	9	9	8.3	1.2
30	11	12	12	11.7	0.6
40	16	15	14	15.0	1.0
50	22	19	17	19.3	2.5
75	31	31	33	31.7	1.2
100	42	45	48	45.0	3.0
150	61	65	65	63.7	2.3
200	70	76	76	74.0	3.5
300	90	81	90	87.0	5.2
400	93	84	91	89.3	4.7
500	92	92	92	92.0	0

Sample, 1 M NaCl treated PSII membranes were treated by NH_2OH at 1.6-2 mg Chl/ml for 30 minutes at 4°C in the dark.

100 % Mn release corresponds 4.2 Mn/RC.

Table 5

Oxygen evolving activity of NaCl PSII treated by various concentrations of NH_2OH

[NH_2OH]	Oxygen evolution rate of Exp. 1	Oxygen evolution rate of Exp.2	Oxygen evolution rate of Exp. 3	mean value	std. dev.
10	94 %	90 %	93 %	92.3	2.1
20	89	85	89	87.7	2.3
30	77	76	78	77.0	1.0
40	68	64	69	67.0	2.6
50	63	58	65	62.0	3.6
75	51	47	46	48.0	2.6
100	42	35	31	36.0	5.6
150	24	19	11	18.0	6.6
200	17	10	7	11.3	5.1
300	2	6	2	3.3	2.3
400	0	4	0	1.3	2.3
500	0	0	0	0	0

Sample, 1 M NaCl treated PSII membranes were treated by NH_2OH at 1.6-2 mg Chl/ml for 30 minutes at 4°C in the dark.

100 % O_2 evolution corresponds 600 μM/mg Chl/ml.

Figure 13. Mn release by various concentrations of NH_2OH on 1 M NaCl treated PSII membranes lacking the 17 and 23 kD polypeptides. The NaCl PSII was treated with NH_2OH for 30 minutes at 4 °C in the dark and centrifuged. Both the pellet and the supernatant were analyzed for Mn^{2+} concentrations by room temperature EPR.

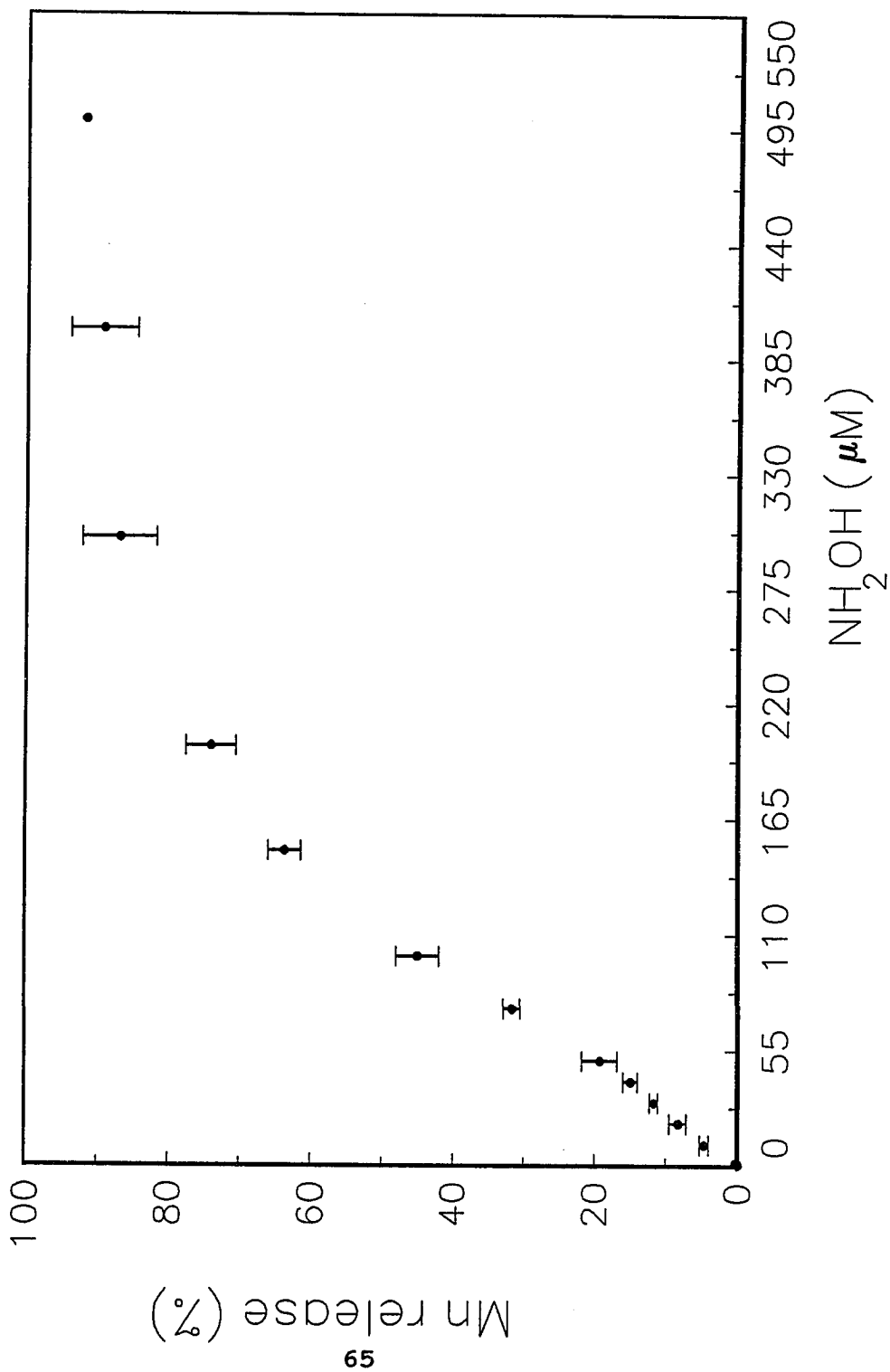

Figure 14. Oxygen evolving activity after treatment with various concentrations of NH_2OH on 1 M NaCl treated PSII membranes lacking the 17 and 23 kD polypeptides. The NaCl PSII was treated with NH_2OH for 30 minutes at 4 °C in the dark at 1.6-2 mg Chl/ml. After centrifugation, the pellet was resuspended and an aliquot was used for measuring the oxygen evolving activity at 1200 $\mu E \cdot m^{-2} \cdot s^{-1}$. 100 % Oxygen evolving activity corresponds to 600 μM/mg Chl/hr.

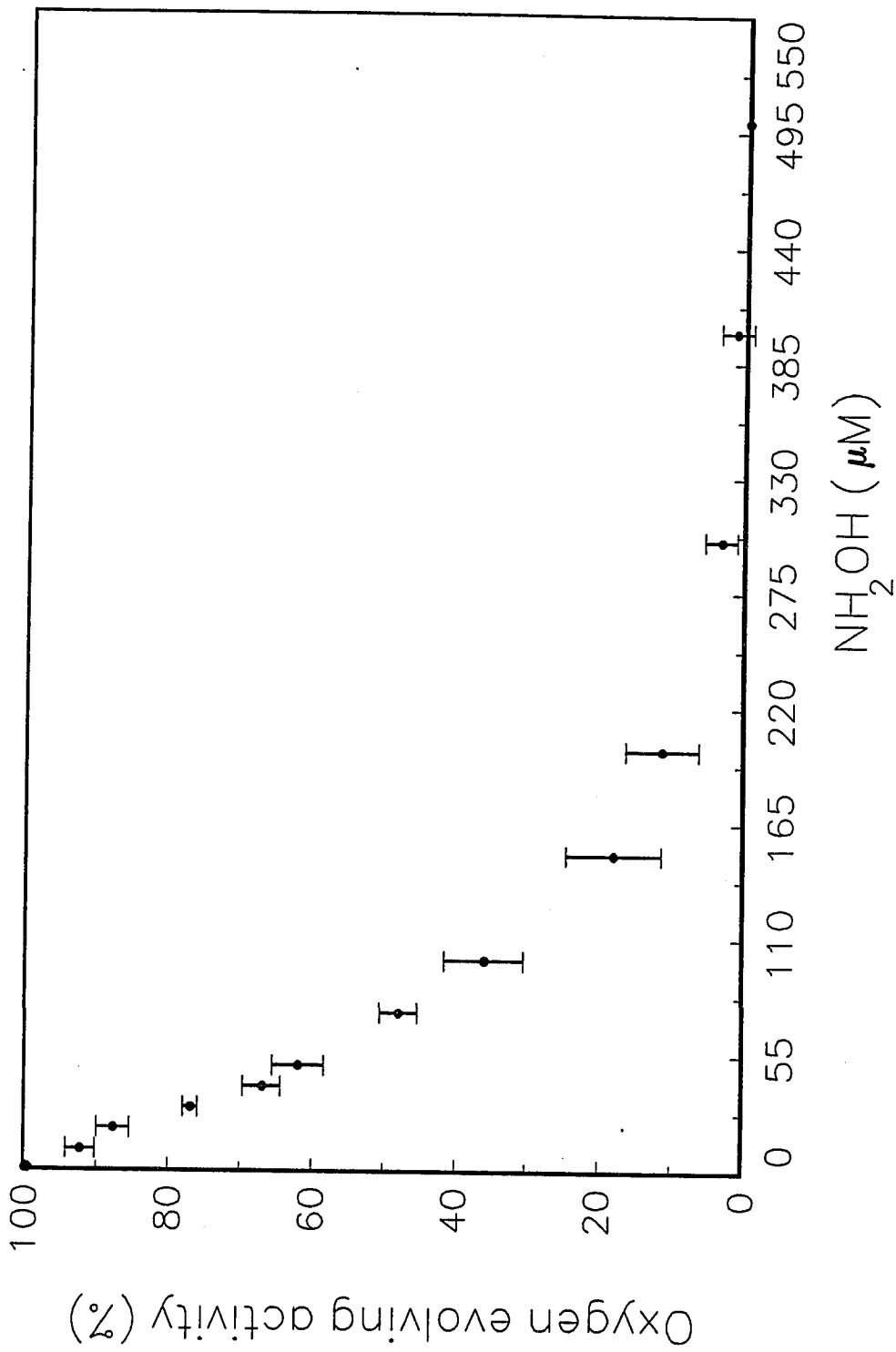

Figure 15. The oxygen evolving activity as a function of Mn release (based on data in figure 13 and 14.

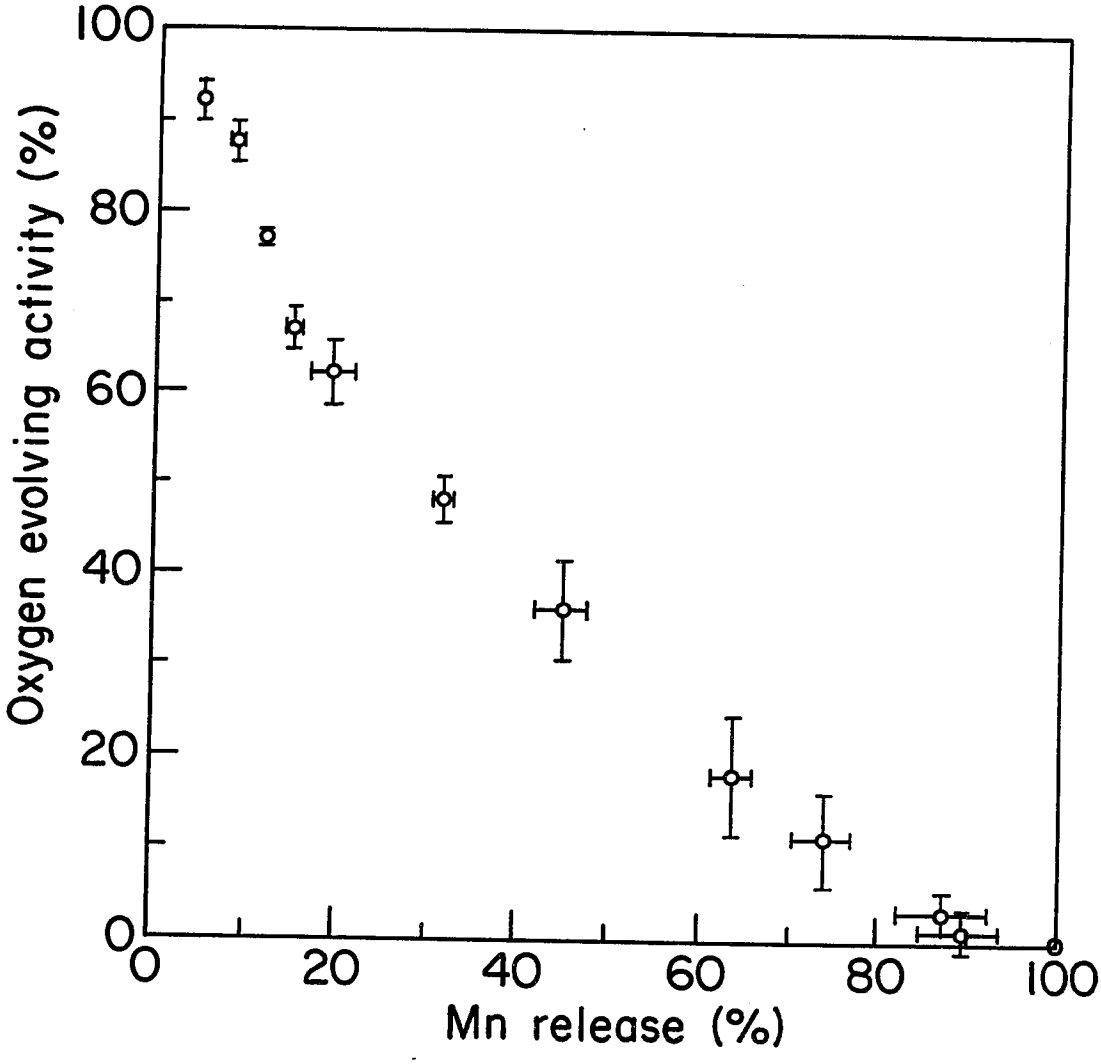

Therefore, a plot of log (y/(1-y)) versus log [H] yields a straight line with a slope of n. This representation is called a Hill plot and its slope n at the midpoint of the binding (y = 0.5) is called the Hill coefficient. If we identify y with the fraction of Mn released we can found an approximate Hill coefficient as follows.

In figure 13, 45 % of the Mn was released by 100 μM NH_2OH, 50 % of Mn was released by 109 μM NH_2OH, and 55 % of Mn was released by 120 μM NH_2OH.

$$\log \frac{y}{1-y} \quad \text{vs.} \quad \log [H]$$

$$45\ \% \qquad \log \frac{0.55}{1-0.55} \quad \text{vs} \quad \log 100$$

$$55\ \% \qquad \log \frac{0.45}{1-0.45} \quad \text{vs} \quad \log 120$$

$$\text{Hill coefficient} = \frac{0.087 + 0.087}{2.083 - 2.000} = 2.2$$

The Hill coefficient of 2.2 for NH_2OH binding to Mn in the WOC means that the binding is cooperative. NH_2OH binding at one binding site of the WOC facilitates the NH_2OH binding at another Mn site of the same WOC. The following is one of the possible interpretations of the Mn release by various concentrations of NH_2OH. Let us assume that the sequential binding of NH_2OH is in equilibrium (Segel, 1975; Förster and Junge, 1985, 1986):

$$M \underset{K_d}{\overset{+H}{\longleftrightarrow}} M(H) \underset{aK_d}{\overset{+H}{\longleftrightarrow}} M(H)_2 \underset{bK_d}{\overset{+H}{\longleftrightarrow}} M(H)_3 \underset{cK_d}{\overset{+H}{\longleftrightarrow}} M(H)_4$$

where M is the manganese center, H is NH_2OH, K_d is a dissociation constant and a, b, and c are sequential interaction factors. The degeneracies of the states $M(H)_n$ follow the pattern:

$$M:M(H) = 1:1 \text{ for } n = 1$$

$$M:M(H):M(H)_2 = 1:2:1 \text{ for } n = 2$$

$$M:M(H):M(H)_2:M(H)_3 = 1:3:3:1 \text{ for } n = 3$$

$$M:M(H):M(H)_2:M(H)_3:M(H)_4 = 1:4:6:4:1 \text{ for } n = 4$$

With the assumption that a = b = c, the percentages of manganese bound by NH_2OH, T_n, are:

$$T_1 = X/(1 + X)$$

$$T_2 = (2X + X^2/a)/(1 + \text{numerator})$$

$$T_3 = (3X + 3X^2/a + X^3/a^3)/(1 + \text{numerator})$$

$$T_4 = (4X + 6X^2/a + 4X^3/a^3 + X^4/a^6)/(1 + \text{numerator})$$

where X is $[H]/K_d$, is a normalized NH_2OH concentration. The first line for n = 1 represents the hyperbolic plot.

Figure 16 is the result of simulations for n = 1, 2, 3, and 4 on a log scale. The simulation with n = 3 or n = 4 fit the data better than n = 1 or n = 2. The simulation with n = 3 fits the data somewhat better, but n = 4 still gives a reasonable fit. Table 6 lists the fitting parameters a and K_d as well as X^2, the sum of squares of the deviations calculated with and without weighting

Figure 16. Fits of the Mn^{2+} released from the NaCl PSII versus log [NH_2OH]. The data (solid circles) are from figure 13 after division by 92 %, the maximum Mn release. The 4 lines represents the best fits by the model described in the text for n = 1, 2, 3, and 4. For n = 1, K_d = 95 μM; for n = 2, K_d = 340 μM and a = 0.2; for n = 3, K_d = 760 μM and a = 0.2; for n = 4, K_d = 1100 μM, a = 0.27.

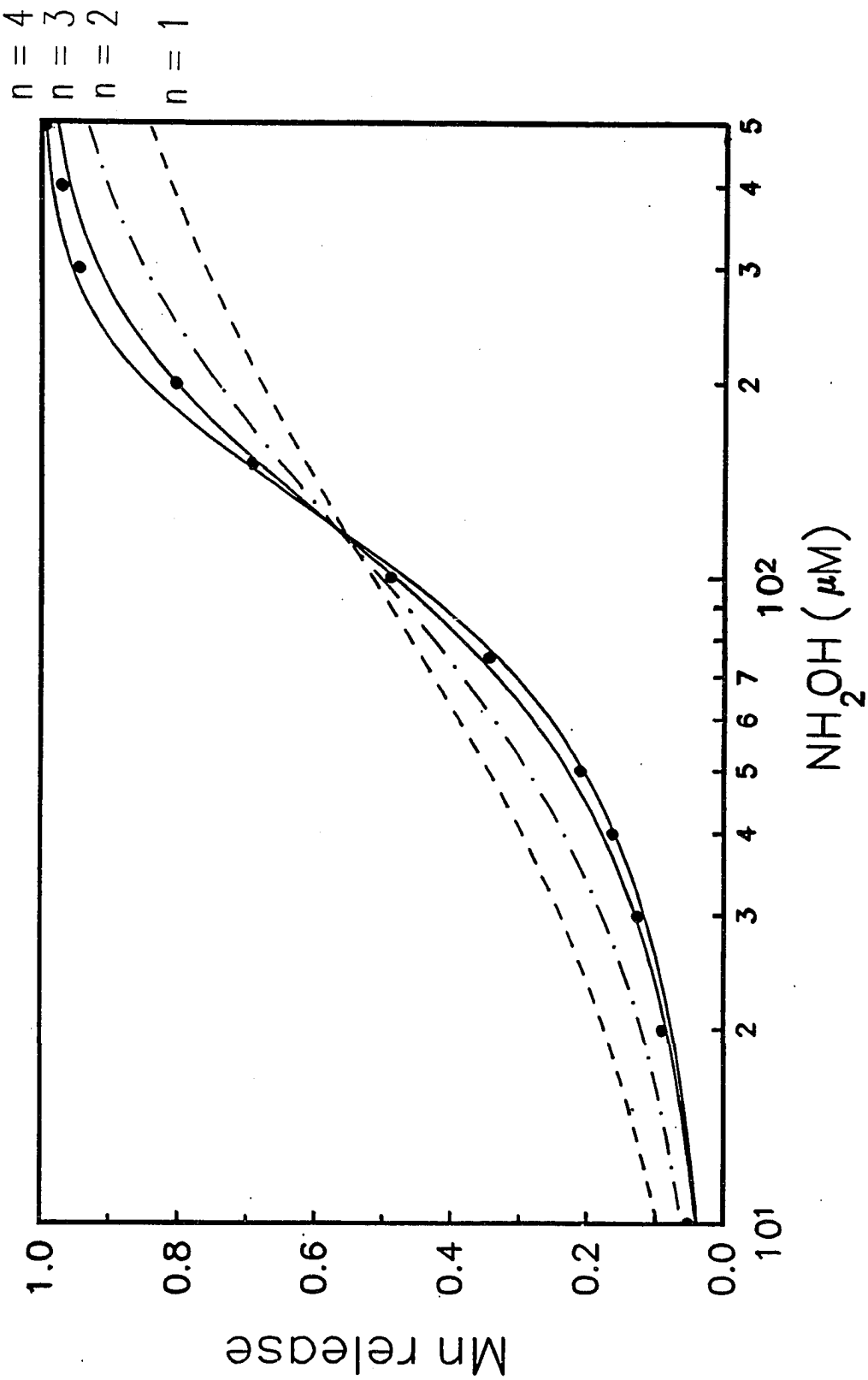

factors x^{-r}, r = ½, 1, 2, which weigh the lower concentrations more strongly.

The oxygen evolution activity, figure 14, has a different functional dependence on the NH_2OH concentration than the Mn release, figure 13, and the two plots are not just the complement of each other. It is clear that a hyperbolic dependence on [NH_2OH] does not fit the data and a Hill plot (not shown) suggests some cooperativity. Figure 15, which shows oxygen evolution versus Mn released, confirms thses observations. It is plausible to assume that the released any one Mn from a WOC eliminates its oxygen evolution. Accordingly, the relation between oxygen evolution and manganese released then must fall between the following two limiting cases. If one of the four Mn is easily released by NH_2OH while the others are not, the oxygen evolution should drop linearly with Mn released and reach zero for 25 %, i.e., one Mn released per RC. If, on the other hand, the Mn is not stable against NH_2OH once a first atom has been removed, then figure 15 should be a straight line along the diagonal, i.e., x % oxygen evolution corresponds to (100 - x) % Mn released. Clearly, the experimental data lie between the two limiting cases, the slope being steepest between 10 % and 20 % Mn released, while it is equal to -1 from 20 % to 70 % Mn released.

Table 6

Various types of X^2 which show the difference between the experimental data and the theoretical data

X^2	n = 3 a = 0.2, Kd = 760	n = 4 a = 0.27, Kd = 1100
$\Sigma\ (t-y)^2$	0.0025	0.0034
$\Sigma\ \frac{(t-y)^2}{\sqrt{x}}$	0.0017	0.0023
$\Sigma\ \frac{(t-y)^2}{x}$	0.0002	0.0002
$\Sigma\ \frac{(t-y)^2}{x^2}$	0.000002	0.000002

t is the theoretical value calculated according to the equations in chapter III-3, y is the experimental value, x is $[NH_2OH]$, n is the cooperativity, a is the sequential interaction factor, and K_d is the dissociation constant.

Chapter IV: FUNCTION OF THE 33 KD POLYPEPTIDE

1 M $CaCl_2$ treated PSII membranes lack the 3 extrinsic polypeptides but with 200 mM NaCl and 15 mM $CaCl_2$ in the washing and resuspension medium (0.4 M sucrose and 20 mM MES (pH 6.5) (Ono and Inoue, 1984) they retain all the Mn. The oxygen evolving activity of these preparations, on the other hand, is only 40 % of that of 1 M NaCl treated PSII membranes (Miyao and Murata, 1984) (Table 3). Apparently, the high salt concentration protects the Mn of the OEC, but the function of the complex is impaired.

There is disagreement as to whether or not PSII lacking the three extrinsic polypeptides can undergo the $S_1 \rightarrow S_2$ transition (Imaoka et al., 1986; Ono and Inoue, 1985). Thermoluminescence studies of 1 M $CaCl_2$ treated PSII suggest that the S_2 and S_3 states can be attained (Ono and Inoue, 1985). The flash dependent yield of oxygen indicates that the $S_3 \rightarrow S_0$ state transition, in particular, is retarded (Miyao et al., 1987).

The following experiments were undertaken to explore the reasons for the lower oxygen evolution rate of 1 M $CaCl_2$ treated PSII membranes.

IV-1. The effect of NH_2OH on 1 M $CaCl_2$ treated PSII.

IV-1-1 Rationale

In III-3-3 it was shown that a plot of Mn released from NaCl PSII versus NH_2OH concentration shows a sigmoidal shape, which could be interpreted in terms of a cooperativity model. In this

Figure 17. Mn release by various concentrations of NH_2OH on 1 M $CaCl_2$ treated spinach PSII membranes with 200 mM NaCl and 15 mM $CaCl_2$ in the resuspending medium. The $CaCl_2$ PSII was treated with NH_2OH for 30 minutes at 4 °C in the dark and centrifuged to collect the pellet and the supernatant for measuring Mn concentration by room temperature EPR. [Chl] for NH_2OH treatment was 1.6 - 2 mg/ml and 100 % Mn corresponds to 4.2 Mn/RC.

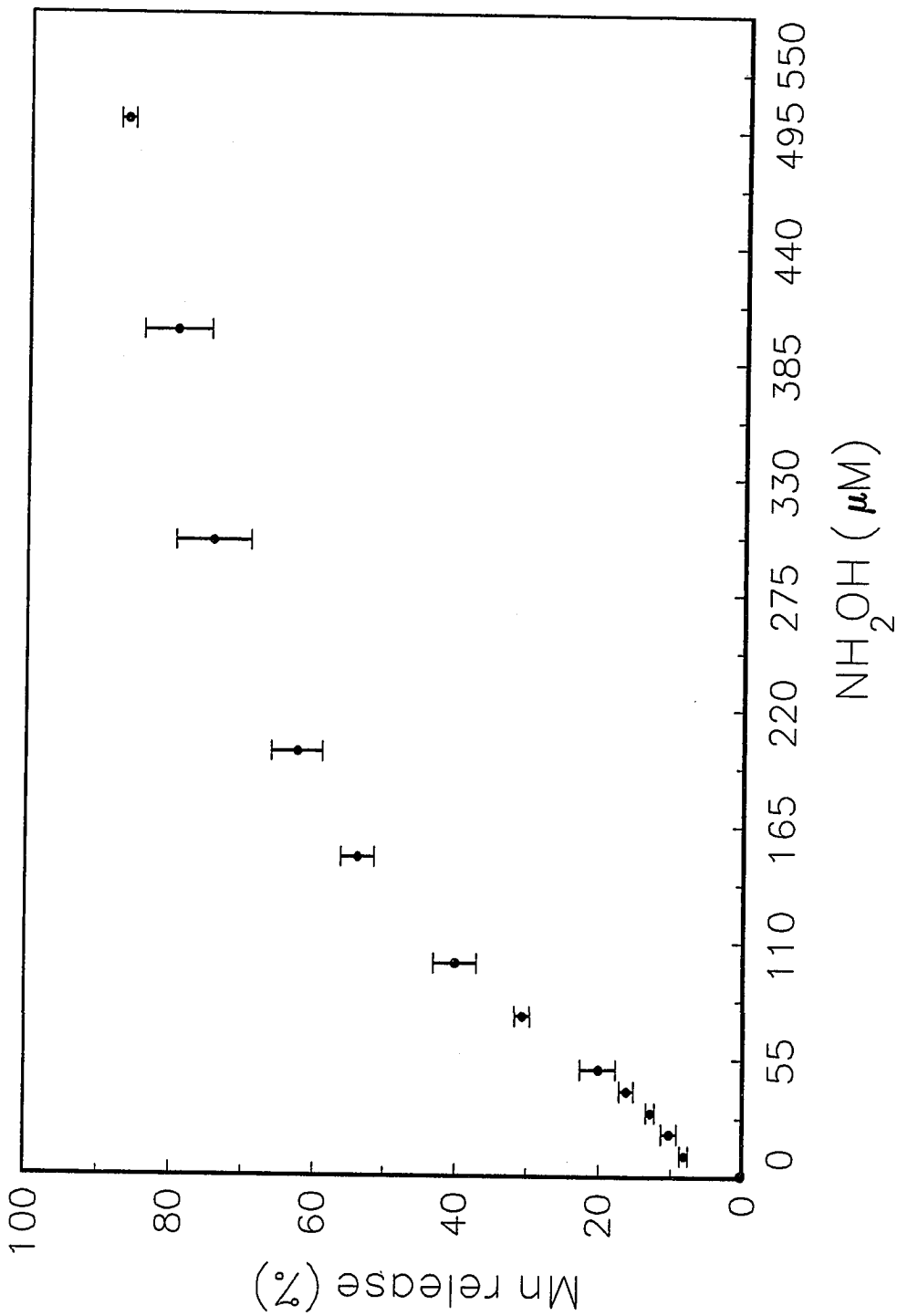

section it will be shown that the release of Mn by NH_2OH is not greatly affected by the presence or absence of the 33 kD polypeptide.

IV-1-2 Results

Two aliquots of the same sample were used for measuring Mn concentration and oxygen evolving activity. Figure 17 shows a plot of Mn released from 1 M $CaCl_2$ treated PSII by various concentration of NH_2OH. Comparison with the corresponding plot for 1 M NaCl treated PSII (figure 13) shows great similarity in the Mn release of 1 M $CaCl_2$ treated PSII but with 200 mM NaCl and 15 mM $CaCl_2$ in the resuspending medium ($CaCl_2$ PSII). 200 mM NaCl and 15 mM $CaCl_2$ can thus replace the 33 kD extrinsic polypeptide in terms of protecting Mn from release by NH_2OH (Table 3). Figure 18 shows how the oxygen evolving activity changes with various NH_2OH concentration (100 % is the maximum activity of 1 M NaCl treated PSII membranes (NaCl PSII)). Figure 19 compares the O_2 evolution of the NaCl PSII with that of $CaCl_2$ PSII (closed circles), where the maximum activity of the latter has been normalized to 100 %.

IV-1-3 Discussion

The equations in section III-3-3 were used to fit the data of Mn release by NH_2OH in 1 M $CaCl_2$ treated PSII. The maximum Mn release by NH_2OH in the preparation was 86 % and the y values were divided, accordingly, by 0.86. A best fit ($X^2 = 0.0118$, see figure 20) is obtained with $n = 3$, $K_d = 780\ \mu M$ and $a = 0.22$ or $X^2 = 0.0292$ with $n = 4$, $K_d = 1125\ \mu M$ and $a = 0.29$. Compared to the NaCl PSII,

Figure 18. Oxygen evolving activity in 1 M $CaCl_2$ pretreated spinach PSII membranes treated with various concentrations of NH_2OH. $CaCl_2$ PSII membranes were treated with NH_2OH for 30 minutes at 4 °C in the dark at 1.6 - 2 mg Chl/ml and centrifuged to collect the pellet for measuring the oxygen evolving activity. 100 % corresponds to 600 μM O_2/mg Chl/hr. The oxygen evolving assay was done at 1200 $\mu E \cdot m^{-2} \cdot s^{-1}$ in the presence of 200 μM PPBQ at 10 μg Chl/ml.

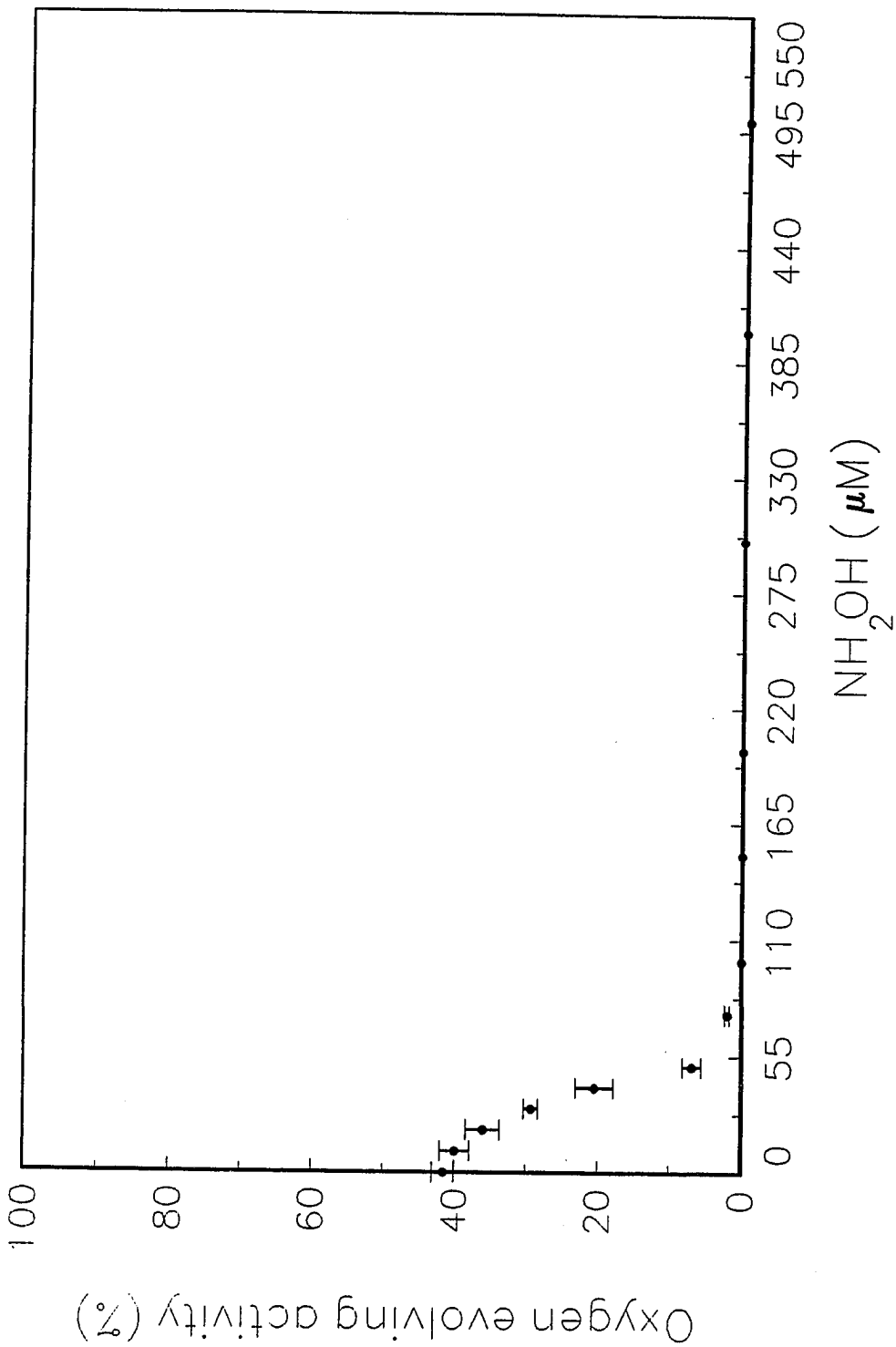

Figure 19. Oxygen evolving activity in 1 M $CaCl_2$ pretreated spinach PSII membranes treated with various concentrations of NH_2OH (closed circles, 100 % is the maximum activity of 1 M $CaCl_2$ treated PSII, 240 μM O_2/mg Chl/hr) and the same for spinach PSII samples pretreated with 1 M NaCl (crosses, 100 % is the maximum activity of the NaCl PSII, 600 μM O_2/mg Chl/hr). $CaCl_2$ PSII and NaCl PSII were treated with NH_2OH for 30 minutes at 4 °C in the dark at 1.6 - 2 mg Chl/ml and centrifuged to collect the pellet for measuring the oxygen evolving activity. The oxygen evolving assay was done at 1200 $\mu E \cdot m^{-2} \cdot s^{-1}$ in the presence of 200 μM PPBQ at 10 μg Chl/ml.

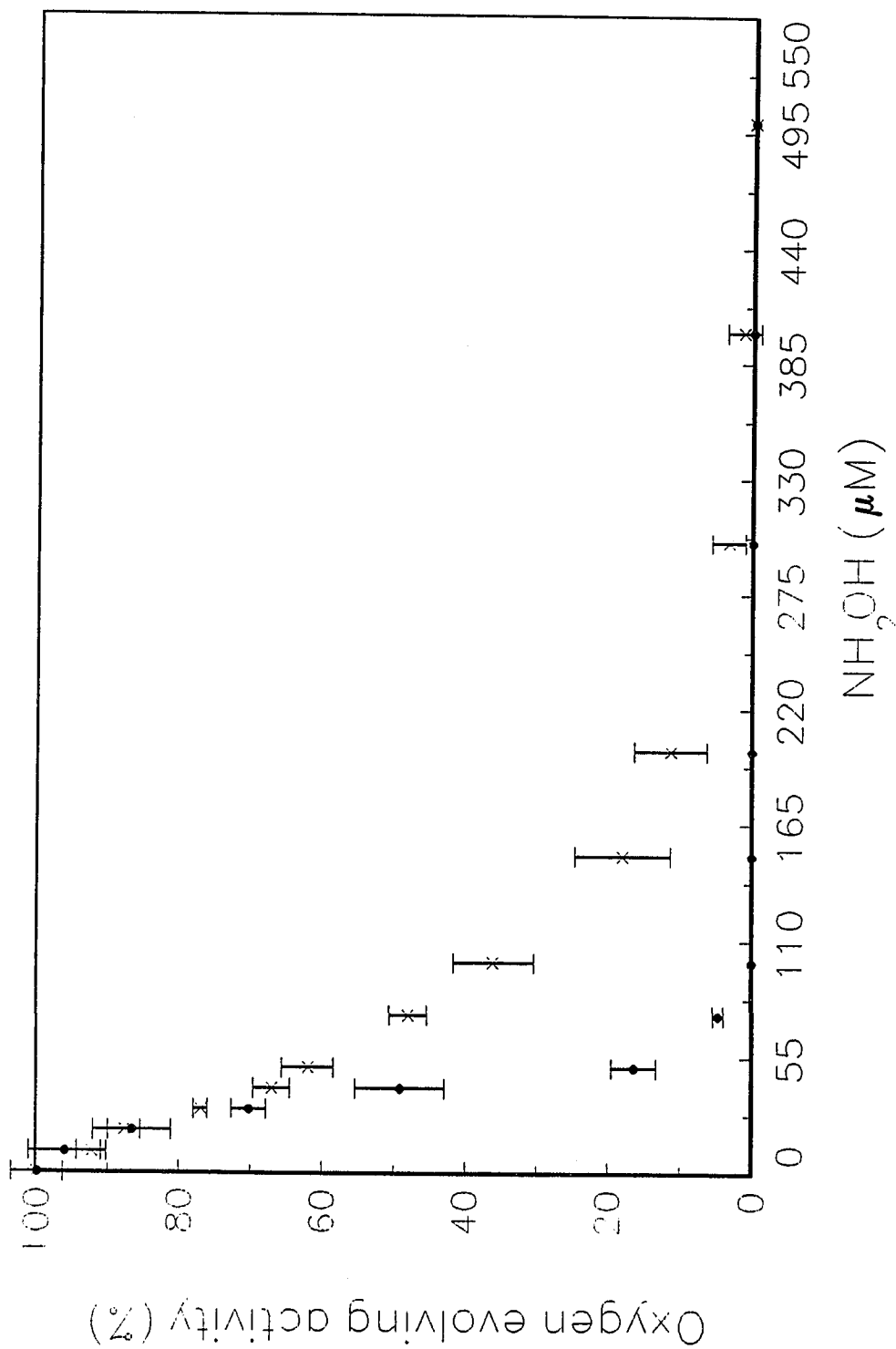

the sequential interacting factor, a, and the K_d values are similar. Therefore, 200 mM NaCl and 15 mM $CaCl_2$ have replaced the 33 kD polypeptide in the sense that the accessibility of the substrate analog, NH_2OH, to Mn has not changed by the removal of the 33 kD protein.

IV-2. PSII activity as a function of light intensity

IV-2-1 Rationale

As shown in Table 3, 1 M $CaCl_2$ treated PSII membranes have low oxygen evolving activity at 1200 $\mu E \cdot m^{-2} \cdot s^{-1}$ although all the Mn was retained. One possible explanation is that the S-state turnover rate slowed down and the high light intensity caused earlier saturation or possibly photoinhibition. To check this possibility, the O_2 evolution was measured at decreased light intensity. To measure the activity of the acceptor side, the DCIP reduction rate was monitored in parallel experiments.

IV-2-2 Results

Table 7 shows the data of oxygen evolving activity. Numbers in parenthesis are normalized to the light intensity of 1200 $\mu E \cdot m^{-2} \cdot s^{-1}$, i.e., they are a measure of the yield per photon. As the light intensity decreases to 70 $\mu E \cdot m^{-2} \cdot s^{-1}$, 1 M $CaCl_2$ treated PSII can evolve the same amount of O_2 as the NaCl PSII. Removal of the 33 kD polypeptide, therefore, did not inactivate the Mn centers. Moreover, at 100 $\mu E \cdot m^{-2} \cdot s^{-1}$ the normalized oxygen evolution activity

Table 7

Oxygen evolving activity and DCIP reduction rate as a function of light intensity

Light intensity ($\mu E \cdot m^{-2} \cdot s^{-1}$)	Oxygen evolution NaCl PSII	Oxygen evolution $CaCl_2$ PSII
60.0	7 (140)	6 (120)
67.2	8 (143)	7 (125)
74.4	9 (145)	7 (113)
90.7	11 (145)	8 (106)
108.0	13 (144)	9 (100)
300.0	33 (132)	16 (64)
672.0	69 (123)	24 (43)
1200.0	100 (100)	36 (36)

The numbers in parenthesis are the normalized oxygen evolving activities calculated as follows,

$$x = \frac{1200}{I} \frac{A}{A_o}$$

where A is the oxygen evolving activity at the light intensity, I, and A_o is the oxygen evolving activity with 1200 $\mu E \cdot m^{-2} \cdot s^{-1}$.

Oxygen evolution activity was assayed in the presence of 200 μM PPBQ at 10 μg Chl/ml

Figure 20. Fit of the Mn^{2+} released from $CaCl_2$ PSII versus NH_2OH concentration. The data are from figure 20 after division by 86 %, the maximum Mn release. The solid line represents the best fit of the data by the cooperativity model described in the text for n = 3 with K_d = 780 μM, and a = 0.22.

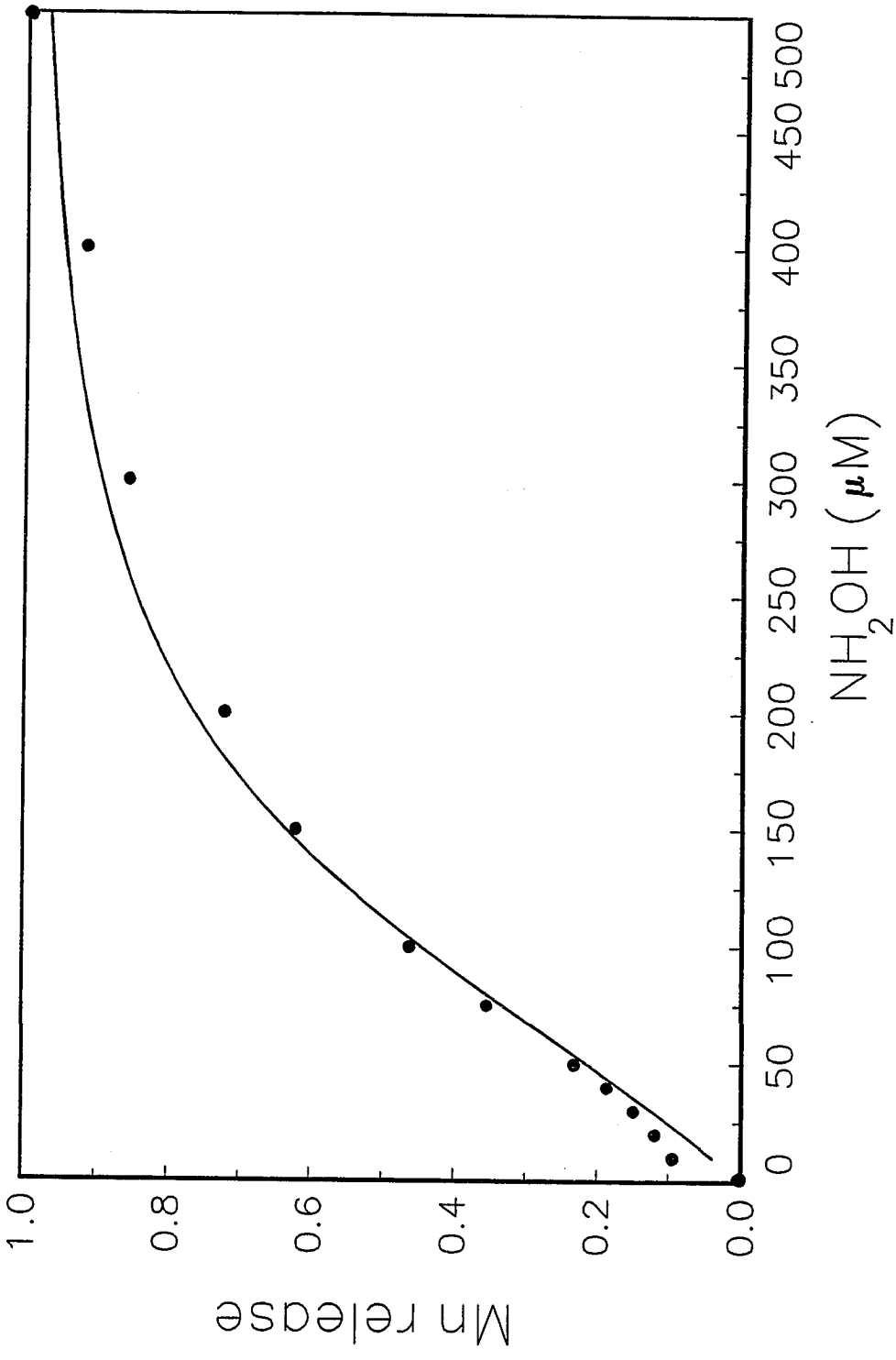

of the NaCl PSII has increased to 143 % of that observed at 1200 $\mu E \cdot m^{-2} \cdot s^{-1}$.

IV-2-3 Discussion

In the presence of 200 mM NaCl and 15 mM $CaCl_2$ in the resuspension medium the WOC of 1 M $CaCl_2$ treated PSII lacking the 17, 23, and 33 kD polypeptides not only retains four Mn per reaction center (Table 3), but at sufficiently low light intensity it evolves oxygen at the same rate as the NaCl PSII lacking the 17 and 23 kD polypeptides. It thus appears to be fully functional albeit at a slower rate. While each RC of NaCl PSII evolves 225 molecules of O_2 per second under saturating conditions (600 μM O_2/mg Chl/ml), the maximum rate for $CaCl_2$ PSII is 80/RC/sec. The time for one full cycle thus increases from 4.4 ms to roughly 12 ms. Usually, the bottleneck is not in the electron transfer from Z to P680, which normally occurs on a 20 - 300 ns time scale and is thus much faster than the rate of electron flow from the Mn complex to Z, which occurs on a 30 μs - 1 ms range (Kramer et al., 1990). Since $CaCl_2$ PSII does not have the 33 kD extrinsic polypeptide, which is closest to the Mn site, while the acceptor is on the opposite side of the membranes. In principle, the rate limitation could also be due to the acceptor, but since the acceptor is on the opposite side of the membranes from the 33 kD polypeptide, the slowdown most likely occurs in the Kok cycle. It remains to be seen if an individual step of the cycle is too slow or if all five steps are affected.

The normalized oxygen evolution activity of the NaCl PSII increased monotonically with decreasing light intensity to level off at 143 % for intensities of ≤ 100 $\mu E \cdot m^{-2} \cdot s^{-1}$. Oxygen evolution from PSII is thus saturated at 1200 $\mu E \cdot m^{-2} \cdot s^{-1}$.

These results agree well with current ideas about the noncatalytic role for the 33 kD polypeptide. Several workers found that the millisecond kinetics of oxygen release after the third flash was retarded by the removal of the 33 kD protein and stimulated by its rebinding, suggesting that the transition from S_3 to S_0 is accelerated by the 33 kD protein (Henry et al., 1982; Andersson et al., 1984; Ghanotakis et al., 1984; Miyao and Murata, 1984; Nakatani, 1984; Vass et al., 1987; Ono and Inoue, 1985; Miyao et al., 1987a, b). In section IV-3, we will explore the delay of the microsecond kinetics of the transition from S_1 to S_2 by the removal of the 33 kD polypeptide.

IV-3. Chl a fluorescence

IV-3-1 Rationale

Chlorophyll a fluorescence has long been used as an intrinsic indicator of the photosynthetic reactions of isolated chloroplasts of green plants. Since Chl a fluorescence is in competition with photochemical reactions and other processes in chloroplasts, it has been widely used to monitor variations in photosynthetic activity (see e.g., Duysens, 1986).

Light-induced charge separation initiates the electron transport from the reaction center (P680) to the plastoquinone pool

via Q_A and Q_B. Q_A is a tightly bound one electron acceptor and Q_B is a loosely bound two electron acceptor (see e.g., Crofts and Wraight, 1983). The Chl a fluorescence yield depends, among other factors, upon the redox state of Q_A. By measuring the change in the variable Chl a fluorescence yield, which correlates with the concentration of Q_A^-, it is possible to estimate the kinetics and equilibrium parameters for the reaction of Q_A with Q_B (see e.g., Xu et al., 1989). Furthermore, effects on the electron donor side can be studied by monitoring Chl a fluorescence yield changes with and without external donors such as hydroxylamine or hydroquinone.

By reducing the light intensity, it was possible to demonstrate in section IV-2 that in 1 M $CaCl_2$ treated PSII the overall rate of the donor side of is slowed down compared to that of 1 M NaCl treated PSII. As will be discussed in the next section, Chl a fluorescence following saturating flashes was used to get more information.

IV-3-2 Results

The Chl a fluorescence transients were measured according to section II-6. Figure 21A shows the transients of the NaCl PSII and $CaCl_2$ PSII, figure 21B shows those of the samples in the presence of 10 μM DCMU as inhibitor, and figure 21C shows those of samples in the presence of 2 mM hydroquinone as electron donor.

Figure 22 shows the decay of the Chl a fluorescence in dark adapted NaCl PSII and $CaCl_2$ PSII after 1 (A), 2 (B), 3 (C), and 4 (D) saturating flashes measured according to section II-6. The first data point is at 40 μs after the saturating flash. The F_o

Figure 21. Chl a fluorescence transients at room temperature. (A) shows the transients of the 1 M NaCl treated PSII membranes and 1 M $CaCl_2$ treated PSII membranes, (B) the transients of samples in the presence 10 μM DCMU, and (C) the transients of samples in the presence of 2 mM HQ.

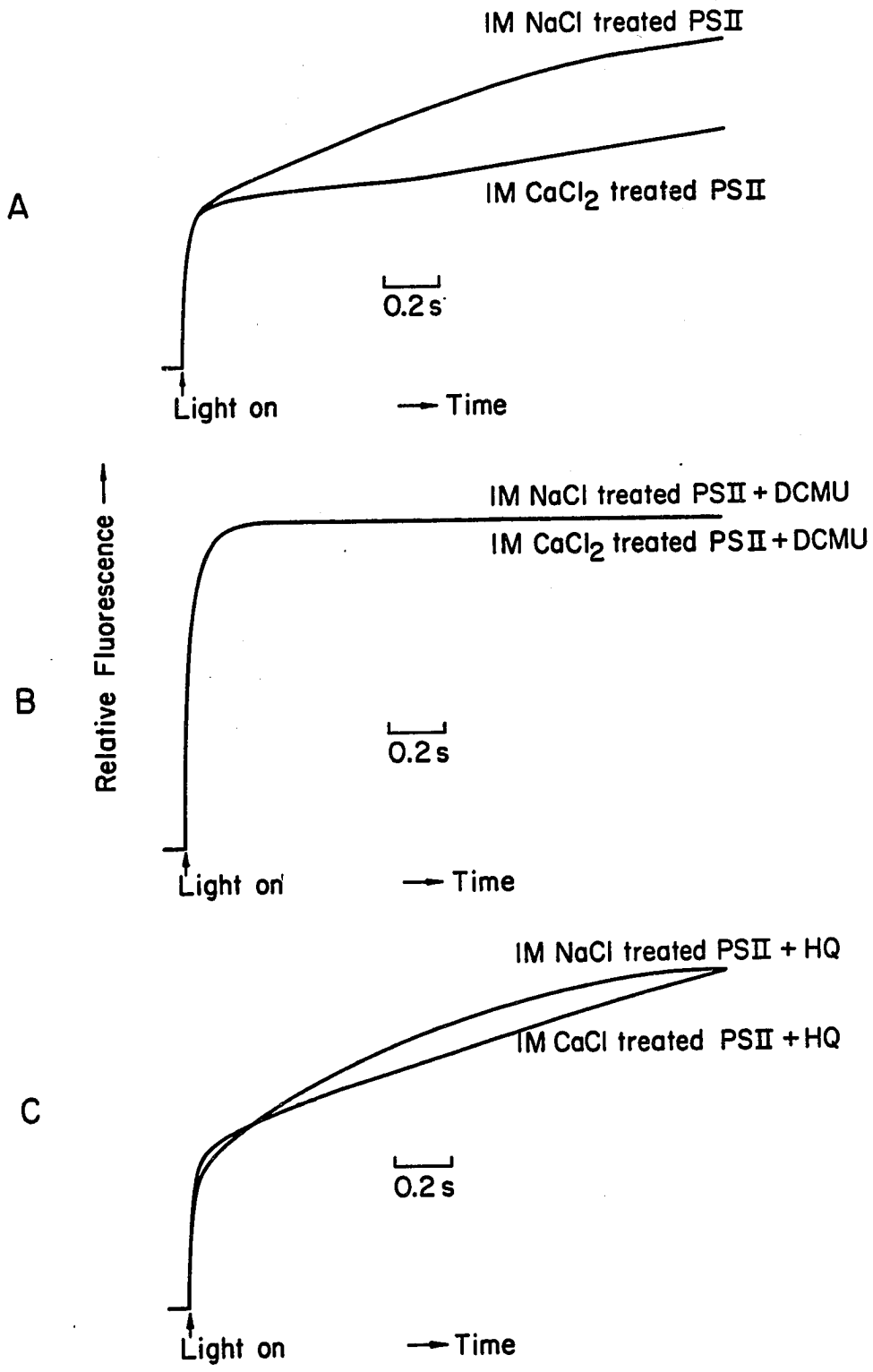

Figure 22. Variable Chl a fluorescence in dark adapted NaCl treated PSII and $CaCl_2$ treated PSII after the first (A), second (B), third (C), and fourth (D) saturating flash measured according to section II-6. The first data point is at 40 μs after the flash.

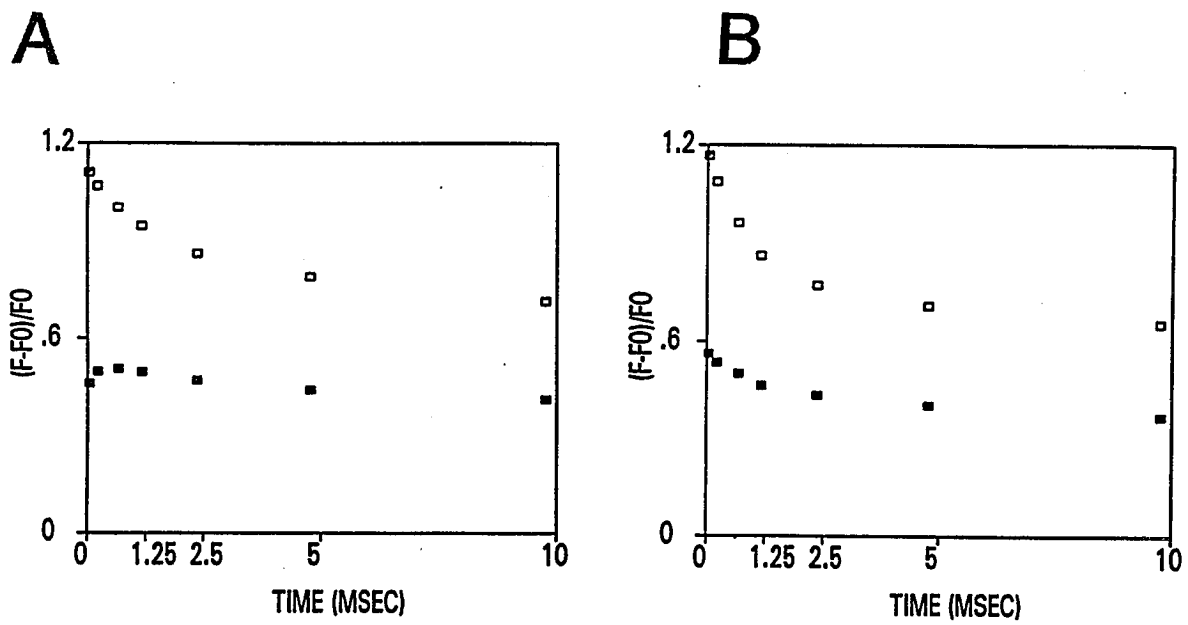

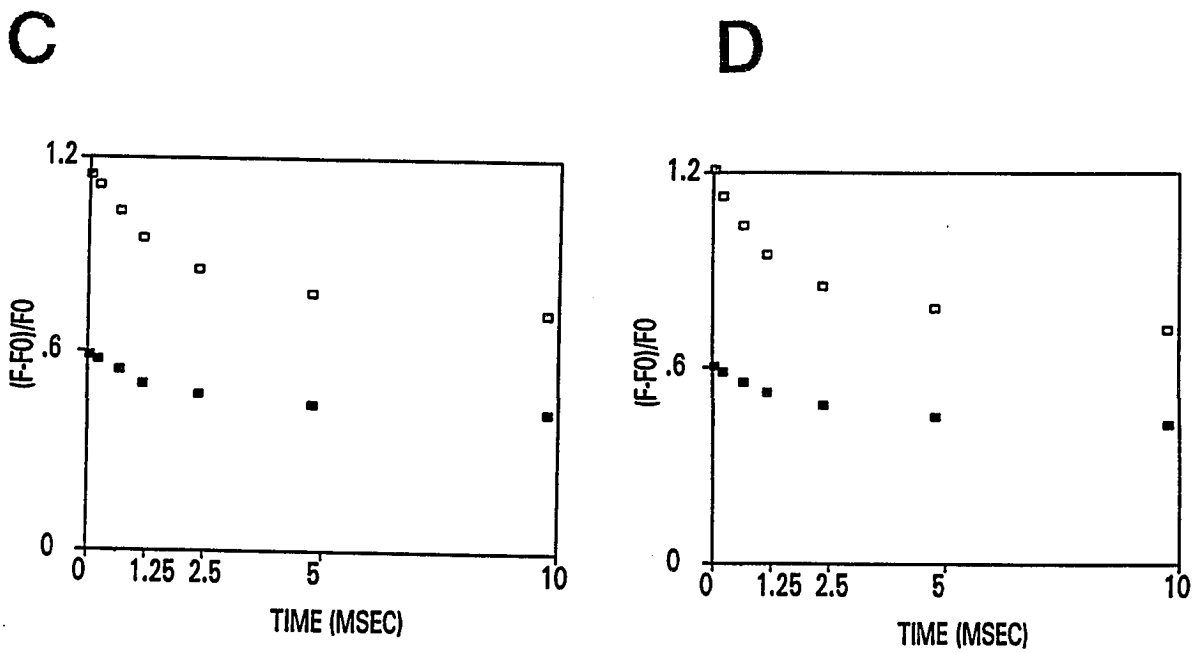

Table 8

The F_o levels for different samples used for the data in figure 25 - 31.

Samples	F_o (relative units)
NaCl PSII	.80
NaCl PSII + DCMU	.78
$CaCl_2$ PSII	.78
$CaCl_2$ PSII + DCMU	.74
$CaCl_2$ PSII + DCMU + HQ	.79

[DCMU] was 20 μM and [HQ] was 2 mM at sample concentration of 5 μg Chl/ml.

levels used in these calculations are listed in Table 8. $CaCl_2$ treated PSII shows a slower rise after the first actinic flash compared to the others (second, third and fourth). $CaCl_2$ treated PSII also shows lower variable Chl a fluorescence than the NaCl PSII. One possible explanation for the lower Chl a fluorescence is the existence of fluorescence quenchers (e.g., Chl^+) in $CaCl_2$ PSII. As a matter of fact, Miller et al. (1987) reported that Chl is the alternative in $CaCl_2$ PSII at low temperature (about 70 % of the electrons came from the WOC, the other 30 % from Chl). Figure 21B and EPR data in the next section show that $[Q_A^-]_{max}$, which can be obtained by one electron photochemistry, reaches the same value in $CaCl_2$ PSII as in NaCl PSII. The slower rise in figure 22A (only after the first flash) indicates a delay in electron flow during the S_1 to S_2 transition.

Figure 23 shows a plot of the flash number dependence of variable Chl a fluorescence of the NaCl PSII measured at different times after each flash. The data sets for times longer than 220 μs show the biphasic oscillations.

Figure 24 shows the flash number dependence of the variable Chl a fluorescence of 1 M $CaCl_2$ treated PSII membranes. The data sets for times longer than 670 μs show the biphasic oscillations.

Figure 25 shows the flash number dependence of the variable Chl a fluorescence of NaCl PSII with 10 μM DCMU, $CaCl_2$ PSII with 10 μM DCMU, and $CaCl_2$ PSII with 10 μM DCMU and 1.5 mM HQ measured at 2.2 ms, 258 ms, and 4858 ms after each flash. HQ seems like a very slow donor to $CaCl_2$ PSII. 4858 ms after each flash, the variable Chl a fluorescence of the $CaCl_2$ PSII with 10 μM DCMU and 1.5 mM HQ

Figure 23. The flash number dependence of variable Chl a fluorescence of the 1 M NaCl treated PSII membranes lacking the 17 and 23 kD polypeptides, measured at different times after each flash. Open squares are for 40 μs data, closed squares for 220 μs, open triangles for 670 μs, and closed squares for 1170 μs.

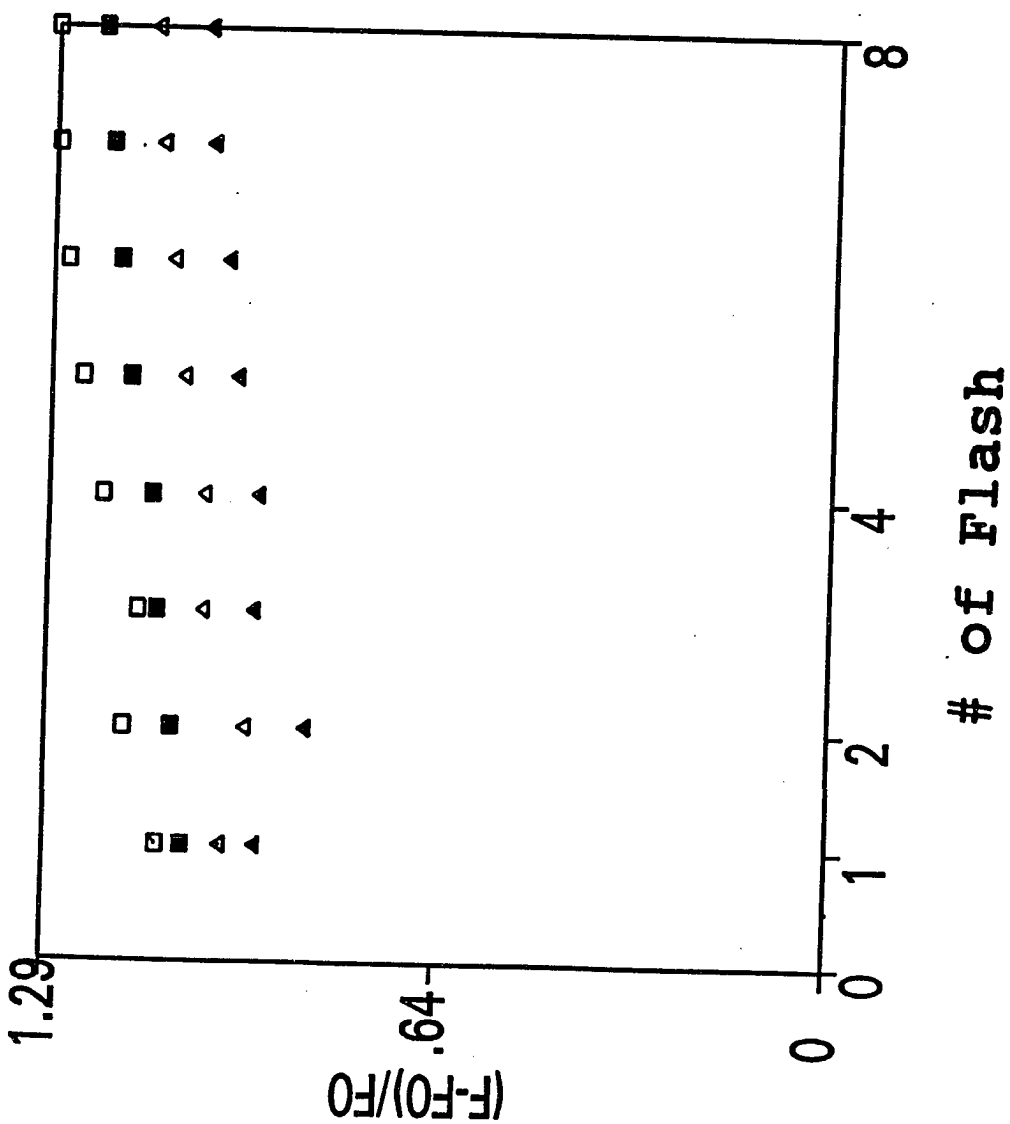

Figure 24. The flash number dependence of variable Chl a fluorescence of 1 M $CaCl_2$ treated PSII membranes measured at different times after each flash. Open squares are for 40 μs, closed squares for 220 μs, open triangles for 670 μs, and closed squares for 1170 μs.

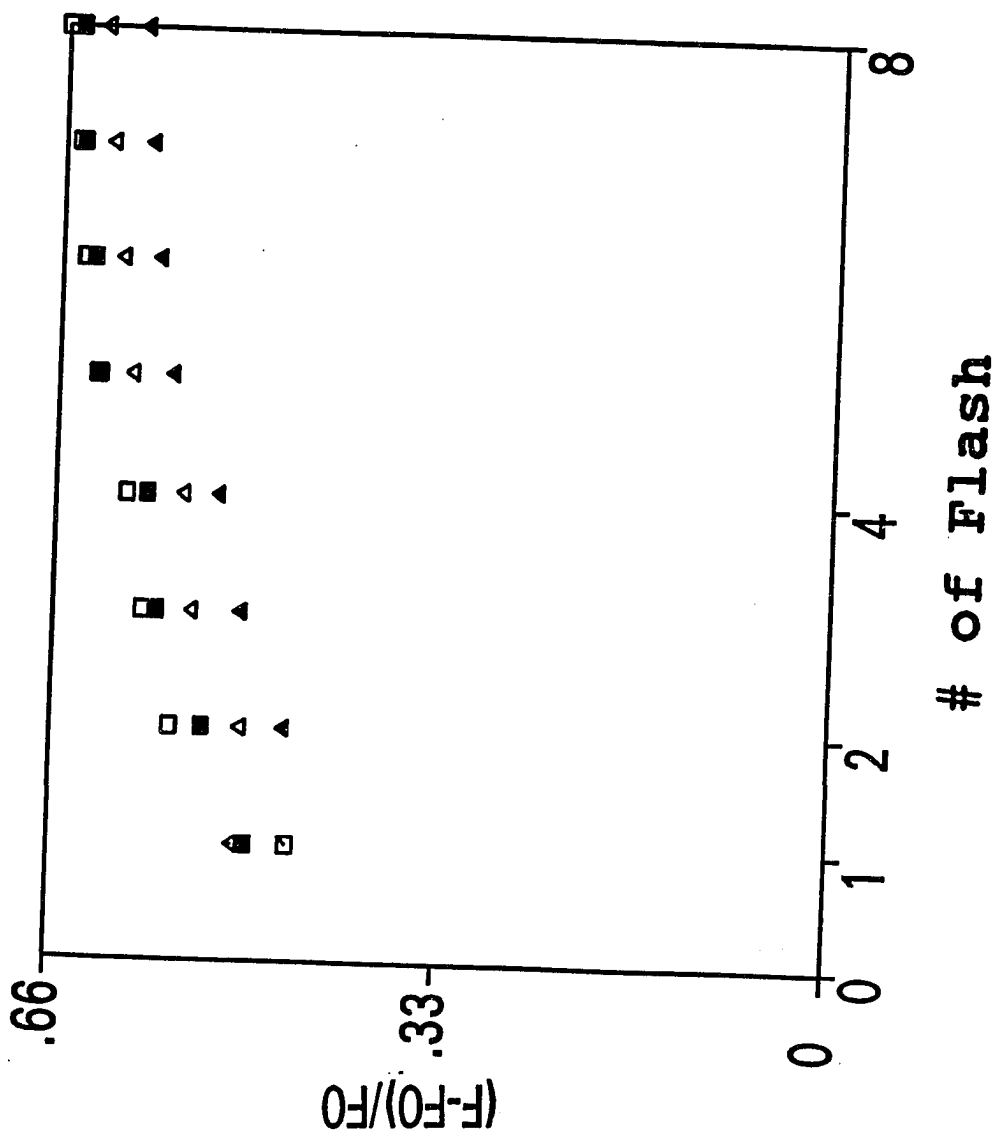

Figure 25. The flash number dependence of variable Chl *a* fluorescence of 1 M NaCl treated PSII membranes in the presence of 10 μM DCMU (a), 1 M $CaCl_2$ treated PSII membranes in the presence of 10 μM DCMU (b), and 1 M $CaCl_2$ treated PSII membranes in the presence of 10 μM DCMU and 1.5 mM hydroquinone (c) measured at 2.2 ms (A), 258 ms (B), and 4858 ms (C) after each flash.

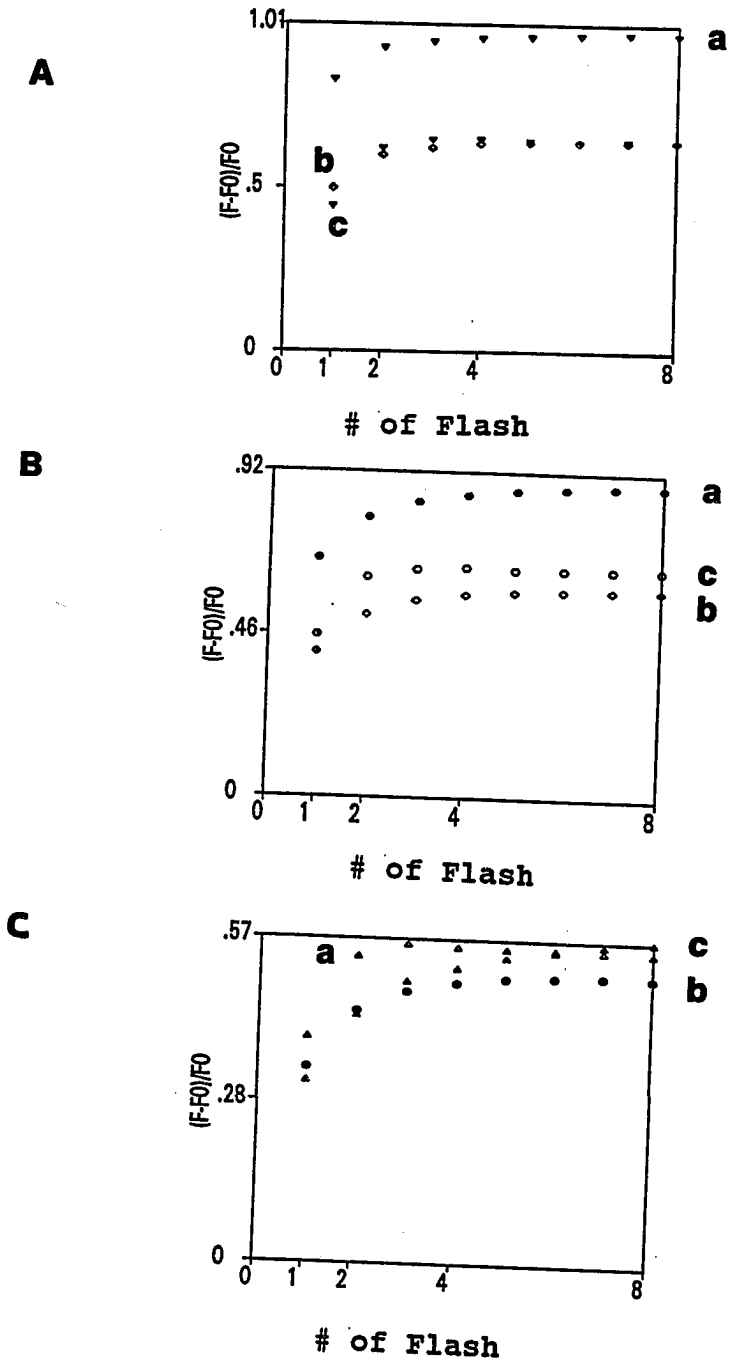

Figure 26. Variable Chl a fluorescence of 1 M $CaCl_2$ treated PSII membranes with 10 μM DCMU after the second flash on an extended time scale. Closed squares are with 2 mM HQ and open squares are without HQ.

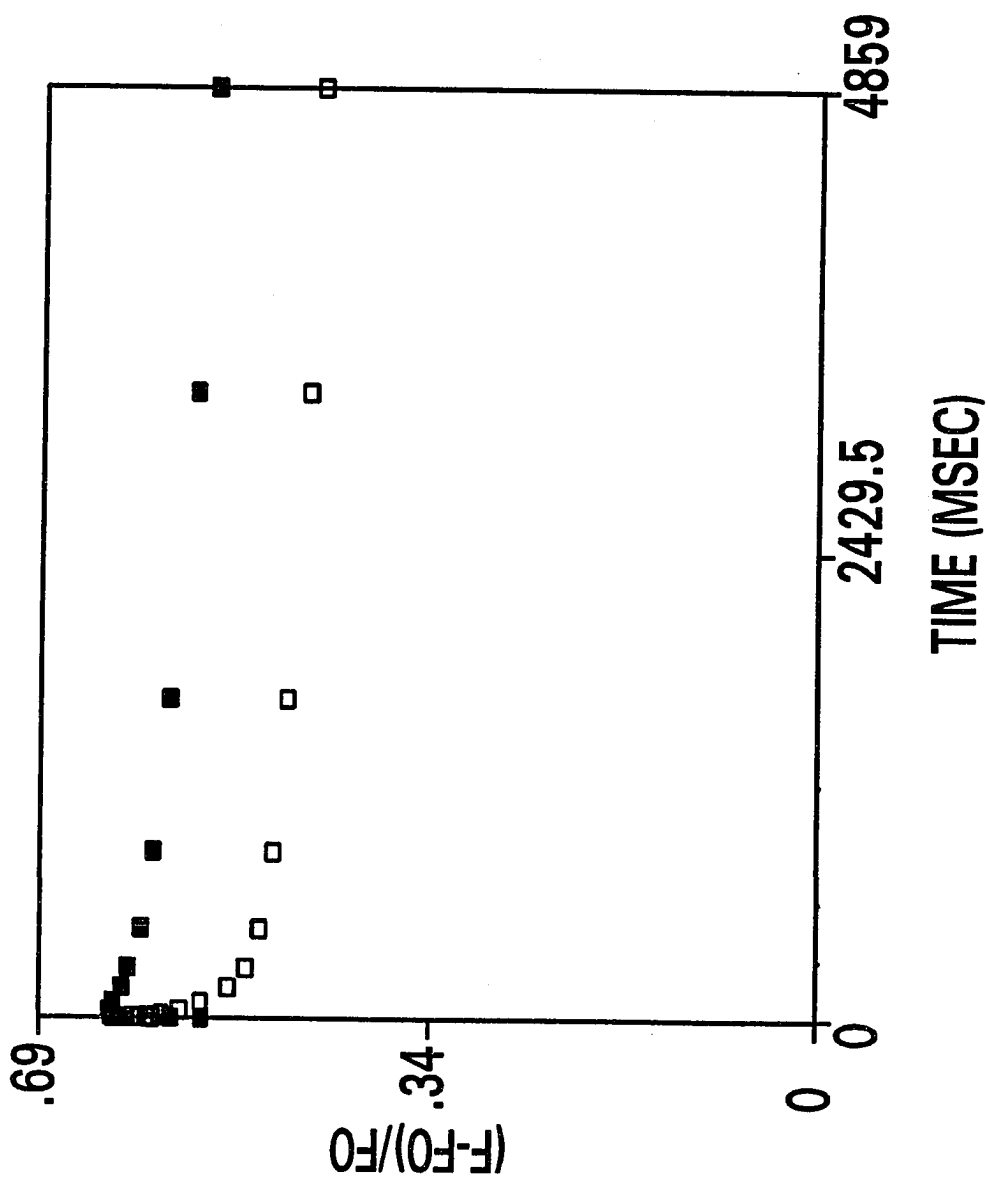

Figure 27. Variable Chl *a* fluorescence of 1 M NaCl treated PSII membranes and 1 M $CaCl_2$ treated PSII membranes with 10 μM DCMU after the first (a), the second (b), and the third flash (c): (A) 1 M NaCl treated PSII membranes; (B) 1 M $CaCl_2$ treated PSII membranes.

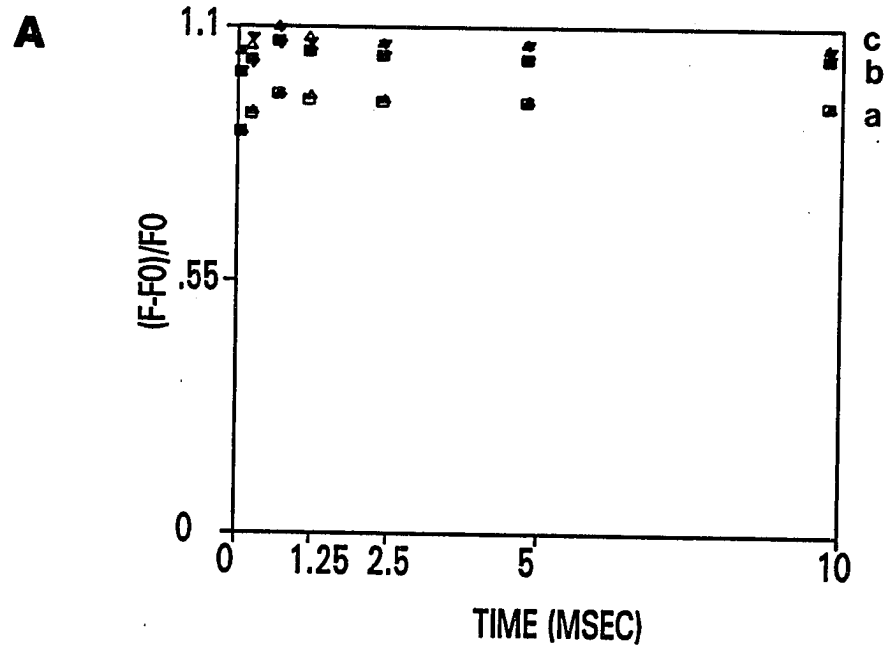

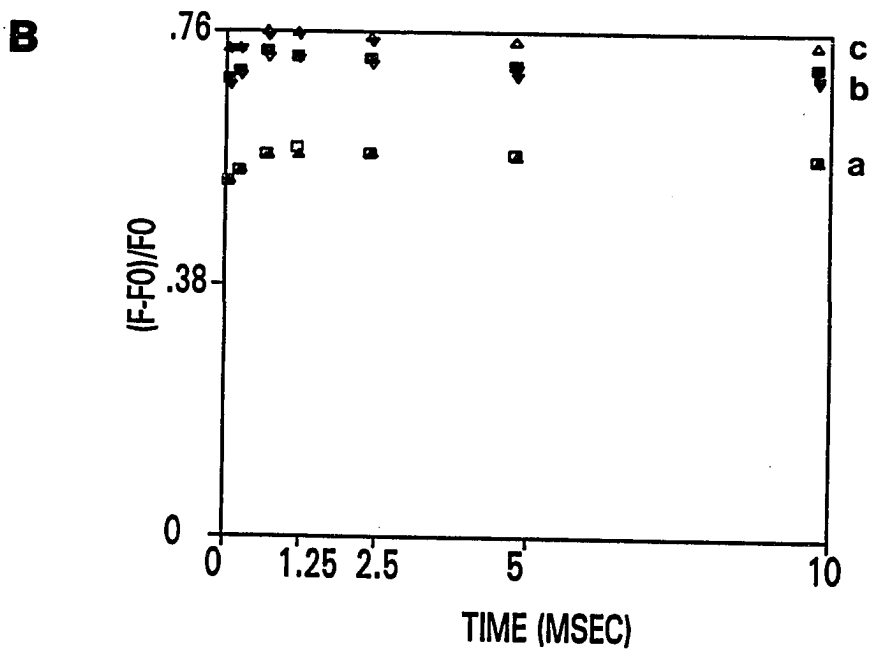

approaches the same value as that of the NaCl PSII with 10 μM DCMU. The results support the idea of the existence of a fluorescence quencher in $CaCl_2$ PSII.

Figure 26 shows the variable Chl a fluorescence of $CaCl_2$ PSII with 10 μM DCMU after the second flash on a time scale of seconds. Closed squares are with 2 mM HQ and open squares are without HQ. The difference between these two data sets shows the amount of back reaction from $Z^+PQ_A^-$ to $ZP^+Q_A^-$ (refer to scheme 1). Figure 27A shows the variable Chl a fluorescence of the standard with DCMU after the first, the second, and the third flash and figure 27B shows that of the $CaCl_2$ treated PSII.

IV-3-3 Discussion

The period-two oscillations in figures 23 and 24 can be explained in terms of scheme 1, modified from Kramer et al. (1990). After a saturating single-turnover actinic flash, $S_nZP^+Q_A^-$ forms on the subnanosecond time scale (Eckert, et al., 1991). An equilibrium between S_nZP^+ and S_nZ^+P will be reached in less than 1 μs. The equilibrium constant between these two states has been found to vary depending on which S-state is present at the time of the flash ($K \approx 2.2$ to 29 for thylakoids (Bretel et al., 1984). The turnover of the acceptor side of PSII has been extensively studied by fluorescence changes due to changes in $[Q_A^-]$ (see reviews by Crofts and Wraight, 1983). In the dark-adapted state and in PSII samples in which Q_B^- has been converted to Q_B (Van Gorkom et al., 1986), the system is in the state Q_AQ_B (both reduced). After the first saturating flash, the state $Q_A^-Q_B$ is formed; it becomes $Q_AQ_B^-$ after

Scheme 1

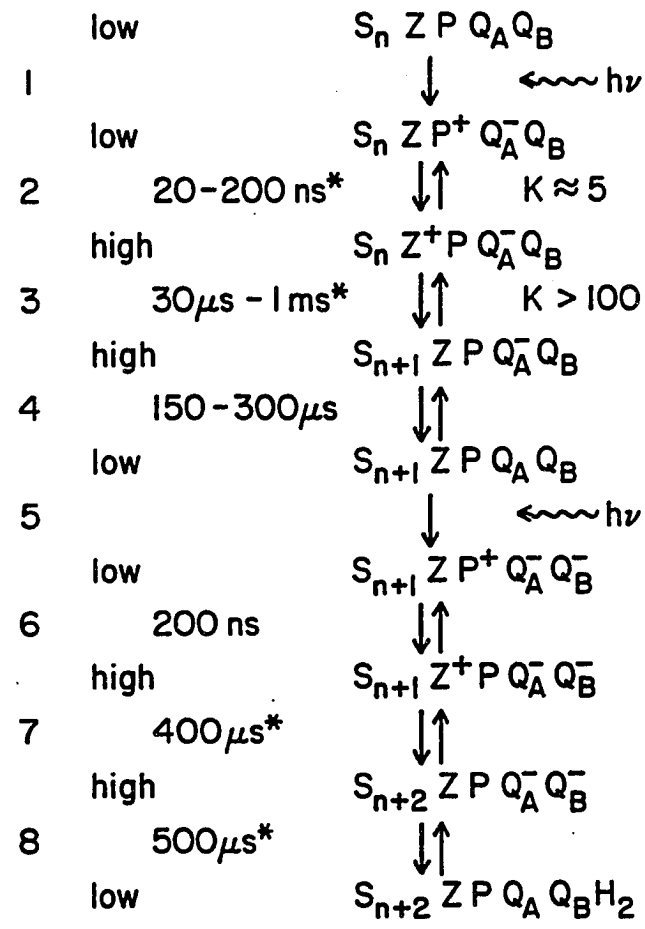

* dependent on S-state

"low" and "high" in the second column represents low and high fluorescence.

S_n is the S-state of the Kok cycle; Z is the donor to P_{680}^+; P is P_{680}; Q_A is the primary acceptor quinone of PSII; Q_B is the secondary acceptor quinone of PSII.

Figure 28. Normalized data of figure 27. The light energy transfer rate to P_{680} was assumed to be 0.05, F_{max} = 1.1 for 1 M NaCl treated PSII membranes and F_{max} = 0.76 for 1 M $CaCl_2$ treated PSII membranes. Open symbols are for NaCl PSII and the closed symbols are for $CaCl_2$ PSII.

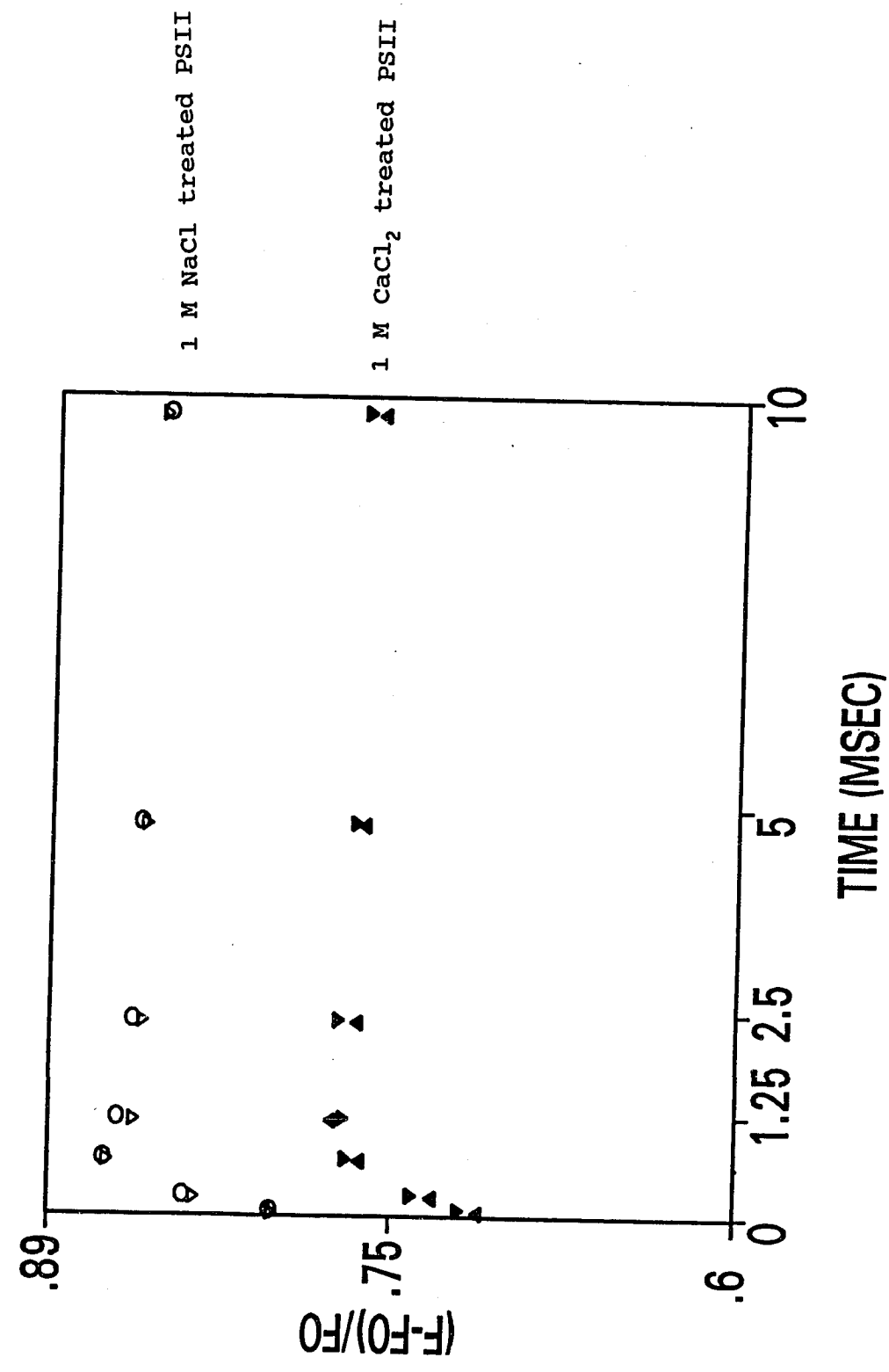

110

Figure 29. A plot of log $((y_{max} - y)/y_{max})$ versus time. The early rise of $y = (F - F_o)/F_o$ up to y_{max} is due to the transition from $S_1Z^+PQ_A^-Q_B$ to $S_2ZPQ_A^-Q_B$, both of which are highly fluorescent. Extrapolation of the first 4 points of figure 28 (refer to section IV-3-3): (a) 1 M NaCl treated PSII membranes; (b) 1 M $CaCl_2$ treated PSII membranes.

(a)

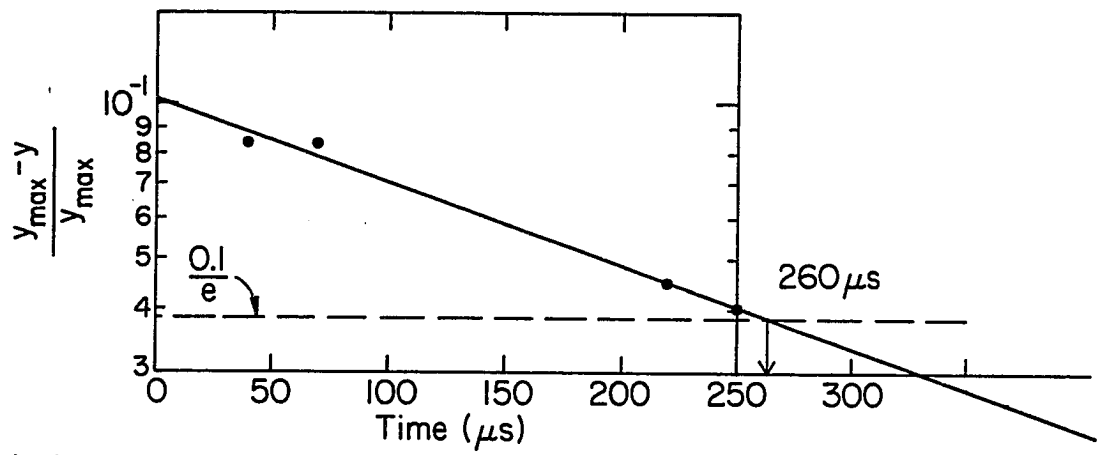

(b)

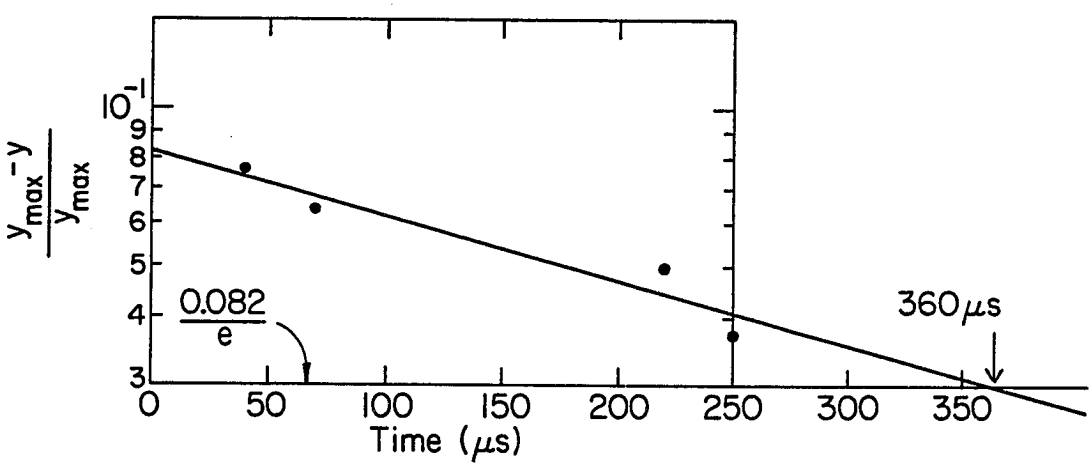

an electron is transferred to Q_B. After the second flash, the state $Q_A^-Q_B^-$ is formed, which upon protonation, becomes $Q_AQ_BH_2$. The Q_BH_2 diffuses away from the binding site and another plastoquinone from the PQ pool binds to the Q_B site. The Chl *a* fluorescence yield, reflecting $[PQ_A^-]$, therefore changes, giving rise to a binary pattern of decay rates for the state Q_A^- (Bowes and Crofts, 1980).

Figure 28 contains the normalized data of figure 27 assuming the probability p of light energy transfer to P_{680} is 0.05 and F_{max} is 1.1 for the standard and F_{max} is 0.76 for $CaCl_2$ treated PSII (Kramer et al, 1990). Open symbols are for the NaCl PSII and the closed symbols are for $CaCl_2$ PSII. As shown in scheme 1, the highly fluorescent state $S_1Z^+PQ_A^-Q_B$ is in equilibrium with the nonfluorescent state $S_1ZP^+Q_A^-Q_B$ long before the first measurement at 40 μs. The early rise of $y = (F - F_o)/F_o$ up to y_{max} is due to the transition from $S_1Z^+PQ_A^-Q_B$ to $S_2ZPQ_A^-Q_B$, both of which are highly fluorescent. A plot of log $((y_{max} - y)/y_{max})$ versus t then yields K as the intercept at t = 0 and the transition rate $S_1Z^+PQ_A^-Q_B$ to $S_2ZPQ_A^-Q_B$ as the slope. Figure 29 shows this extrapolation for the NaCl PSII (A) and the $CaCl_2$ PSII (B) using the first 4 points of figure 28. In figure 29A, the K value of the transition from $S_1ZP^+Q_A^-Q_B$ to $S_1Z^+PQ_A^-Q_B$ for the NaCl PSII is about 10 while in figure 29B, that for the $CaCl_2$ PSII is about 12. Without further experiments it is impossible to state that these K values are significantly different. The transition time from $S_1Z^+PQ_A^-Q_B$ to $S_2ZPQ_A^-Q_B$ for the NaCl PSII is about 260 μs, shile it is 360 μs for $CaCl_2$ PSII.

The time for the S_1 to S_2 transition of $CaCl_2$ PSII is thus 40 % longer than that of NaCl PSII. This time is still a small

fraction of the overall oxygen evolution cycle, which was found to be 12 ms in IV-2-3, for $CaCl_2$ PSII. The bulk of the slow-down then must be found in the other transitions including dark reactions.

IV-4 EPR

IV-4-1 Rationale

When the three extrinsic polypeptides (17, 23, and 33 kD) are removed from PSII, Mn remains bound to PSII membranes, but under normal assay conditions less than 40 % of the oxygen evolving activity of the NaCl PSII is retained.

Here, the $S_1 \rightarrow S_2$ state transition in $CaCl_2$ treated PSII has been investigated by the S_2 state multiline EPR signal, which is a sensitive indicator of the Mn complex.

IV-4-2 Results

The NaCl PSII did not produce the S_2 state g = 4.1 EPR signal nor a cyt b_{559}^+ signal (cyt b_{559} is in the low potential form which can not be photooxidized). Instead, a Chl^+ was the alternative electron donor at low temperature illumination (77 K). The intensity of the $Fe^{2+} \cdot Q_A^-$ can be used as a measure of the extent of stable charge separation from the total population of oxidized electron donors. In $CaCl_2$ treated PSII membranes, the two species that donate electrons are Chl and the Mn complex (Miller et al., 1987).

Figure 30 A and B show the 'light' minus 'dark' EPR difference spectra near g = 2 of the NaCl PSII and the $CaCl_2$ PSII membranes in

Figure 30. EPR multiline difference spectra of the S_2 state ('light') minus the S_1 state ('dark') of (a) 1 M NaCl treated PSII membranes; (b) 1 M $CaCl_2$ treated PSII membranes in the presence of PPBQ, an electron acceptor. [Chl] = 6 mg Chl/ml illuminated at 200 K. Instrumental conditions are the same as figure 5 except microwave frequency = 9.14 GHz.

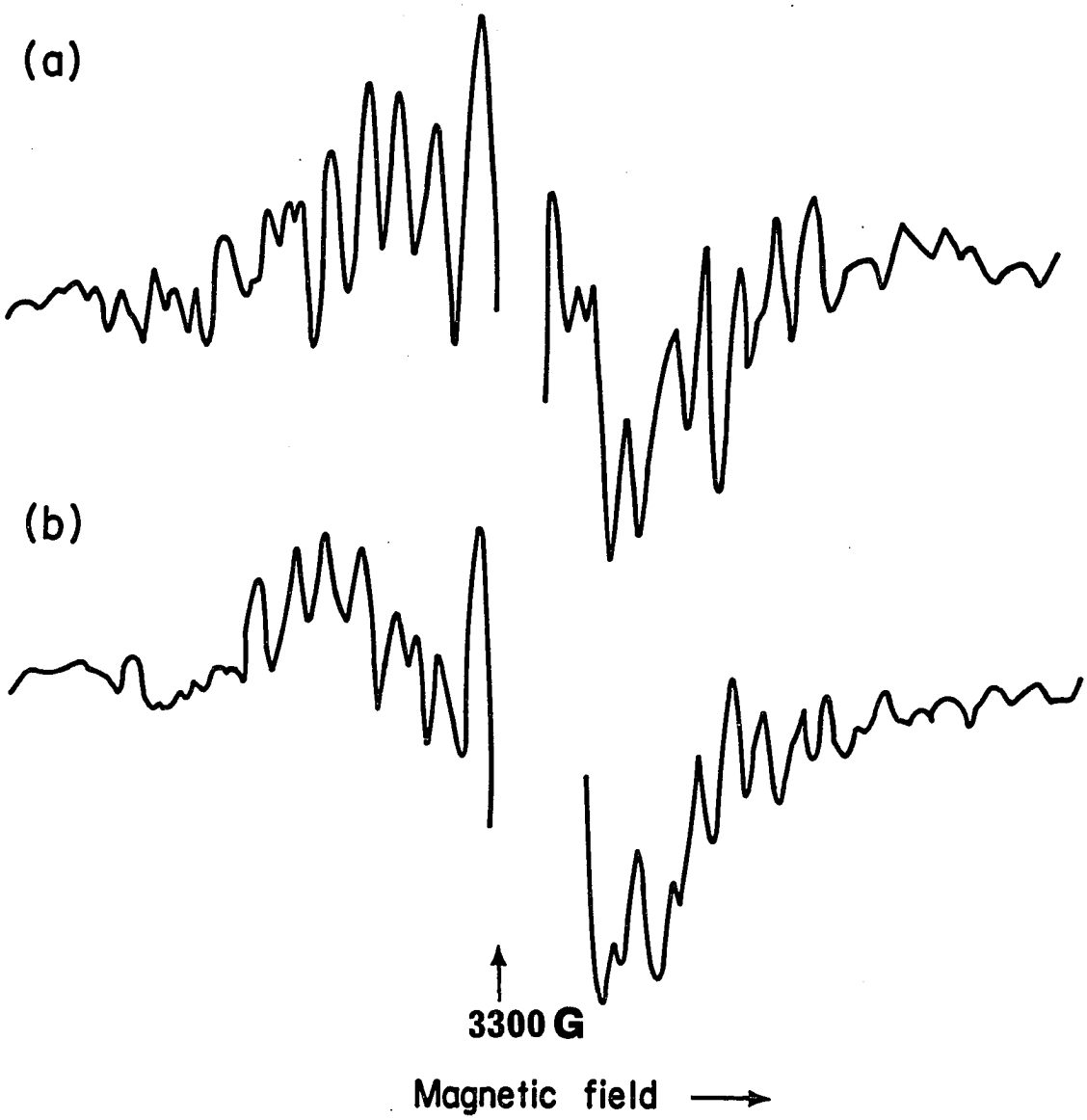

the presence of PPBQ as electron acceptor. They were obtained by subtracting the EPR spectra of the dark adapted samples from those of a sample illuminated at 200 K. The difference signal is mainly due to the manganese in the S_2 state of the oxygen evolving complex except for the Q_A^- signal near g = 1.84. The sample concentrations based on the content of chlorophyll were the same in figure 30 A and B but the intensity of the multiline signal in $CaCl_2$ PSII is about 60 % of that in the NaCl PSII while the intensity of the Q_A^- signal (g = 1.82) is same for both spectra.

IV-4-3 Discussion

The sample concentrations based on the content of chlorophyll were the same in figure 30 A and B but the intensity of the multiline signal in the $CaCl_2$ PSII is about 60 % of that in the NaCl PSII while the intensity of the Q_A^- signal (g = 1.82) is same for both spectra. It could have been possible to get more than 60 % multiline signal if the sample had no PPBQ. The sample was illuminated at 200 K for 5 minutes and warmed up to room temperature for 30 minutes for dark-adaptation and the illumination was repeated. This process could cause photoinhibition which will be discussed in more detail in chapter V. EPR data shows that $CaCl_2$ PSII reduces Q_A^- fully as much as the NaCl PSII because at low temperature, there is an alternative donor, Chl which donates electron to Z^+.

From the results, the 33 kD polypeptide does not seem to supply ligands to Mn because the S_2 signal is normal in shape. However, PSII without the 33 kD polypeptide is slowed down in the

S-state transition and only 40 % oxygen is evolved at 1200 $\mu E \cdot m^{-2} \cdot s^{-1}$ compared to PSII with 33 kD polypeptide.

In summary, the 33 kD polypeptide is not required for low-level oxygen evolution and therefore has no catalytic role in the WOC. The same conclusion was reached by Andersson and Styring (1991). Interestingly, the 33 kD protein of cyanobacteria may not be required for oxygen evolution as suggested by recent studies on a genetically engineered Synechocystis sp. PCC 6803 mutant lacking the 33 kD protein (Burnap and Sherman, 1990). The removal of the 33 kD protein, on the other hand, slows down the S cycle by an overall factor of three. The rate of the S_1 -> S_2 transition, however, decreased by a factor of 1.4 only, and one may speculate that the other steps are slowed down more, in particular the dark reaction, which may involve considerable conformational change. The present data do not allow to deduce any change on the acceptor side, but the low fluorescence of $CaCl_2$ treated PSII remains to be explained. The presence of quenchers may be responsible for the low fluorescence, and Chl^+ as an alternate donor to P_{680}^+ is a likely candidate. Again, the slow electron transfer rate from the normal donor, the WOC, could explain an excessive level of Chl^+.

Chapter V. PHOTOACTIVATION AND PHOTOINHIBITION

V-1. Optimizing conditions for photoactivation

V-1-1 Rationale

The Mn cluster is dissociated from the complex by treatment with NH_2OH with concomitant inactivation of oxygen evolution. It can be reassembled from the inactivated complex by incubation with Mn^{2+} under illumination to restore partial oxygen evolution (Radmer and Cheniae, 1977). This light-dependent reconstitution of the Mn-cluster or photoactivation presumably involves binding at normal binding sites oxidation of Mn^{2+} by PSII followed by assembly of the oxidized Mn into a functionally active Mn cluster in the water-oxidation site of the PSII complex (Radmer and Cheniae, 1971; Cheniae and Martin, 1973; Inoue et al., 1975; Ono and Inoue, 1987; Tamura and Cheniae, 1987, 1988). The process requires not only Mn^{2+} but also Ca^{2+} (Yamashita and Tomita, 1974, 1976; Ono and Inoue, 1983a and b; Miller and Brudvig, 1989) and Cl^- (Yamashita and Ashizawa, 1985) as essential inorganic cofactors. Tamura and Cheniae (1987) succeeded in photoactivating oxygen evolution in NH_2OH treated PSII membranes by illuminating the treated membranes in the presence of 1 mM $MnCl_2$, 50 mM $CaCl_2$ and 100 μM DCIP. Miyao and Inoue (1991) reported that they achieved higher photoactivation by lowering the DCIP concentration to 5 μM. In our experiment, lowered [DCIP] did not increase photoactivation in contradiction of Miyao and Inoue (1991).

In this study, the conditions for photoactivation are reexamined in more detail by using the NaCl PSII, i.e., PSII membranes lacking the 17 and 23 kD extrinsic polypeptides.

V-1-2 Results

NH_2OH (0.25 mM) treatment of the NaCl PSII lacking the 17 and 23 kD polypeptides at 4°C for 30 minutes in the dark reduced the oxygen-evolving activity at 1200 $\mu E \cdot m^{-2} \cdot s^{-1}$ to 4 % of that before the treatment while over 80 % Mn was depleted. In some experiments, the sample was treated with 0.25 mM NH_2OH twice. When NH_2OH treated NaCl PSII was incubated under illumination with 1 mM Mn^{2+} but without DCIP, the oxygen evolving activity did not recover. Table 9 shows the effect of different DCIP concentrations on photoactivation: with 40 μM DCIP about 24 % of the original activity was recovered (see the legend of Table 9 for other conditions). Table 10 shows the effect of different light intensities on the photoactivation rate with 40 μM DCIP: 20 - 33 $\mu E \cdot m^{-2} \cdot s^{-1}$ (desk fluorescent lamp) gave essentially the same photoactivation (27 %) (for other details, see the legend of Table 10). With 40 μM DCIP, the optimum illuminating time was 20 - 30 minutes for photoactivation as shown in Table 11. Furthermore, 0.8 - 1 M sucrose in the reconstitution medium gave the best results (data not shown).

By applying all of the above optimized conditions, I was able to get the results shown in Table 12. The Mn depleted (NH_2OH-treated) PSII had 4 % of the original activity of the NaCl PSII. Incubation in the reconstitution buffer alone had no effect, but the activity recovered to 25 % of the original after illumination

Table 9

The effect of different DCIP concentration on photoactivation of 1 M NaCl PSII samples lacking the 17 and 23 kD extrinsic proteins

DCIP concentration (μM)	Oxygen evolving activity
0	3.1 %
3	15.9 %
6	19.2 %
9	15.9 %
20	22.3 %
40	24.0 %
60	22.3 %

100 % is for the NaCl PSII, i.e., 600 μM O_2/mg Chl/ml. The photoactivation medium had 0.4 M sucrose, 110 mM NaCl, 1 mM $MnCl_2$, 20 mM MES (pH 6.5), and 20 mM $CaCl_2$ at 250 μg Chl/ml. The light intensity was 12 $\mu E \cdot m^{-2} \cdot s^{-1}$. 10 ml beaker for the sample size 0.5 ml (2 mm sample thickness), 30 min photoactivation.

Oxygen evolution activity was assayed in the presence of 200 μM PPBQ at 10 μg Chl/ml.

Table 10

The effect of different light intensity on the photoactivation with 40 μM DCIP

Light intensity ($\mu E \cdot m^{-2}s^{-1}$)	Oxygen evolving activity
33	26.8 %
20	27.2 %
18	24.5 %
14	23.5 %
12	20 %
8	12.7 %

100 % is for the NaCl PSII, i.e., 600 μM O_2/mg Chl/ml. The photoactivation medium had 0.8 M sucrose, 110 mM NaCl, 1 mM $MnCl_2$, 20 mM MES (pH 6.5), and 20 mM $CaCl_2$ at 250 μg Chl/ml. 10 ml beaker for the sample size 0.5 ml (2 mm sample thickness), 30 min photoactivation.

Oxygen evolution activity was assayed in the presence of 200 μM PPBQ at 10 μg Chl/ml.

Table 11

The effect of different illumination time on photoactivation with 40 μM DCIP

Photoactivation time (min)	Oxygen evolving activity
10	22 %
20	27 %
30	26 %
40	20 %

100 % is for the NaCl PSII, i.e., 600 μM O_2/mg Chl/ml. The photoactivation medium had 0.8 M sucrose, 110 mM NaCl, 1 mM $MnCl_2$, 20 mM MES (pH 6.5), and 20 mM $CaCl_2$ at 250 μg Chl/ml. 10 ml beaker for the sample size 0.5 ml (2 mm sample thickness) at 12 $\mu E \cdot m^{-2}s^{-1}$.

Oxygen evolution activity was assayed in the presence of 200 μM PPBQ at 10 μg Chl/ml.

Table 12

The oxygen evolving activity and DCIP reduction rate of different preparations

Samples	Oxygen activity	DCIP reduction
NaCl PSII	100 %	100 %
NH_2OH treated on NaCl PSII	4 %	2 %
Before photoactivation (in reconstitution buffer)	4 %	-
After photoactivation (After illumination)	25 %	-
After 2 mM EDTA wash	30 %	32 %

Photoactivation buffer contained 110 mM NaCl, 0.8 M sucrose, 20 mM $CaCl_2$, 20 mM MES (pH 6.5), 40 μM DCIP, and 1 mM Mn. Light intensity was 25 - 35 $\mu E \cdot m^{-2} \cdot s^{-1}$ of cool fluorescent lamp. Sample size was 2.5 ml of 0.25 mg Chl/ml at a time, 100 ml beaker was used to have 2 mm sample thickness. Photoactivation was done on the shaker (gently shaking) for 30 min.

The oxygen evolving activity or DCIP reduction with 1200 $\mu E \cdot m^{-2} \cdot s^{-1}$. Oxygen evolution activity was assayed in the presence of 200 μM PPBQ at 10 μg Chl/ml; DCIP reduction rate was assayed in the presence of 50 μM DCIP at 10 μg Chl/ml. The rates were determined by following the diasppearance of absorbance at 600 nm.

of the sample. This activity improved further to a value of 30 % after a 2 mM EDTA wash; evidently, the EDTA wash removed the excess Mn only, but not the one bound in the photoactivation process.

V-1-3 Discussion

As a result of several trials the following conditions were found to optimize photoactivation: The photoactivation buffer contained 110 mM NaCl, 0.8 M sucrose, 20 mM $CaCl_2$, 20 mM MES (pH 6.5), 40 μM DCIP, and 1 mM Mn. The light intensity was 25 - 35 $\mu E \cdot m^{-2} \cdot s^{-1}$ of a cool fluorescent lamp. Samples of 2.5 ml with 0.25 mg Chl/ml at a time were used in a 100 ml beaker to have a sample thickness of 2 mm. Photoactivation was done on a shaker (gently shaking) for 30 minutes. I also tried EDTA wash for the first time on photoactivated samples. EDTA washed out the unnecessary extraneous Mn and improved oxygen evolving activity (see Table 12 2and refer to section V-3).

V-2. Effect of other metal ions on the photoactivation

V-2-1 Rationale

In view of the successful reconstitution of NH_2OH treated PSII with Mn^{2+}, it would be interesting to find out whether any other metal ions can replace Mn, bind in Mn binding sites, and inhibit oxygen evolution. Such metal complexes might show interesting EPR and/or ENDOR spectra that may allow one to identify the ligands at that binding site.

V-2-2 Results

Figure 31 shows the oxygen evolving activity of different preparations used in our study. $FeCl_2$ (1 mM) and $CoCl_2$ (1 mM) could not reconstitute the oxygen evolving activity of NH_2OH treated PSII membranes in contrast to $MnCl_2$ (1 mM). Different metal ions were then added along with Mn to see whether there is competetive binding between those metal ions and Mn. The results are shown in Table 13. In this experiment, Mn (1 mM) alone reconstituted 37 % of the original activity, Mn with Co (1 mM) reconstituted only 10 %, Mn with Fe^{2+} (1 mM) reconstituted only 2 %, and Mn with Fe^{3+} (1 mM) reconstituted 27 %. It is shown that these metal ions interfered with Mn rebinding in the order (highest to lowest): $Fe^{2+} > Co^{2+} > Fe^{3+}$.

Table 14 shows the metal concentrations determined by plasma emission spectroscopy of different reconstituted samples. While NaCl PSII has 4.1 Mn/RC, i.e., the full complement, the Mn^{2+} reconstituted and EDTA washed sample had only 1.6 Mn/RC, i.e., 40 % of the full complement. Both samples also contained ~ 7.8 Fe/RC, although only 3 Fe/RC are known to be bound spedifically, two in Cyt b-559 and one in the Q_A Q_B binding site. Addition of 1 mM Fe^{2+} to the Mn^{2+} in the reconstitution medium with or without subsequent EDTA wash, reduced the bound Mn to 0.43/RC or 10 % of the full complement, while the number of bound iron increased to 270/RC. Addition of 1 mM Co^{2+} to the Mn^{2+} in the reconstitution medium followed by EDTA wash, finally, reduced the Mn content to 0.57/RC, while only 0.2 Co/RC were bound and the Fe^{2+} stayed as 7.7/RC.

Figure 31. Trace of the oxygen evolving activity after photoactivation by different metal ions: (a) 1 M NaCl treated PSII membranes lacking the 17 and 23 kD proteins; (b) 0.25 mM NH_2OH treated (a); (c) Fe^{2+} (1 mM) "reconstituted" NH_2OH treated PSII membranes. 1 mM Co^{2+} addition gave the same result; (d) Mn^{2+} reconstituted NH_2OH treated PSII membranes. NH_2OH treated membranes were resuspended in reconstitution buffer (0.8 M sucrose, 110 mM NaCl, 40 μM DCIP, 20 mM MES (pH 6.5), and 20 mM $CaCl_2$) to 250 μg Chl/ml. The oxygen evolution assay was done at 1200 $\mu E \cdot m^{-2} \cdot s^{-1}$ in the presence of 200 μM PPBQ at 10 μg Chl/ml.

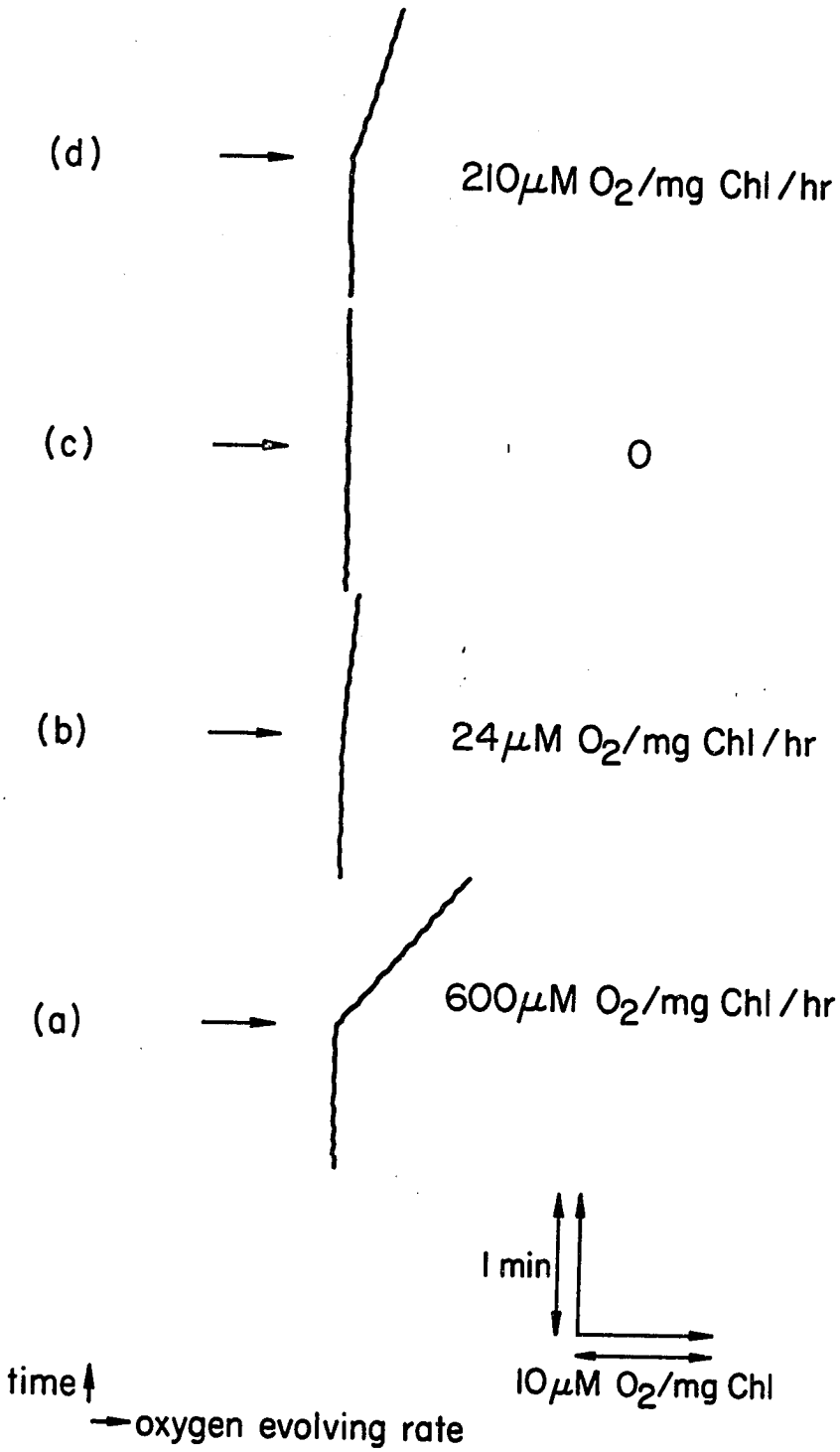

Table 13

The oxygen evolving activity of samples photoactivated with Mn^{2+} and other metal ions.

Samples	Oxygen evolving activity
NaCl PSII	100 %
NH_2OH treated NaCl PSII	4 %
Mn^{2+} (1 mM) reconstituted + 2 mM EDTA wash	37 %
Co^{2+} (1 mM) + Mn^{2+} (1 mM) reconstituted	15 %
Co^{2+} (1 mM) + Mn^{2+} (1 mM) reconstituted + 2 mM EDTA wash	10 %
Fe^{2+} (1 mM) + Mn^{2+} (1 mM) reconstituted + 2 mM EDTA wash	2 %
Fe^{3+} (1 mM) + Mn^{2+} (1 mM) reconstituted + 2 mM EDTA wash	27 %

Photoactivation buffer contained 110 mM NaCl, 0.8 M sucrose, 20 mM $CaCl_2$, 20 mM MES (pH 6.5), 40 μM DCIP, and 1 mM Mn. Light intensity was 25 - 35 $\mu E \cdot m^{-2} \cdot s^{-1}$ of cool fluorescent lamp. Sample size was 2.5 ml of 0.25 mg Chl/ml at a time, 100 ml beaker was used to have 2 mm sample thickness. Photoactivation was done on the shaker (gently shaking) for 30 min.

The oxygen evolving activity was measured at 1200 $\mu E \cdot m^{-2} \cdot s^{-1}$. Oxygen evolution activity was assayed in the presence of 200 μM PPBQ at 10 μg Chl/ml.

Table 14

Ion concentrations measured by plasma emission spectroscopy of different reconstitution samples

Samples	Concentration* (mg/l)
NaCl PSII	4.1 Mn/RC 7.9 Fe/RC 0 Co
Mn^{2+} (1mM) reconstituted + 2 mM EDTA wash	1.6 Mn/RC 7.8 Fe/RC 0 Co
Mn^{2+} (1mM) + Fe^{2+} (1mM) reconstituted	0.43 Mn/RC 270 Fe/RC 0 Co
Mn^{2+} (1mM) + Fe^{2+} (1mM) reconstituted + 2 mM EDTA wash	0.35 Mn/RC 270 Fe/RC 0 Co
Mn^{2+} (1mM) + Co^{2+} (1mM) reconstituted + 2 mM EDTA wash	0.57 Mn/RC 7.7 Fe/RC 0.2 Co/RC

All data were obtained against the blank buffer (110 mM NaCl, 0.8 M sucrose, 20 mM $CaCl_2$, 20 mM MES (pH 6.5)).

The plasma emission data were obtained at the Chl concentration of 0.5 mg/ ml.

The inability to reconstitute 100 % of oxygen evolution activity by photoactivation seems to be due to the inability to reconstitute fully the 4 Mn/RC. If 4 Mn/RC gives 100 % activity, 1.6 Mn/RC would give a maximum of 40 % activity. This fits well with the 37 % reconstitution.

V-2-3 Discussion

The oxygen evolving activity of the EDTA washed, reconstituted sample is 30 - 37 % of the original while the Mn content is 40 %. Therefore about 60 % of the centers have Mn free reaction center. It is possible that our Mn depleted PSII (0.25 mM NH_2OH treated in 1 M NaCl pretreated PSII) lost the ability of reconstitution due to the modifications of the center, possibly its destruction, or due to photoinhibition during photoactivation process.

In figure 31, it was shown that Fe^{2+}, Fe^{3+}, and Co^{2+} could not reconstitute the oxygen evolving activity in Mn depleted PSII but they interfered with Mn reconstitution as shown in Table 13. It remains to be studied whether Fe^{2+} and Co^{2+} inhibit Mn^{2+} binding 'competitively' or not. Table 15 summarizes the configurations and ionic radii of Mn, Fe, and Co. Since the radius of Co^{2+} and Fe^{2+} are the same as that of Mn^{2+} and the radius of Co^{3+} and Fe^{3+} are the same as that of Mn^{3+}, it is plausible that Co^{2+} and Fe^{2+} can bind to Mn^{2+} binding sites; all these metal ions are known to be stable in aqueous solutions as Mn^{2+}, Co^{2+}, and Fe^{3+}. Mn^{2+} is believed to be oxidized to Mn^{3+} when it binds to PSII membranes. Fe^{2+} has a stronger tendency to be oxidized to Fe^{3+} (d^5 is more stable than d^6) than Mn^{2+}

and Co^{2+}. According to the result in Table 14, Fe^{2+} binds not only to the Mn site but also to many nonspecific sites in PSII membranes. There must be many possible Fe binding sites in PSII membranes unrelated to the WOC. Fe^{2+} tends to be oxidized to Fe^{3+} in aqueous solution, and Fe^{3+} will bind more strongly to the proteins. Co^{2+} interferes with Mn reconstitution in Mn depleted PSII but it does not affect the function of the Mn complex of the NaCl PSII with intact Mn complex (see section V-3).

V-3 Photoinhibition

V-3-1 Rationale

Photoactivation is the process by which the catalytic Mn complex of PSII is assembled from Mn^{2+} ions and oxygen evolving activity is restored. The term photoactivation reflects the finding that assembly of the Mn complex is dependent on illumination of PSII (Cheniae and Martin, 1967). Illumination is necessary for photoactivation, but it can also result in photoinhibition, causing loss of primary photochemical activity. Photoinhibition has been proposed to result from oxidative damage to PSII, a consequence of the powerful oxidant (P_{680}^{+}) generated upon light-induced charge separation (Thompson and Brudvig, 1988).

We need to explain why the photoactivation process is not 100 % and about 60 % of the WOC remain without bound Mn. Several papers have been published on the inactivation of PSII even by Mn (Izawa et al., 1983) and Co (Tripathy and Mohanty, 1981, 1983). It is

Table 15

Summary of the configurations and ionic radii of Mn, Fe, and Co.

	Configuration	ionic radius (Å)
Mn^{2+}	$3d^5$	0.80
Mn^{3+}	$3d^4$	0.66
Fe^{2+}	$3d^6$	0.74
Fe^{3+}	$3d^5$	0.64
Co^{2+}	$3d^7$	0.72
Co^{3+}	$3d^6$	0.63

likely that the photoactivated PSII complexes are inevitably exposed to this type of inactivation during the photoactivation treatment. The following section deals with photoinhibition which happens during the process of photoactivation described in sections V-1 and V-2.

V-3-2 Results

Table 16 shows the effect of various treatments on the oxygen evolving activity of the NaCl PSII. Illuminating the NaCl PSII at 30 $\mu E \cdot m^2 \cdot s^{-1}$ in 40 μM PPBQ at room temperature reduced oxygen evolving activity to 74 % of the original after 30 minutes while 40 μM DCIP reduced the activity to 60 %. Comparison of lines 3 and 5 in Table 16 showed that DCIP is a more efficient chemical not only for photoactivation but also for photoinhibition than PPBQ. In the presence of 40 μM DCIP, 1 mM Co did not influence the effects of 30 minute illumination at 30 $\mu E \cdot m^{-2} \cdot s^{-1}$ on the oxygen evolution activity of the NaCl PSII. In contrast, 1 mM Mn reduced oxygen evolving activity to 14 % of the original.

Figure 32 shows the oxygen evolving activity assay of the NaCl PSII for 5 minutes at 1200 $\mu E \cdot m^{-2} \cdot s^{-1}$ with and without the divalent metal ions, Mn^{2+}, Co^{2+}, or Fe^{2+} in the assay medium. The presence of 1 mM Co^{2+} in the assay medium did not affect the activity but the presence of 1 mM Mn^{2+} and 1 mM Fe^{2+} decreased significantly the rate of oxygen evolution with Fe^{2+} being most effective followed by Mn^{2+}.

Table 16

The effect of various treatments on the oxygen evolving activity of 1 M NaCl treated PSII membranes lacking 17 and 23 kD proteins.

Samples	Oxygen evolving activity w/ 20 μM PPBQ	Oxygen evolving activity w/ 40 μM DCIP
NaCl PSII	100 %	13 %
Std, 30 min dark[a] incubated	97 %	-
Std + 40 μM PPBQ[a] 30 min, illuminated[b]	74 %	-
Std + 40 μM DCIP[a] 30 min, dark	100 %	-
Std + 40 μM DCIP[a] 30 min, illuminated[b]	60 %	5 %
Std + 1 mM Mn[a] 30 min, dark	83 %	10 %
Std + 1 mM Mn + 40 μM DCIP[a] 30 min, illuminated[b]	14 %	-
Std + 1 mM Co[a] 30 min, dark	88 %	10 %
Std + 1 mM Co + 40 μM DCIP[a] 30 min, illuminated[b]	60 %	-

[a] The sample had been diluted to 0.25 mg Chl/ml for the treatment.

[b] Light intensity was 30 $\mu E \cdot m^{-2} \cdot s^{-1}$.

Photoactivation buffer contained 110 mM NaCl, 0.8 M sucrose, 20 mM $CaCl_2$, 20 mM MES (pH 6.5). Light intensity was 25 - 35 $\mu E \cdot m^{-2} \cdot s^{-1}$ of cool fluorescent lamp. The sample size was 2.5 ml of 0.25 mg Chl/ml at a time, 100 ml beaker was used to have 2 mm sample thickness. Illumination was done on the shaker (gently shaking) for 30 min.

The oxygen evolving activity was measured at 1200 $\mu E \cdot m^{-2} \cdot s^{-1}$ at 10 μg Chl/ml.

Figure 32. Time dependence of the oxygen evolving activity of 1 M NaCl treated PSII lacking the 17 and 23 kD polypeptides at 1200 $\mu E \cdot m^{-2} \cdot s^{-1}$ with and without metal ions (1 mM Mn^{2+}, 1 mM Co^{2+}, or 1 mM Fe^{2+}) in the presence of PPBQ at 10 μg Chl/ml.

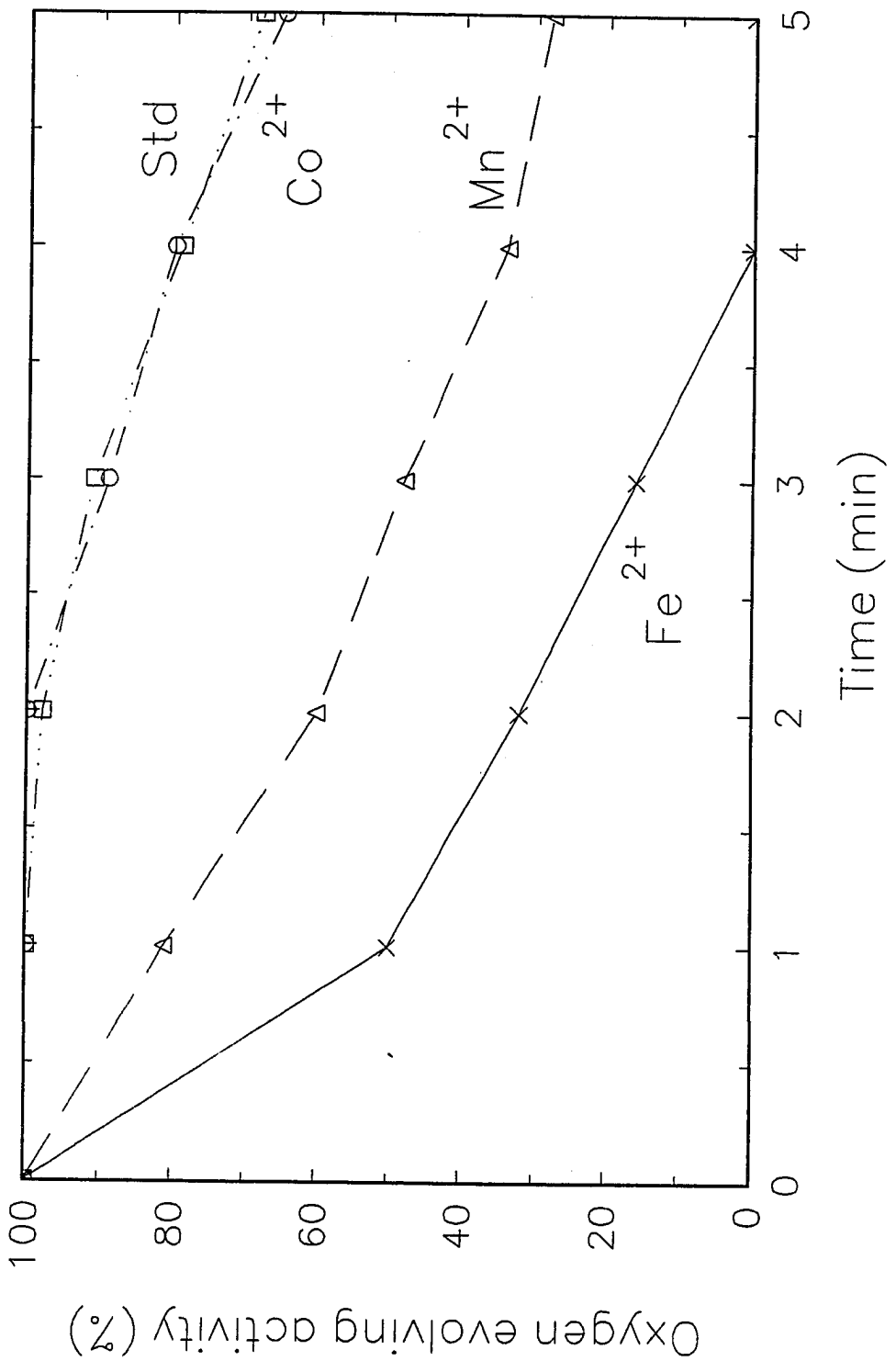

V-3-3 Discussion

Strong illumination of oxygen-evolving organisms inhibits the electron transport through PSII (Jones and Kok, 1966; Callahan et al., 1986; Thompson and Brudvig, 1988). In addition, strong illumination leads to a rapid turnover of the D_1 protein in the reaction center of PSII (Jegerschöld et al., 1990; Kuhn and Böger, 1990; Blubaugh and Cheniae, 1990; Fine and Frasch, 1990; Eckert et al., 1991). Both the D_1 protein and the inhibition of the oxygen evolution are much more sensitive to illumination in the modified PSII (e.g., 1 M $CaCl_2$ treated, NH_2OH treated) than in the NaCl PSII.

DCIP is a more efficient electron acceptor not only for photoactivation (Tamura and Cheniae, 1987) but also for photoinhibition than PPBQ. A possible explanation is that DCIP is hydrophilic and has easier access to the Q_B site which is hydrophilic while PPBQ is hydrophobic. This also can explain why DCIP accelerates the photoinhibition process during the oxygen evolving assay (light intensity is 1200 $\mu E \cdot m^{-2} \cdot s^{-1}$, 40 times the photoactivation light intensity). Izawa et al. (1983) reported that Mn inhibition (the oxygen evolving center can be irreversibly inactivated by dark incubation with exogenous Mn (Muallem and Izawa, 1980) can be prevented by the presence of Cl^- during Mn treatment. The resuspension and assay medium had enough Cl^-, so that Cl^- was not the limiting factor in ths treatment in Table 16.

Scheme 2 shows the reactions that lead to the accumulation of abnormally long-lived, highly oxidizing radicals on the donor side

in PSII. When the S_n state turnover is not fast enough for normal reduction of P_{680}^+, (in the absence of a fast donor), the life time of the oxidized primary donor, Z, is increased to 40 - 50 μs (Ono et al., 1986). Under these circumstances it is highly likely that P_{680}^+ (possibly also Z^+), due to its high oxidative potential, can oxidize nearby amino acid residues or close-lying redox components (Thompson and Brudvig, 1988), which might destroy the tertiary structure of the D_1 protein. The modified D_1 proteins are then excised from the reaction center and further degraded in proteolytic reactions (Mattoo et al., 1989). Since D_1 most likely harbors Mn (see e.g., Coleman and Govindjee, 1987 and figure 3), the degradation of D_1 may prevent the reconstitution of the WOC.

The above effect is more severe in the Cl^--depleted system. The presence of DCMU during the illumination prevents the formation of these radicals (Jegerschöld et al., 1990) because even though continuous illumination results in formation of the radical pair P_{680}^+ - $Pheo^-$ this recombines in a few nanoseconds in the presence of Q_A^- (Takahashi et al., 1987).

The presence of metal ions further accelerates the light-induced protein damage of tertiary structure and inhibition. Especially, Fe^{2+}, the metal ion which has a stronger tendency to get oxidized from +2 to +3, induces more photoinhibition.

Scheme 2

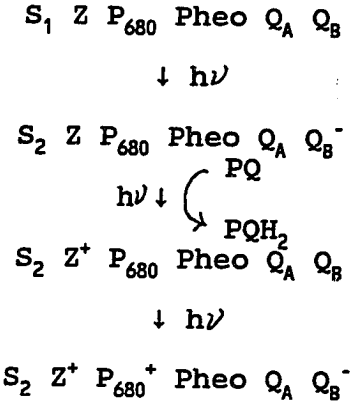

S_n is the S-state of the Kok cycle; Z is the donor to P_{680}^+; P is P_{680}; Q_A is the primary acceptor quinone of PSII; Q_B is the secondary acceptor quinone of PSII; PQ is plastoquinone from the PQ pool.

High intensity of illumination causes photoinhibition because S-state turnover is slower than primary charge separation, and the Mn complex can not supply electrons fast enough to reduce Z^+ or P_{680}^+.

Chapter VI: CONCLUSIONS

In this thesis an attempt was made to take apart the OEC in a controlled way (chapter III) and to reconstitute it again to its functional form (chapter V). In the process, it was found that photoinhibition originating from the powerful oxidant, P_{680}^{+}, is always a limiting factor as shown in chapter V. Photoinhibition occurs whenever the light intensity is so high that the electron transfer rate to the acceptor side exceeds the rate at which electrons can be supplied from the OEC, the intrinsic donor. This situation arises even in the standard assay of oxygen evolution at a light intensity of 1200 $\mu E \cdot m^{-2} \cdot s^{-1}$, where the electron transfer rate on the acceptor side is 1.4 times faster than the maximum rate on the donor side (chapter IV-2). This point has to be taken into account in assays of the oxygen evolution in modified PSII. It is shown in chapter III-1, for instance, that in a proper buffer, PSII lacking all extrinsic proteins not only has the full complement of four Mn per RC, but it also evolves the same number of O_2 molecules per photon as the standard PSII as long as the light intensity and therefore the electron transfer rates are sufficiently low. This observation was confirmed and further elaborated using time dependent fluorescence, which allowed one to deduce electron transfer rates and other kinetic parameters. Overall, a consistent picture emerged although it was impossible to resolve all S-state transitions.

In chapter III, the mechanism of photosynthetic water oxidation has been probed by the use of the substrate analogue NH_2OH: (a) NH_2OH reduces Mn in the water oxidation complex and releases Mn from the reaction center. Earlier studies of the NH_2OH effect on PSII did not take account of the simultaneous release of extrinsic polypeptides. (b) When Mn is released from 1 M NaCl treated PSII membranes (the 17 and 23 kD extrinsic proteins depleted PSII) by NH_2OH treatment in the dark, a plot of the Mn released versus [NH_2OH] shows a sigmoidal shape. The results were interpreted in terms of a cooperativity model.

(c) The plot of Mn release versus oxygen evolving activity shows all 4 Mn/RC are essential for active oxygen evolution as illustrated in figure 33.

In Chapter IV, it was shown that 1 M $CaCl_2$ treated PSII membranes, which lack all 3 extrinsic polypeptides (17, 23, and 33 kD) have low oxygen evolving activity in spite of the full complement of 4 Mn per RC: (a) If the light intensity is sufficiently low, $CaCl_2$ treated PSII evolve the same number of oxygen molecules per photon as NaCl treated PSII. Therefore, removal of the 33 kD polypeptide did not inactivate the Mn center and all Mn centers are intact. (b) If the light intensity is high, Chl is suggested to act as an alternative electron donor to P_{680}^+ in $CaCl_2$ treated PSII. As a result, the fluorescence and the oxygen evolving activity are low. (c) Chl a fluorescence transient data with and without HQ (electron donor) show that in $CaCl_2$ treated PSII the donor side is slowed down. (d) To investigate the slow-

down of the S_n -> S_{n+1} transition rate in more detail, I analyzed the fluorescence data of the S_1 -> S_2 transition in DCMU-treated samples. For $CaCl_2$ PSII the transition time, 360 μs, is a factor of 1.4 times longer than in NaCl PSII (260 μs). It is clear that some other S state transition, including the dark reaction, must be slowed down as well.

In chapter V, photoactivation and photoinhibition were studied: (a) I succeeded in reconstituting 37 % of the oxygen evolving activity with 40 % Mn concentration in the reconstituted sample. Therefore, about 40 % of the centers have all 4 Mn while the other 60 % of the centers have no Mn. It is very plausible that Mn rebinding also involves cooperativity. (b) Other divalent transition metal ions like Fe^{2+} and Co^{2+} can not reconstitute the oxygen evolving activity in Mn depleted PSII, but they apparently compete for the Mn binding sites and interfere with Mn reconstitution. (c) Comparison of the oxygen evolving activity at 1200 $\mu E \cdot m^{-2} \cdot s^{-1}$ of NaCl treated PSII with and without the divalent metal ions, Mn^{2+}, Co^{2+}, or Fe^{2+} in the assay medium showed that Fe^{2+}, which has the strongest tendency to get oxidized, induces most photoinhibition. Some photoinhibition is likely to occur also in the process of photoactivation, which is done at lower light intensity but at comparable Mn^{2+} concentration. (d) Other divalent transition metals like Fe^{2+} and Co^{2+} apparently compete for the Mn binding sites and may form mixed metal clusters. If such clusters can be prepared in a well defined manner their magnetic properties

Figure 33. The cooperativity model indicates that a WOC that has lost one Mn at a given NH_2OH concentration has an increased probability of losing the second, third and forth Mn. In the extreme limit of cooperativity all four Mn would be released simultaneously, and the fractional loss of oxygen evolving activity would equal the fractional loss of Mn. The result implies that there is mixture of the centers which already lost Mn (3 or 4 according to the cooperativity model) and which start to lose Mn, and the centers that have one to three Mn bound lost oxygen evolution activity.

might give insight into the spin coupling of the cluster and, if ENDOR is feasible, into the nature of the ligands.

REFERENCES

Akabori, K., Imaoka, A., and Toyoshima, Y. (1984) FEBS Lett. 173, 36-40.

Åkerlund, H.-E., Jasson, C., and Andersson, B. (1982) Biochim. Biophys. Acta 681, 1-10.

Andersson, B., Critchley, C., Ryrie, I.J., Jansson, C., Larsson, C., and Anderson, J.M. (1984) FEBS Eltt. 168, 113-117.

Andersson, B., and Styring, S. (1991) Current Topics in Bioenergetics 16, 1-80.

Andréasson, L.-E., and Hansson, O. (1987) Prog. Photosyn. Res. Proc. Int. Congr. Photosyn., 7th, 1987 1, 503-510.

Andréasson, L.-E., and Vänngård, T. (1988) Ann. Rev. Plant Physiol. Plant Mol. Biol. 39, 379-411.

Babcock, G.T. (1987) In New Comprehensive Biochemistry Photosynthesis (Amesz, J., ed.) pp. 125-158, Elsevier/North-Holland, Amsterdam.

Baumgarten, M., Philo, J.S., and Dismukes, G.C. (1990) Biochemistry 29, 10814-10822.

Beck, W.F., and Brudvig, G.W. (1987) Biochemistry 26, 8285-8295.

Bennoun, P., and Joliot, A. (1969) Biochim. Biophys. Acta 189, 85-96.

Berthold, D.A., Babcock, G.T., and Yocum, C.F. (1981) FEBS Lett. 61, 231-234.

Blubaugh, D.J. (1987) Ph.D. Thesis, Biology, University of Illinois at Urbana-Champaign.

Blubaugh, D.J., and Cheniae, G.M. (1990) Biochemistry 29, 5109-5118.

Bouges, B. (1971) Biochim. Biophys. Acta 234, 103-112.

Boussac, A., Zimmerman, J.L., and Rutherford, A.W. (1989) Biochemistry 28, 8984-8989.

Boussac, A., Zimmermann, J.-L., Rutherford, A.W., and Lavergne, J. (1990) Nature 347, 303-306.

Bowes, J.M., and Crofts, A.R. (1980) Biochim. Biophys. Acta 590, 373-384.

Brettel, K., Schlodder, E., and Witt, H.T. (1984) Biochim. Biophys. Acta 766, 403-415.

Brudvig, G.W., Beck, W.F., and De Paula, J.C. (1989) Annu. Rev. Biophys. Biophys. Chem. 18, 25-46.

Brudvig, G.W., Casey, G.L., and Sauer, K. (1983) Biochim. Biophys. Acta 723, 366-371.

Burnap, R.L., and Sherman, L.A. (1991) Biochemistry 30, 440-446.

Callahan, F.E., Becker, D.W., and Cheniae, G.M. (1986) Plant Physiol. 82, 261.

Cheniae, G.M., and Martin, I.F. (1967) Biochem. Biophys. Res. Commun. 28, 89-95.

Cheniae, G.M., and Martin, I.F. (1970) Biochim. Biophys. Acta 197, 219-239.

Cheniae, G.M., and Martin, I.F. (1971) Plant Physiol. 47, 568-575.

Cheniae, G.M., and Martin, I.F. (1973) Photochem. Photobiol. 17, 441-459.

Cole, J.L., Yachandra, V.K., McDermott, A.E., Guiles, R.D., Britt, R.D., Dexheimer, S.L., Sauer, K., and Klein, M.P. (1987) Biochemistry 26, 5967-5973.

Coleman, W.J., Baianu, I.C., Gutowsky, H.S., and Govindjee (1984) In Advances in Photosynthesis Research (Sybesma, C. ed.), Vol I, pp. 283-286, Martinus Nijhoff/ Dr. W. Junk Publishers, The Hague.

Coleman, W.J., and Govindjee (1987) Photosyn. Res. 13, 199-223.

Crofts, A.R., and Wraight, C.A. (1983) Biochim. Biophys. Acta, 726, 149-185.

De Paula, J.C., Li, P.M., Miller, A.-F., Wu, B.W., and Brudvig, G.W. (1986) Biochemistry 25, 6487-6494.

Debus, R.J., Barry, B.A., Babcock, G.T., and McIntosh, L. (1988a) Proc. Natl. Acad. Sci. USA 85, 427-430.

Debus, R.J., Barry, B.A., Sithole, I., Babcock, G.T., and McIntosh, L. (1988b) Biochemistry 27, 9071-9074.

Dekker, J.P., Ghanotakis, D.F., Plijter, J.J., Gorkom, H.J.V., and Babcock, G.T. (1984) Biochim. Biophys. Acta 767, 515-523.

Den Haan, G.A., De Vries, H.A., and Duysens, L.N.M. (1976) Biochim. Biophys. Acta 430, 265-281.

Dexheimer, S.L., Sauer, K., and Klein, M.P. (1990) in Current Research in Photosynthesis (Baltscheffsky, M. ed.), Vol I, pp. 761-764, Kluwer Academic Publishers, Netherlands.

Dismukes, G.C., and Siderer, Y. (1981) Proc. Natl. Acad. Sci. USA 78, 274-278.

Dismukes, G.C. (1986) Photochem. Photobiol. 43, 99-115.

Duysens, L.N.M. (1986) In Light Emission by Plants and Bacteria, (Govindjee, eds.), pp. 4-28, Academic press, Orlando.

Eaton-Rye, J.J. (1987) Ph.D thesis, biology, University of Illinois at Urbana-Champaign.

Eaton-Rye, J.J., and Govindjee (1988) Biochim. Biophys. Acta 935, 248-257.

Eckert, H.-J., Geiken, B., Bernarding, J., Baouwitzjum, A., Eichler, G.-J., and Renger, G. (1991) Photosyn. Res. 27, 97-108.

Fine, P.L., and Frasch, W.D. (1990) In Current Research in Photosynthesis (Baltsheffsky, M., ed.), Vol I, 905-908.

Forbush, B., and Kok, B. (1968) Biochim. Biophys. Acta 162, 243-253.

Förster, V., and Junge, W. (1985) FEBS Lett. 185, 53-57.

Förster, V., and Junge, W. (1986a) FEBS Lett. 186, 153-157.

Förster, V., and Junge, W. (1986b) Photosyn. Res. 9, 197-210.

Ghanotakis, D.F., Babcock, G.T., and Yocum, C.F. (1984) Biochim. Biophys. Acta 765, 388-398.

George, G.N., Prince, R.C., and Cramer, S.P. (1989) Science 243, 789-791.

Goodin, D.B., Yachandra, V.K., Britt, R.D., Sauer, K., and Klein, M.P. (1984) Biochim. Biophys. Acta 767, 209-216.

Govindjee and Coleman, W. (1991) In Photosynthesis and Plant Productivity (Abrol, Y. et al., eds) Oxford University Press/IBH private Ltd., New Delhi, India, in press.

Govindjee and Homann, P.H. (1989) In High Light Modern Biochemistry (Kotyk, A. et al., eds.) Vol. 1, pp. 933-961, The Netherlands.

Govindjee, Kambara, T., and Coleman, W. (1985) Photochem. Photobiol. 42, 187-210.

Govindjee, and Wasielewski, M.R. (1989) In Photosynthesis, Plant biology (Briggs, W.R., ed.) Vol. 8, pp. 71-103, Alan R. Liss Publishers: New York.

Guiles, R.D., Yachandra, V.K., McDermott, A.E., Britt, R.D., Dexheimer, S.L., Sauer, K., and Klein, M.P. (1986) in Progress in Photosynthesis Research (Biggins, J. ed.), Vol. I, pp. 561-564, Martinus Nijhoff, Dordrecht: The Netherlands.

Ghanotakis, D.F., Topper, J.N., Babcock, G.T., and Yocum, C.F. (1984) FEBS Lett. 170, 169-173.

Ghanotakis, D.F., and Yocum, C.F. (1990) Annu. Rev. Plant Physiol. Plant Mol. Biol. 41, 255-276.

Guiles, R.D., Zimmermann, J.-L., McDermott, A.E., Yachandra, V.K., Cole, J.L., Britt, R.D., Dexheimer, S.L., Wieghardt, K., Bossek. U., Sauer, K., and Klein, M.P. (1990) Biochemistry 29, 471-485.

Haddy, A., Aasa, R., and Andreasson, L.-E. (1989) Biochemistry 28, 6954-6959.

Hansson, Ö., Aasa, R., and Vänngård, T. (1986) Biophys. J 51, 825-832.

Henry, L.E.A., Lindberg-Moller, B., Andersson, B,M, and Akerlund, H.-E. (1982) Carlsbergs Res. Commun. 47, 187-198.

Hoganson, C.W., and Babcock, G.T. (1989) Biochemistry 28, 1448-1454.

Homann, P.H. (1988) Biochim. Biophys. Acta 934, 1-13.

Horton, P., and Croze, E. (1977) Biochim. Biophys. Acta 462, 86-101.

Ikeuchi, M., Eggers, B., Shen, G., Webber, A., Yu, J., Hirano, A., Inoue, Y., and Vermaas, W. (1991) J. Biol. Chem. 266, 11111-11115.

Imaoka, A., Akabori, K., Yanagi, M., Izumi, K., Toyoshima, Y., Kawamori, A., Nakayama, H., and Sato, J. (1986) Biochim. Biophys. Acta 848, 201-211.

Inoue, Y., Kobayashi, Y., Sakamoto, E., and Shibata, K. (1975) Plant Cell Physiol. 16, 327-336.

Izawa, S., Muallem, A., and Ramaswamy, N.K. (1983) In The Oxygen Evolving System of Photosynthesis (Inoue, Y., et al., eds.), pp. 293-302, Academic Press: Japan.

Jegerschöld, C., Virgin, I., and Styring, S. (1990) Biochemistry 29, 6179-6186.

Joliot, A., and Joliot, P. (1964) C.R. Acad. Sci. Paris 258, 4622-4625.

Jones, L.W., and Kok, B (1966) Plant Physiol. 41, 1037.

Jursinic, P., and Govindjee (1977a) Photochem. Photobiol. 26, 617-628.

Jursinic, P., and Govindjee (1977b) Biochim. Biophys. Acta 461, 253-267.

Kambara, T., and Govindjee (1985) Proc. natl. Acad. Sci. USA 82, 6119-6123.

Kim, D.H., Britt, R.D., Klein, M.P., and Sauer, K. (1990) J. Am. Chem. Soc. 112, 9389-9391.

Kok, B., Forbush, B., and McGloin, M. (1970) Photochem. Photobiol. 11, 457-475.

Kramer, D.M., Robinson, H.R., and Crofts, A.R. (1990) Photosyn. Res. 26, 181-193.

Kuhn, M., and Böger, P. (1990) Photosyn. Res. 23, 291-296.

Kuwabara, T., Miyao, M., Murata, T., and Murata, N. (1985) Biochim. Biophys. Acta 806, 283-289.

Laemmli, U.K. (1970) Nature 227, 680-685.

Mathis, P., and Paillotin, G. (1981), In The Biochemistry of Plants: Photosynthesis (Hatch, M.D., and Bpard, M.L., eds.), Vol. 8, pp. 97-161, Academic Press, Sydney.

Mattoo, A.K., Marder, J.B., and Edelman, M. (1989) Cell 56, 241-246.

Messinger, J., Wacker, U., and Renger, G. (1991) Biochemistry 30, 7852-7862.

Metz, J.G., Nixon, P.J., Rögner, M., Brudvig, G.W., and Diner, B.A. (1989) Biochemistry 28, 6960-6969.

Miller, A.-F., De Paula, J.C., and Brudvig, G.W. (1987) Photosyn. Res. 12, 205-218.

Miller, A.-F., and Brudvig, G.W. (1989) Biochemistry 28, 8181-8190.

Miller, A.-F., and Brudvig, G.W. (1991) Biochim. Biophys. Acta 1056, 1-18.

Miyao, M., and Inoue, Y. (1991) Biochim. Biophys. Acta 1056, 47-56.

Miyao, M., and Murata, N. (1983) Biochim. Biophys. Acta 725, 87-93.

Miyao, M., and Murata, N. (1984) FEBS Lett. 170, 350-354.

Miyao, M., and Murata, N. (1985) FEBS Lett. 180, 303-308.

Miyao, M., and Murata, N. (1987) in Topics in Photosynthesis (Kyle, D.J. et al. ed.), Vol 9, pp. 289-307, Amsterdam: Elsevier Science Publishers BV.

Miyao, M., Murata, N., Lavorel, J., Maison-Peteri, B., Boussac, A., and Etienne, A.-L. (1987a) Biochim. Biophys. Acta 890, 151-159.

Miyao, M., Murata, N., Maison-Peteri, B., Boussac, A., Etienne, A.-L., and Lavorel, J. (1987b) In Progress in Photosynthesis Research (Biggins, J., ed.), Vol. I, pp. 613-616, Dordrecht:Martinus Nijhoff Publishers.

Muallem, A., and Izawa, S. (1980) FEBS Lett. 115, 49-53.

Murata, N., and Miyao, M. (1985) Trends in Biochem. Sci. 10, 122-124.

Murata, N., Miyao, M., and Kuwabara, T. (1983) in The Oxygen Evolving System of Photosynthesis (Inoue, Y., et al. ed.), pp. 213-222, Tokyo: Academic Press.

Ono, T., and Inoue, Y. (1983a) FEBS Lett. 164, 255-260.

Ono, T., and Inoue, Y. (1983b) Biochim. Biophys. Acta 723, 191-201.

Ono, T., and Inoue, Y. (1984) FEBS Lett. 168, 281-286.

Ono, T., and Inoue, Y. (1985) Biochim. Biophys. Acta 806, 331-340.

Ono, T., and Inoue, Y. (1987) Plant Cell Physiol. 28, 1293-1299.

Ono, J., Zimmermann, J.L., Inoue, Y., and Rutherford, A.W. (1986) Biochim. Biophys. Acta 851, 193-201.

Pace, R.J., Smith, P., Bramley, R., and Stehlik, D. (1991) Biochim. Biophys. Acta 1058, 161-170.

Padhye, S., Kambara, T., Hendrickson, D.N., and Govindjee (1986) Photosyn. Res. 9, 103-112.

Pecoraro, V.L. (1988) Photochem Photobiol 48, 249-264.

Porra, R.J., Thompson, W.A., and Kriedemann, P.E. (1989) Biochim. Biophys. Acta 975, 384-394.

Radmer, R. (1983) In The Oxygen Evolving system of Photosynthesis (Inoue, Y. et al., eds.) pp. 135-144, Academic: Tokyo.

Radmer, R., and Cheniae, G.M. (1971) Biochim. Biophys. Acta 253, 182-186.

Radmer, R., and Cheniae, G.M. (1977) In Primary Processes of Photosynthesis (Barber, J. ed.), pp. 303-348, Elsevier/ North-Holland Biomedical: New York.

Radmer, R., and Ollinger, O. (1983) FEBS Lett. 152, 39-42.

Rawn, J.D. (1989) In Proteins, Energy, and Metabolism, pp. 489-501, Neil Patterson Publisher: Burlington, North Carolina.

Renger, G., and Wydrzynski, T. (1990) Biol. Metals 3, 1-8.

Robinson, H.H., and Crofts, A.R. (1983) FEBS Lett. 153, 221-226.

Sandusky, P.O., and Yocum, C.F. (1984) Biochim. Biophys. Acta 766, 603-611.

Sauer, K., Yachandra, V.K., Britt, R.D., and Klein, M.P. (1991) In Mn Redox Enzymes (Pecoraro, V.L. ed.) VCH Publisher, New York, in press.

Scholes, C.P., Falkowski, K.M., Chen, S., and Bank, J. (1986) J. Am. Chem. Soc. 108, 1660-1671.

Segel, I.H. (1975) In Enzyme Kinetics, pp 161-226, John Wiley and Sons Inc., New York.

Sharp, R.R., and Yocum, C.F. (1981) Biochim. Biophys. Acta 635, 90-104.

Sivaraja, M., and Dismukes, G.C. (1988) Biochemistry 27, 3467-3475.

Sivaraja, M., Tso, J., and Dismukes, G.C. (1989) Biochemistry 28, 9459-9464.

Srivastava, U.C., and Nigam, H.L. (1972) Coord. Chem. Rev. 9, 275-310.

Stewart, A.C., Ljungberg, U., Åkerlund, H.-E., and Andersson, B. (1985) Biochim. Biophys. Acta 808, 353-362.

Stryer, L. (1981) Biochemistry, pp. 65-69, 2nd ed., Freeman and company, New York.

Styring, S., and Rutherford, A.W. (1987) Biochemistry 26, 2401-2405.

Styring, S., and Rutherford, A.W. (1988) Biochim. Biophys. Acta 933, 378-387.

Takahashi, Y., Hansson, Ö., Mathis, P., and Satoh, K. (1987) Biochim. Biophys. Acta 893, 49-59.

Tamura, N., and Cheniae, G.M. (1985) Biochim. Biophys. Acta 809, 245-259.

Tamura, N., and Cheniae, G.M. (1987) Biochim. Biophys. Acta 890, 179-194.

Tamura, N., and Cheniae, G.M. (1988) In Light-Energy Transduction in Photosynthesis: Higher Plant and Bacterial Models (Stevens, S.E. Jr., and Bryant, D.A., eds.), pp. 227-242, The American Society of Plant Physiologists, Rockville.

Thompson, L.K., and Brudvig, G.W. (1988) Biochemistry 27, 6653-6658.

Tripathy, B.C., and Mohanty, P. (1981) Plant Science Letters 22, 253-261.

Tripathy, B.C., and Mohanty, P. (1983) Biochim. Biophys. Acta 722, 88-93.

Tso, J., Sivaraja, M., and Dismukes, G.C. (1991) Biochemistry 30, 4734-4739.

Van Gorkom, H.J., Meiburg, R.F., and De Vos, L.J. (1986) Photosyn. Res. 9, 55-62.

Vass, I., Ono, T, and Inoue, Y. (1987) Biochim. Biophys. Acta 892, 224-235.

Velthuys, B.R., and Kok, B. (1978) Biochim. Biophys. Acta 502, 211-221.

Vermaas, W.F.J., Ikeuchi, M. (1991) In The photosynthetic Apparatus: Molecular Biology and Operation (Bogorad, L and Vasil, I.K., eds.), pp. 26-111, Academic Press, Inc., San Diego.

Vermaas, W.F.J., Ikeuchi, M., and Inoue, Y. (1988a) Photosyn. Res. 17, 97-114.

Vermaas, W.F.J., Rutherford, A.W., and Hansson, Ö. (1988b) Proc. Natl. Acad. Sci. USA 85, 8477-8481.

Xu, C., Rogers, S.M.D., Goldstein, C., Widholm, J.M., and Govindjee (1989) Photosyn. Res. 21, 93-106.

Yamashita, T., and Ashizawa, A. (1985) Arch. Biochem. Biophys. 238, 549-557.

Yamashita, T., and Tomita, G. (1974) Plant Cell Physiol. 15, 69-82.

Yamashita, T., and Tomita, G. (1976) Plant Cell Physiol. 17, 571-582.

Yocum, C.F., Yerkes, C.T., Blankenship, R.E., Sharp, R.R., and Babcock, G.T. (1981) Proc. Natl. Acad. Sci. USA 78, 7507-7511.

Zimmermann, J.-L., and Rutherford, A.W. (1986) Biochemistry 25, 4609-4615.

VITA

Hyunsuk Shim was born in Seoul, Korea on May 15, 1961. She attended Yonsei University receiving a Bacheler of Arts degree in Physics with Honors in 1984. She then continued her education in the Department of Physiology and Biophysics at the University of Illinois at Urbana-Champaign and studied water oxidation in the Mn complex of photosystem II under the guidance of Drs. P.G. Debrunner and Govindjee. She is a co-author of the following publications:

1. Shim, H., Govindjee, and Debrunner, P.G. (1988) Purification of highly active oxygen-evolving photosystem II from *Chlamydomonas reinhardtii*. In 14th Annual Midwest Photosynthesis Conference (Miles, D. ed.), pp. 30.

2. Shim, H., Cao, J., Govindjee, and Debrunner, P.G. (1989) Purification of highly active oxygen-evolving photosystem II from *Chlamydomonas reinhardtii*. Biophysical J. 55, 180a.

3. Shim, H., Cao, J., Govindjee, and Debrunner, P.G. (1990) Purification of highly active oxygen-evolving photosystem II from *Chlamydomonas reinhardtii*. Photosyn. Res. 26, 223-228.

4. Shim, H., Govindjee, and Debrunner, P.G. (1992) Effect of the 33 kD polypeptide on water oxidation of photosystem II. Manuscript in preparation.

5. Shim, H., Govindjee, and Debrunner, P.G. (1992) Binding of NH_2OH to the water oxidation complex. Manuscript in preparation.